

Preliminary Test Results
from a
Liquid Argon/Iron Hadron Calorimeter
Report of the P-541 Collaboration

May 8, 1978

M. Goodman
A. L. Sessoms
Harvard University

S. C. Wright
University of Chicago

B. Eisenstein
L. E. Holloway
W. T. Wroblecka
University of Illinois

R. D. Kephart
Fermilab

Spokesman: A.L. Sessoms
Physics Department
Harvard University
Cambridge, MA 02138
(617) 495-3388

101 pgs.

Summary

We present preliminary results from the test of a liquid argon/iron hadron calorimeter. Our findings can be summarized as follows:

I. It is trivial to maintain the purity of the liquid argon with respect to oxygen to better than 1.5 parts per million. Performance is not noticeably affected until levels of contamination of >10 ppm are reached.

II. Extracting the signals through the cryogenic equipment requires a straightforward procedure with room temperature seals.

III. The electronics we use is stable over long periods of time. The total cost of the electronics was \$20.32/channel.

IV. It is a straightforward matter to calibrate the electronics and it is done continuously during data acquisition.

V. There are no troublesome noise problems as evidenced by our ability to see clean single muon tracks in the chamber. The raw data are clean and easy to analyze.

VI. The measured resolutions presented are uncorrected. No special cuts or sophisticated event selection has been employed and no effort has been made to correct for dispersion in the beam. The preliminary resolutions presented here are therefore upper limits. They are for hadrons:

<u>E in GeV</u>	<u>$\frac{\sigma_E}{E}$</u>	<u>σ_θ in mrad</u>
10	(21 \pm 7)%	68 \pm ?
20	(21 \pm 5)%	57 \pm 17
30	(14.5 \pm 3.5)%	47 \pm 13
40	(15 \pm 3)%	40 \pm 8

Preliminary Test Results from a Liquid Argon/Iron Hadron Calorimeter

We have built and tested a large liquid argon/iron hadron calorimeter. This device is considered a prototype for larger devices to be used as part of experiments to study the interactions of neutrinos and antineutrinos with matter. The mechanical features of the device are discussed briefly in the appended article. A more detailed discussion of the instrument and the analysis will appear later.¹

In this document we give only preliminary results based on first pass analysis and no fine tuning of programs or event selection criteria. There has been no "massaging" of the data by hand and no special fitting. We have not attempted to unfold resolutions related to beam widths and unwanted "junk" events. In other words *all* resolutions derived are upper limits and all distributions are the most straightforward. There is no doubt that the results will improve on further examination. We note, however, that they are encouraging even now and suggest that this technique is even more simple than we had hoped.

We would like to address several questions raised by the PAC and conveyed to us by Tom Groves in his letter of May 6, 1977.

I. Maintenance of the Purity of the Argon

We required that the contamination of oxygen in the liquid argon, by far the most difficult problem, be less than 10 parts per million (ppm), and be maintained at this level for long periods of time. This turned out to be trivial. We did nothing and the measured oxygen contamination in the liquid argon remained at less than 1.5 ppm for the duration of the test (several weeks) with no measurable change. No purification before or during the test was required. Liquid argon of this purity can be obtained directly from the supplier at no additional cost.

II. Techniques for Extracting Signals through the Cryogenic Equipment

The problem of getting the signals out of the device was solved in a straightforward way. The signal cables were attached to the strips and brought to printed circuit boards. These boards were brought through a split ring flange and a room temperature vacuum seal was made around them. Once outside, cables were attached to the PC boards and brought to the electronics. No problems were encountered using this technique.

III. Stability of the Electronics

The electronics were stable to within the measurement errors for the duration of the test.

IV. Ease of Calibration

The relative calibration of the electronics was straightforward. I refer you to a block diagram of the electronics in figure 5 of the attached paper. In addition to addressing the multiplexers on the electronics cards the Read In-Read Out Digital to Analog Converter (RIRODAC) can, on computer control, issue a DC voltage level whose value is determined by the computer and which is applied to the inputs of all amplifiers simultaneously. The values of the signals at the output of the CAMAC ADC's for each channel gives an immediate cross calibration of all channels. Standard running procedures were that several levels be applied to the amplifiers and the results read out to tape before and after every beam spill, thereby sandwiching all the events taken during that spill. Linearities of the quality illustrated in figure 1 were routine. In addition entire tapes of calibration data were taken as a constant, high statistics monitor of the system.

V. Possible Noise Problems

The calorimeter was run under the worst possible condi-

tions in order to see what worst case noise problems might be. No extraordinary shielding (e.g. a Faraday cage) was used. The cables going into the electronics boxes were not shielded individually, inductors were not put on power lines, and so on. This was our standard running configuration. As the results indicate, noise problems are minimal.

A good test of this is our ability to see minimum ionizing particles (muons) traversing the chamber. Figure 2 shows a muon signal for a single set of x-strips (one channel). This is raw data taken directly from the online computer display. The muon signal stands out above the noise-broadened pedestal and indicates that any noise problems are minor.

VI. Cost of Electronics

The *total* cost of the electronics is given in the appendix. This includes all labor charges. The cost is \$20.32 per channel.

One might ask how this compares with the SLAC/LBL system, roughly three times more costly. We have gone over this in detail with Dave Hitlin and find the numbers consistent. We refer you to figure 6 of the appended document. Let us consider only a few of the differences. At the input we use 1N914 diodes that cost five cents apiece. SLAC/LBL found that for their purposes the capacitance of these diodes was too high since they must look at very small (≤ 100 MeV) signals. They use diodes that cost \$3.00 apiece. Their sample and hold circuit is remote from their amplifier while ours is located directly on the chamber. They require an additional line driver, amplifier, and line receiver for each channel in order to do this. The added cost per channel is approximately \$15.00. They require very small dead time and so cannot use a CD4051BE analog switch but must use one that is much faster. The added cost per channel is several dollars. We have 60 channels, up to and including the multiplexers and line drivers, on one

card. SLAC/LBL have only 8 amplifiers per card. This pattern continues throughout the design and accounts for the cost differential.

The Data

We present in figures 3 to 13 raw data dumps of events labeled electrons and hadrons from our online display. These are events as they come into the computer with no subtractions made. The two views, x and y, are shown. The beam enters from the left. There are 12 planes each of x and y strips, each plane being five sets of strips ganged together along the beam direction. Each tick mark in x and y transverse to the beam direction corresponds to a 2 cm wide slice across the face of the shower; this is the width of the strips.

The first striking observation is the cleanliness of the events [note the different scales (SF) for electrons and hadrons] again indicating a relatively noise free environment. The second striking observation is the clear difference between electrons and hadrons. The electrons shower immediately and remain in a narrow cone typically 8 cm wide and 3 planes long. Hadronic showers are much broader, typically 20 cm wide, and go 4 or 5 planes before ending.

Preliminary Results

We present preliminary results on resolutions derived from data taken over the past several weeks. We note again that these data have not been "massaged" in any way and contributions from the momentum spread in the beam have not been taken out. We have also not done road finding or cuts on tails of distributions to improve the data and have done no sophisticated event selection. These results, then, are upper limits and we expect them to improve markedly as we become more adept at the analysis.

I. Energy Resolution

The energy resolutions are derived from curves like that shown in figures 14a-d for hadrons. The measured resolutions are given in Table 1.

Table 1
Measured Energy Resolutions for Hadrons

<u>E (GeV)</u>	<u>σ_E/E</u>
10	(21±7) %
20	(21±5) %
30	(14.5±3.5) %
40	(15±3) %

This corresponds to $\sigma_E/E = (72 \pm 10) \% / \sqrt{E}$

II. Angular Resolution

The angular resolutions are derived from curves like that shown in figures 15. The measured angular resolutions are given in Table 2.

Table 2
Measured Angular Resolutions for Hadrons

<u>E (GeV)</u>	<u>σ_θ (mrad)</u>
10	68±?
20	57±17
30	47±13
40	40±8
muons	11±2

Comments

The measured resolutions are already encouraging. It is clear that once we understand how to define shower roads and widths we will be able to cut on wings of distributions and so on, which will improve the resolutions.

It is also apparent that all resolutions improve with energy. Consider the energy resolutions. In figure 16a we plot the mean of the distribution as a function of the nominal beam energy and find the expected linear dependence. Even though the beam energy is not accurately known, the progression from 10-40 GeV depicted is reasonable.

In figure 16b we plot the quantity $\sqrt{E}(\sigma_E/E)$ vs. nominal energy. This indicates the consistency point to point of the weighted mean quoted for the result.

Conclusions

We are encouraged by our progress so far. The analysis presented is the result of less than two weeks of data taking and study. The small group of people involved point to the ease with which the data taking proceeded once the instrument was on the air; it is truly an easy device to maintain.

Our results compare well at this early stage with those of Willis and coworkers^{2,3} and indicate that liquid argon/iron hadron calorimeters can be useful tools for the study of the interactions of neutrinos with matter.

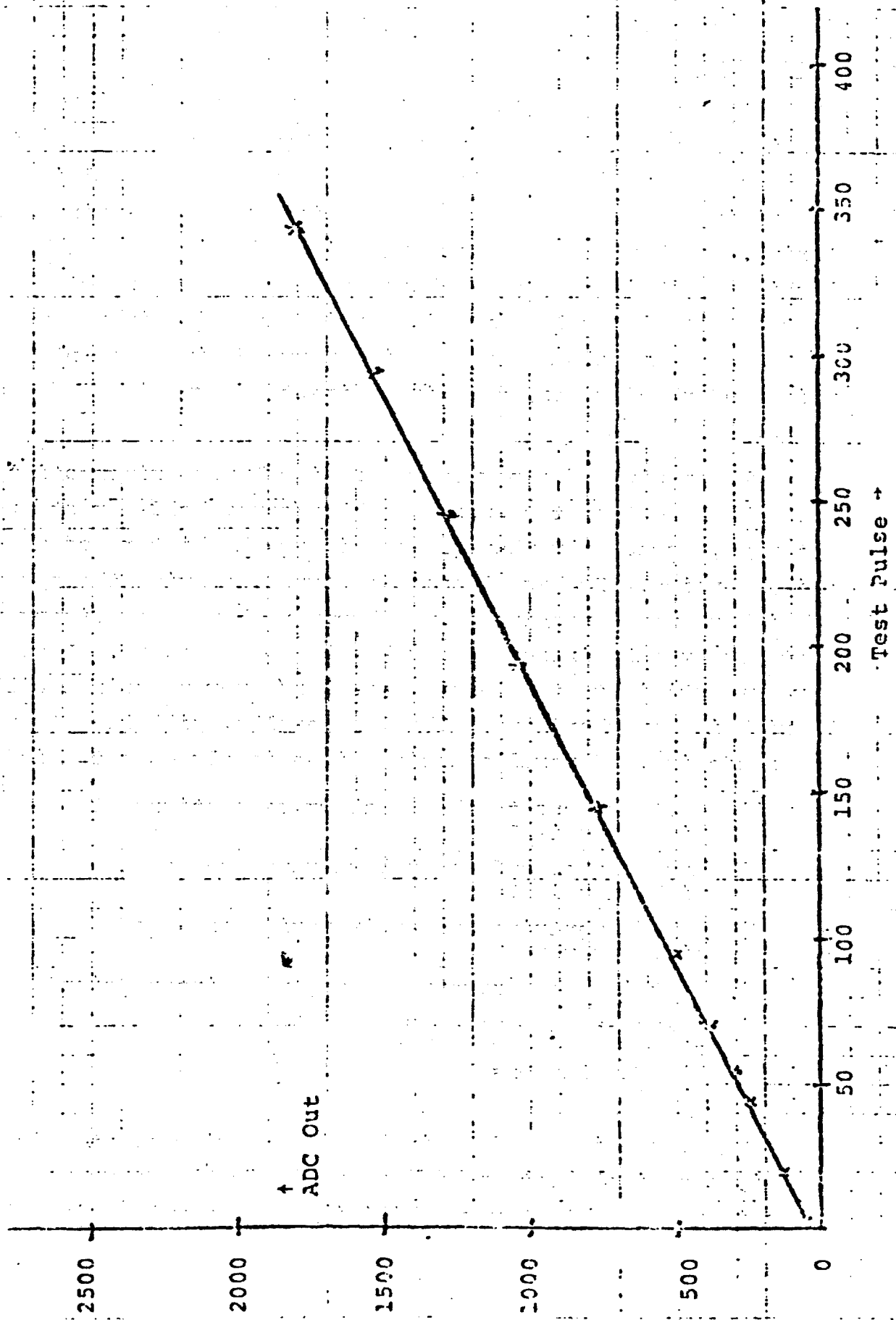


Figure I. Typical Calibration Curve for Liquid Argon Electronics

Σ 836 RN 19 *
λ 1 - 2

HV = 3600

μ-peak.
↓
pedestal
↓

5 K/pulse.

H S I N K 64 L U 64
S F I M S C O E V 9372

29 April 1978

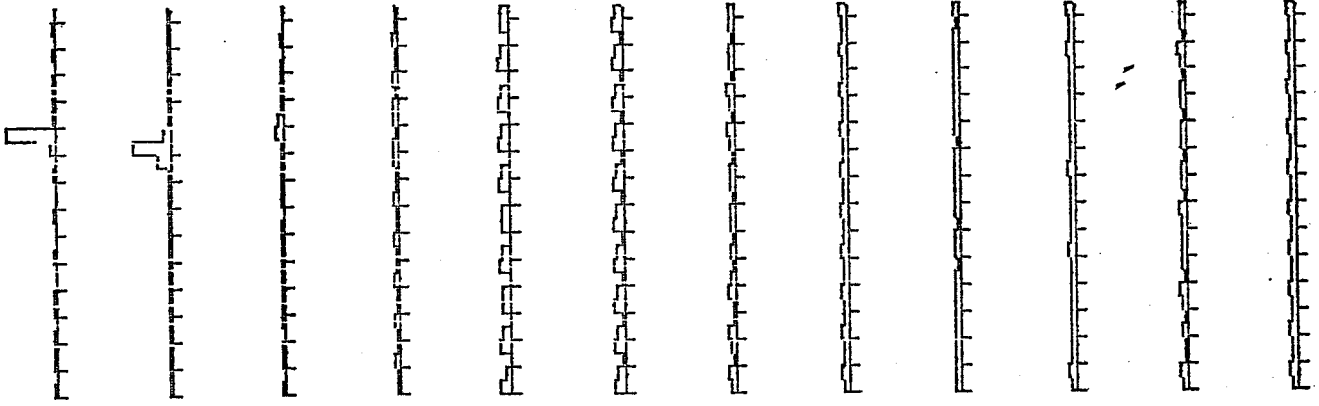
MUON

$\chi, 1, 0.$

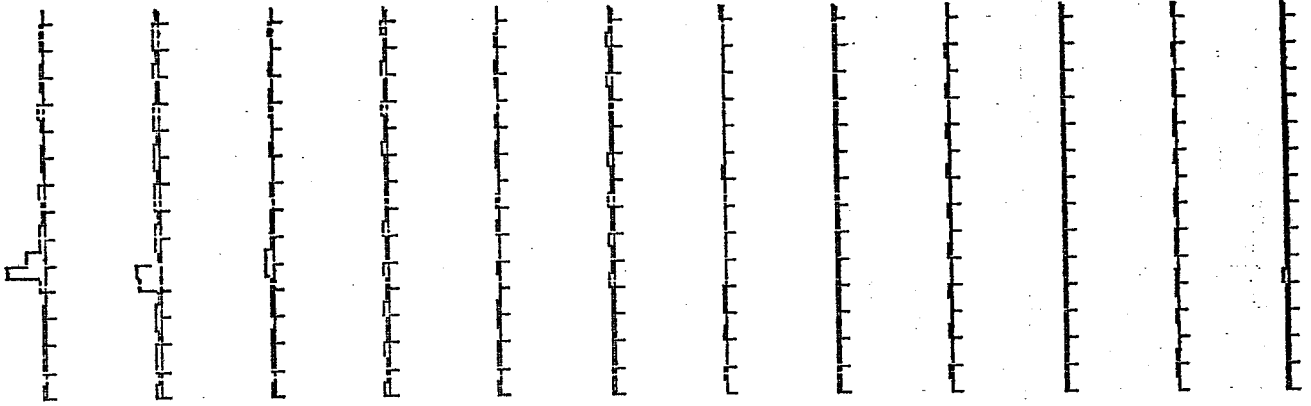
figure 2

EXP 541

Y



X



SF 10

TR 3E

LK 0

LC 0

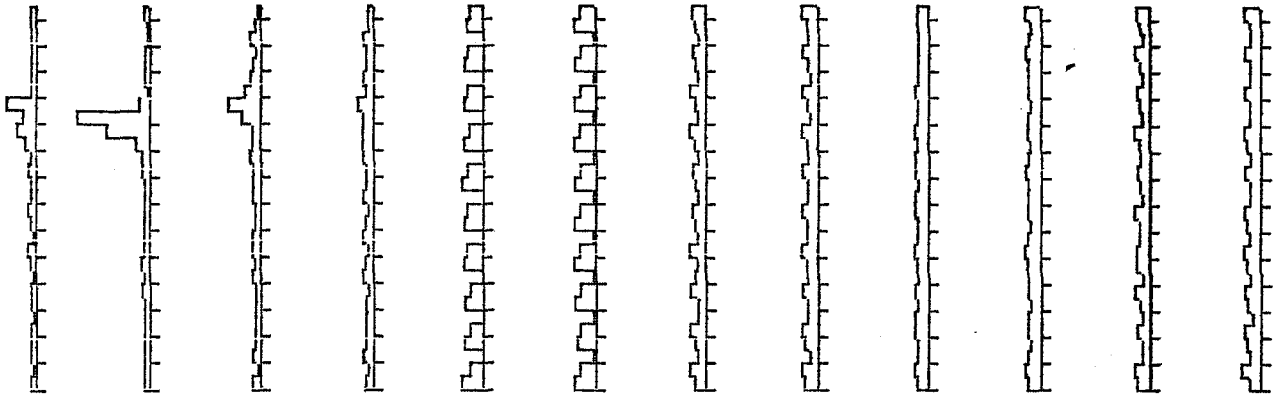
30 April 1978

10 GeV ELECTRON

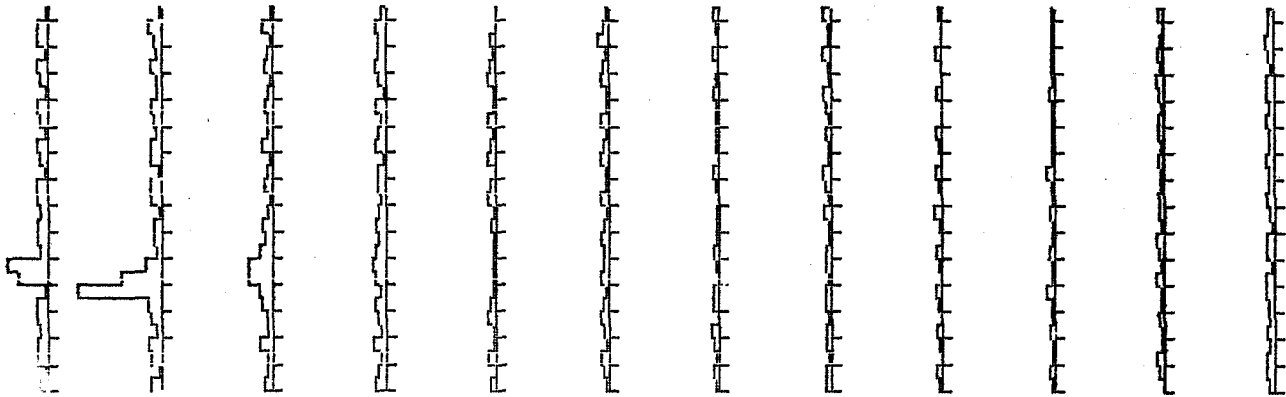
figure 3

EXP 541

Y



X



ST S

LR O

TR 64

LC O

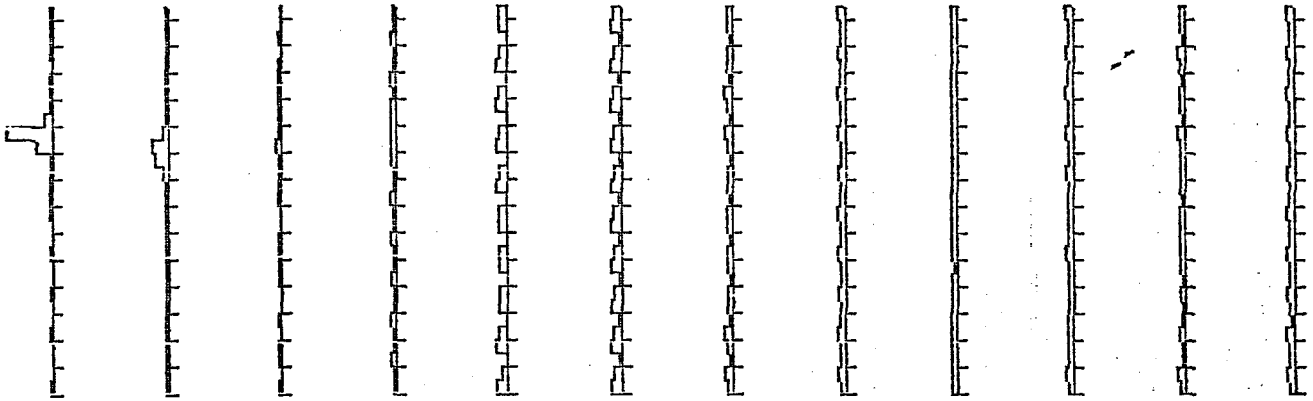
30 April 1978

10 GeV HADRON

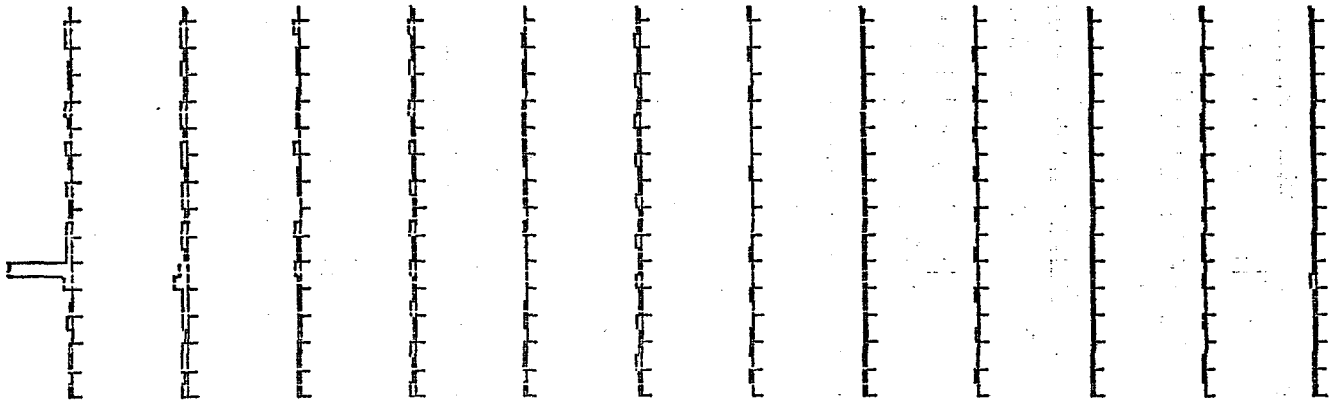
figure 4

EXP 541

Y



X



SF 10

TR 3E'

LK 0

LC 0

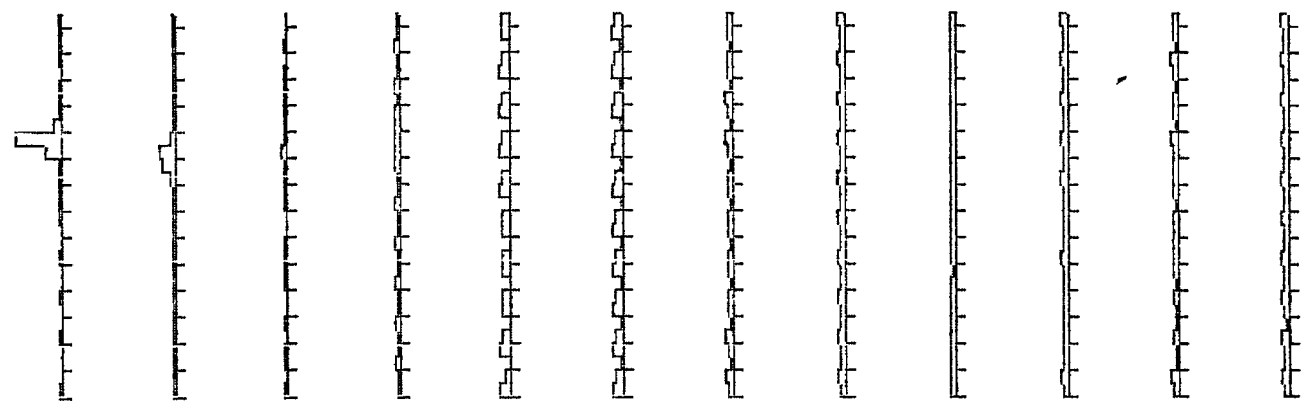
30 April 1978

20 GeV ELECTRON

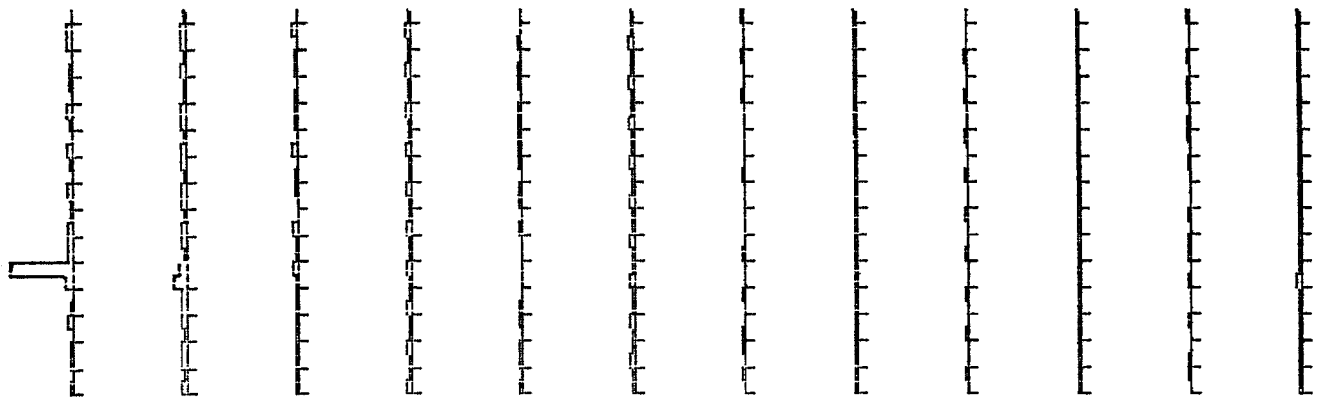
figure 5

EXP 541

Y



X



SF 10

TR 3E'

LK 0

LC 0

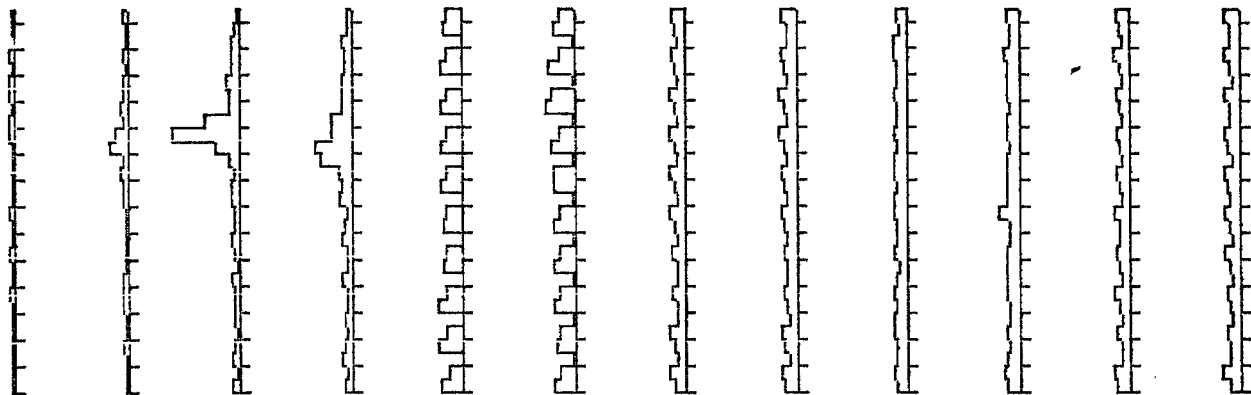
30 April 1978

20 GeV ELECTRON

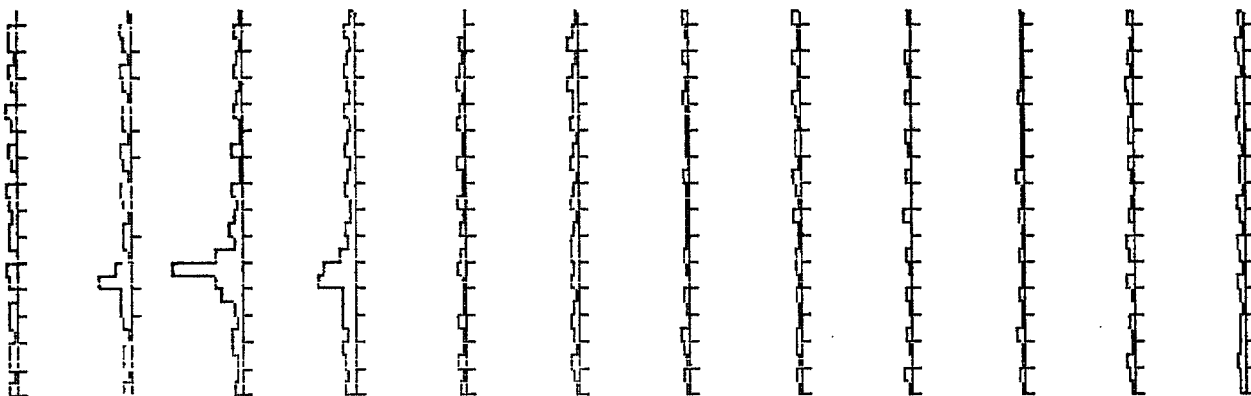
figure 6

EXP 54

Y



X



SF S
L R O

TR S
L O

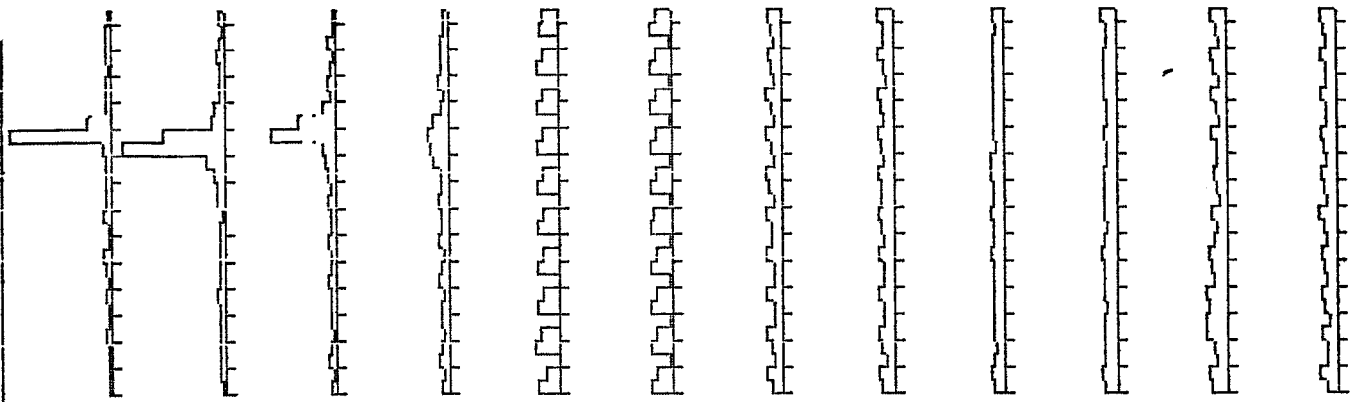
30 April 1978

20 GeV HADRON

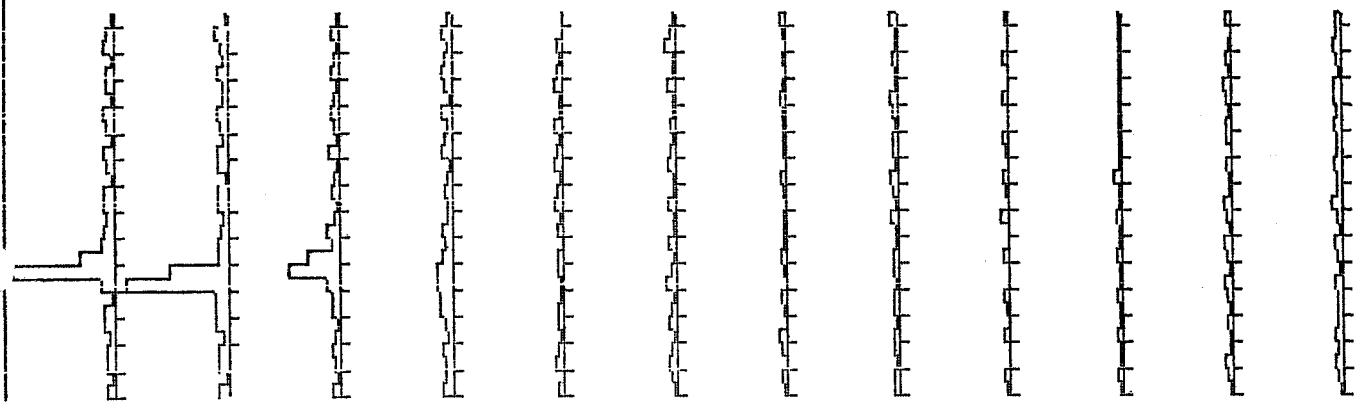
figure 7

EXP 541

Y



X



SF S
L R O

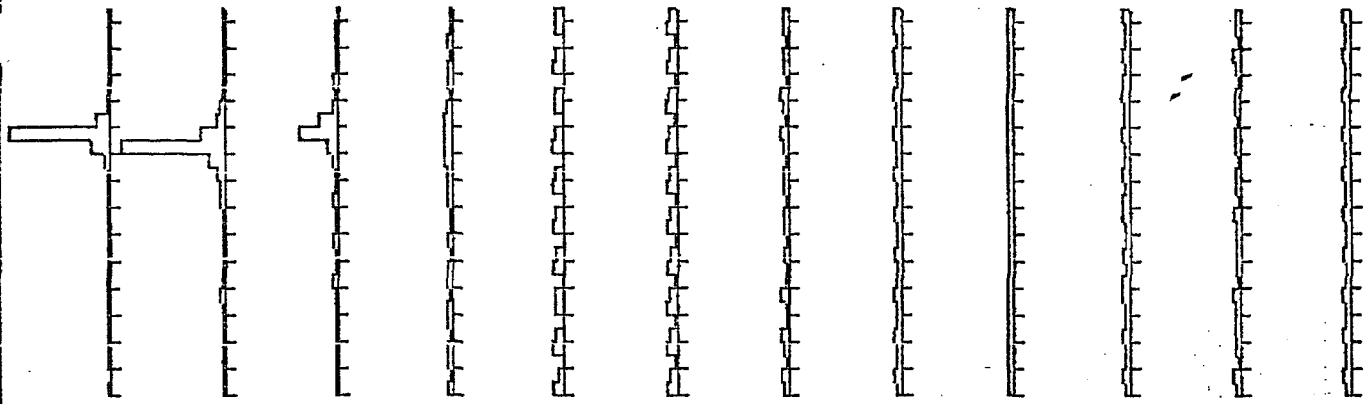
TR T
L O

20 GeV HADRON

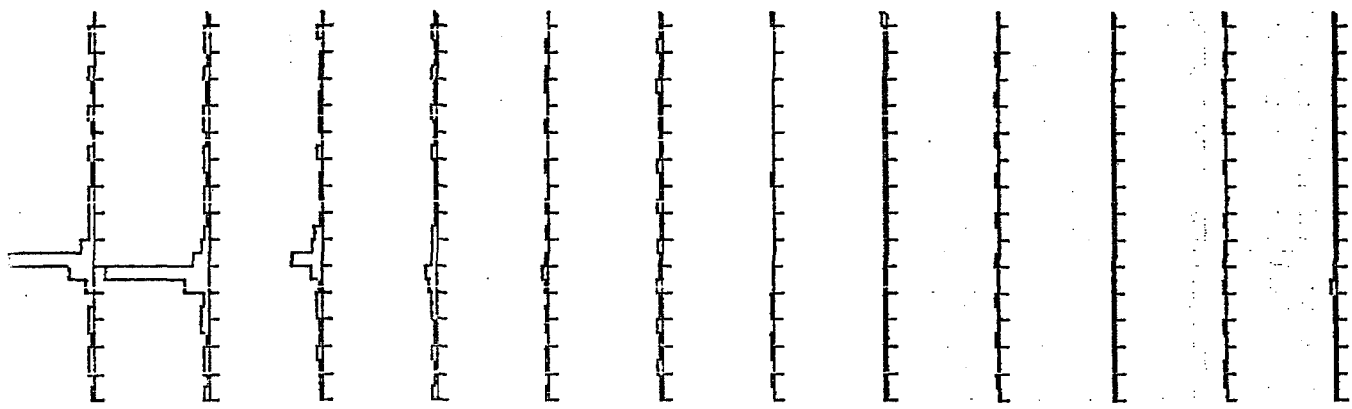
figure 8

EXP 541

Y



X



SF 10

LK 0

TR 32

LC 0

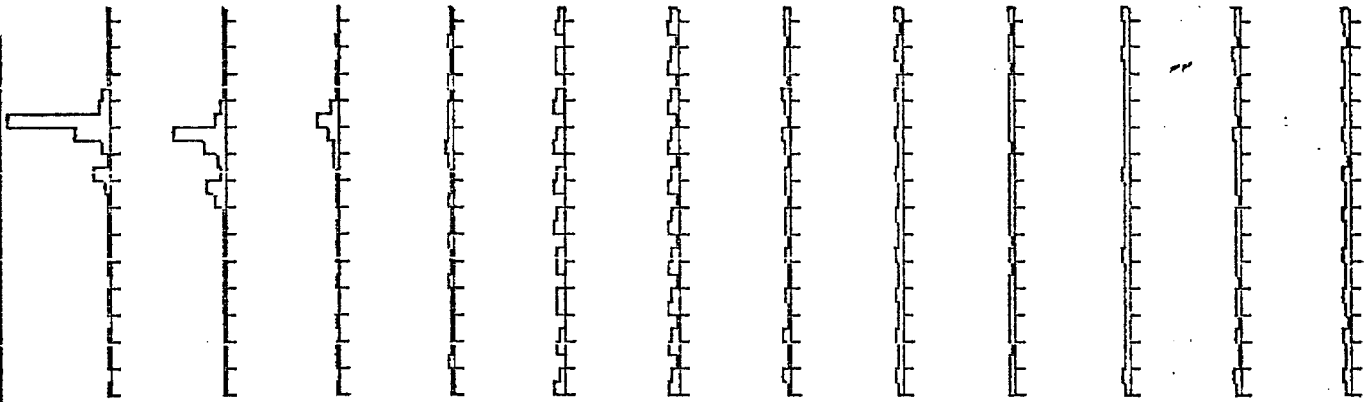
30 April 1978

30 GeV ELECTRON

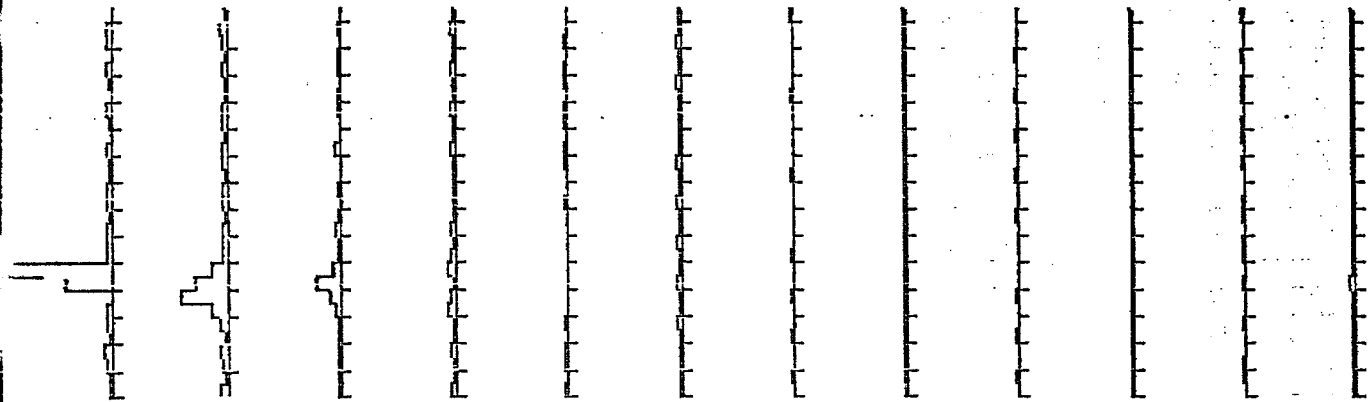
figure 9

EXP 541

Y



X



SF 10

LK 0

TR 32

LC 0

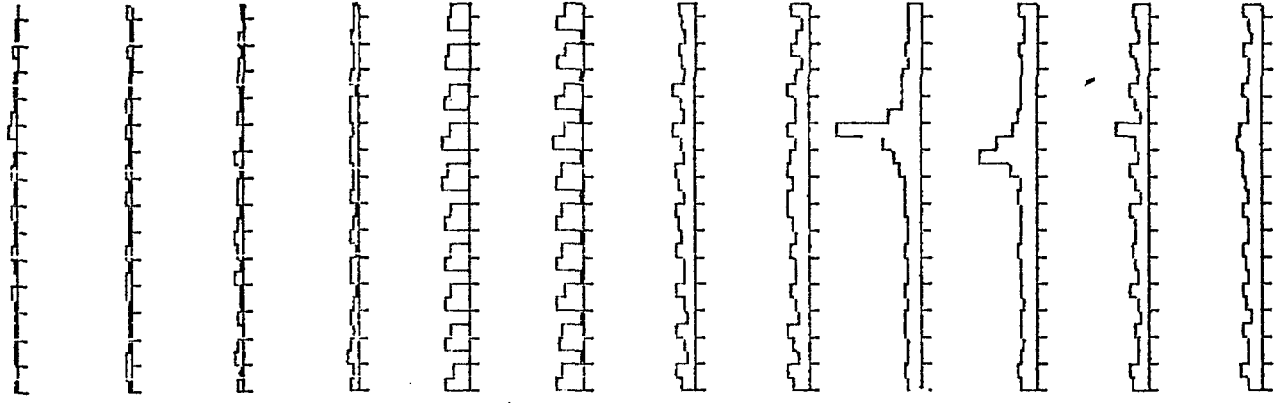
30 April 1978

30 GeV ELECTRON

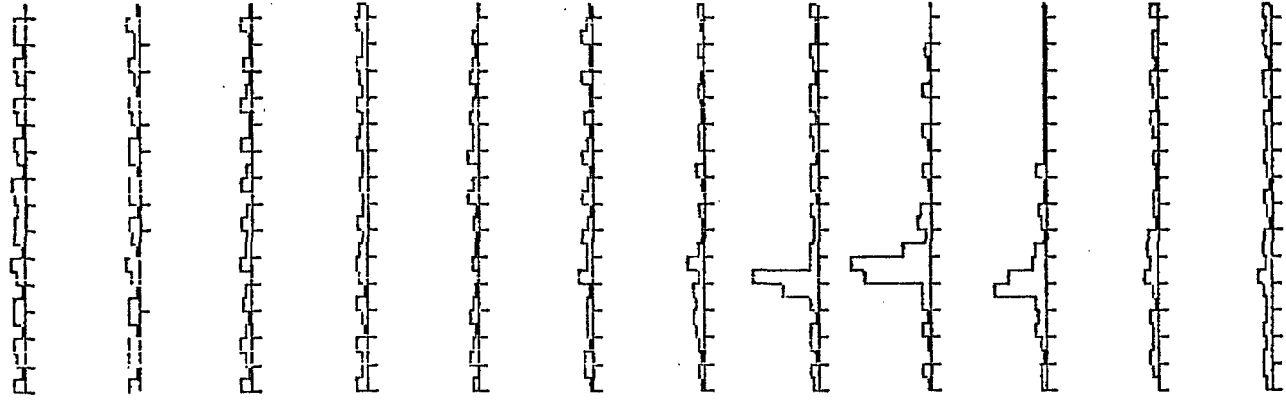
figure 10

EXP 54

Y



X



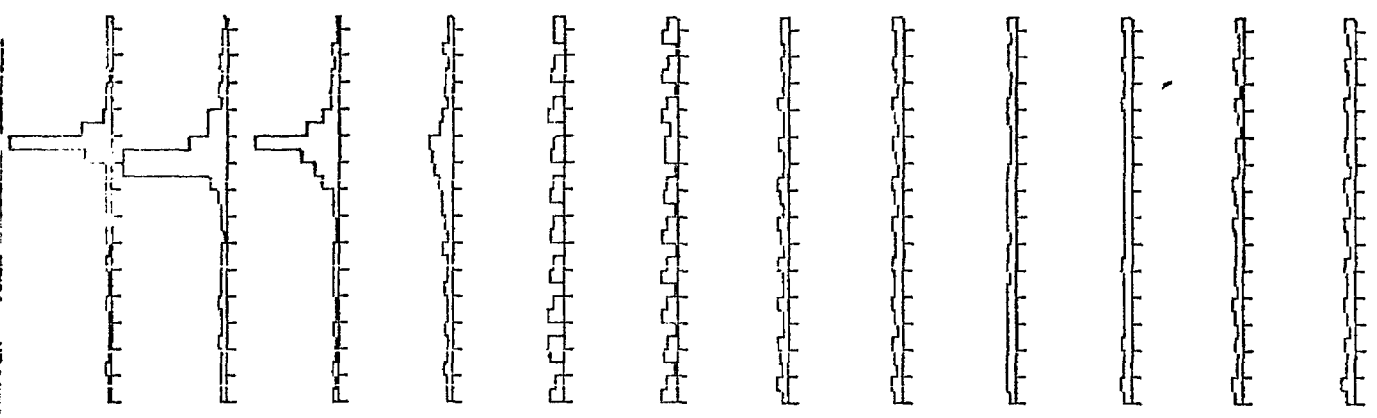
30 GeV HADRON

figure 11

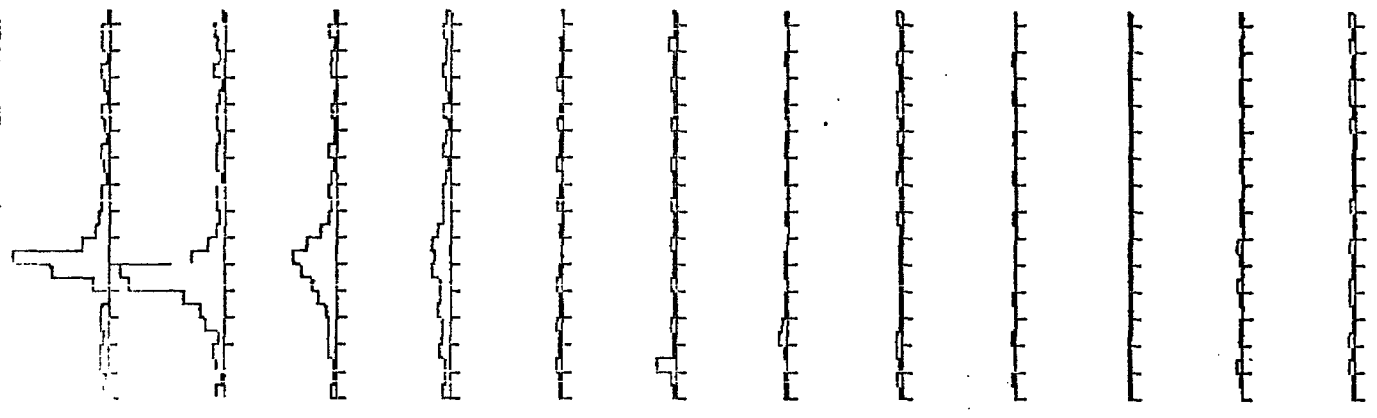
EXP 541

30 GeV

Y



X



EF 7

LR 0

TR 9E

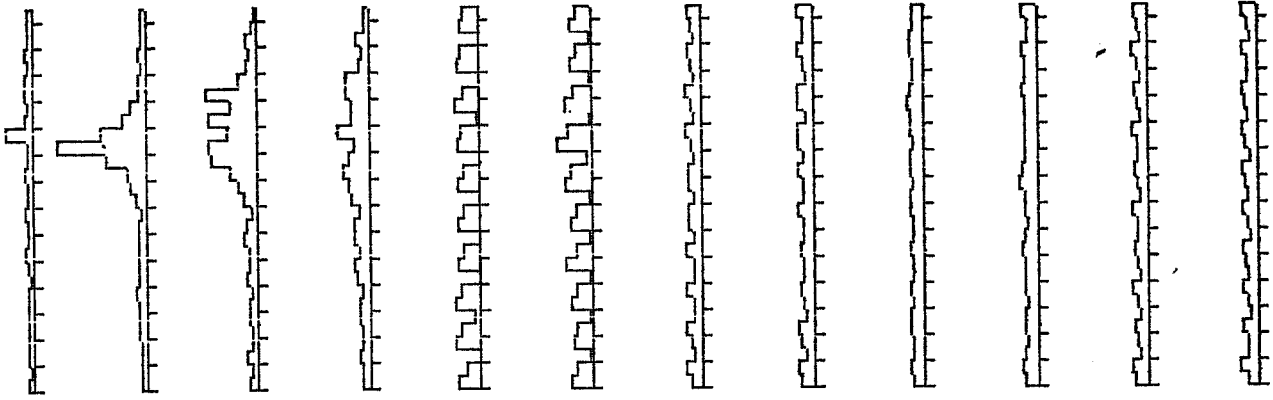
LC 0

30 GeV HADRON

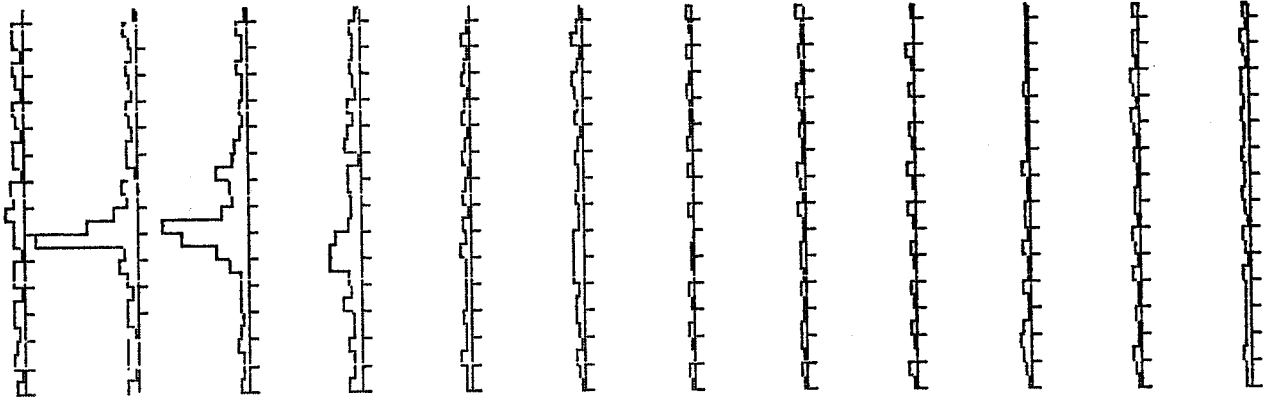
figure 12

EXP 541

Y



X



SF S
LK O

TR S
LO O

1 May 1978

40 GeV HADRON

figure 13

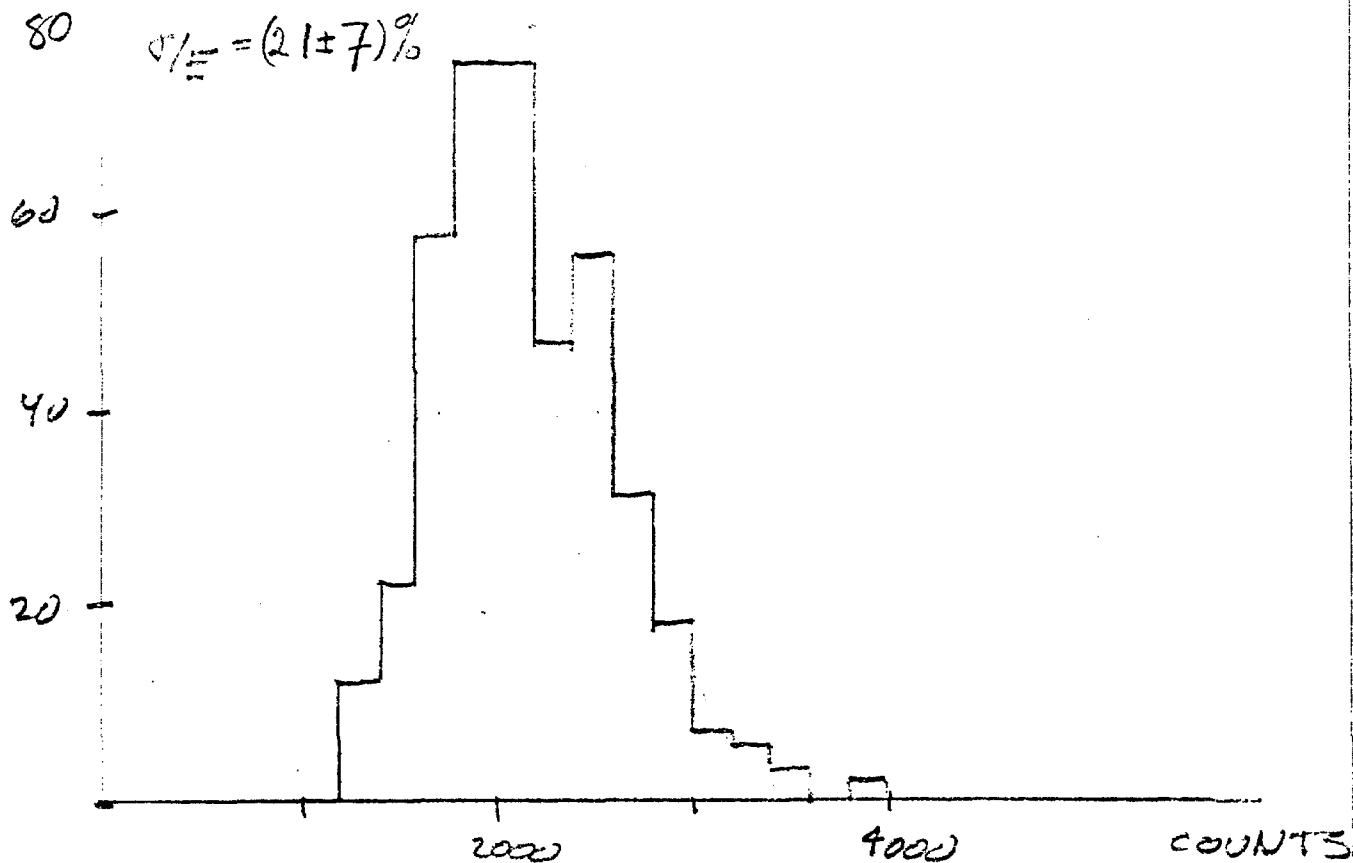
HADRONS AT 10 GEV/C

$$E(\text{MEAN}) = 2200 \pm 400 \text{ COUNTS}$$

$$FWHM = 1100 \pm 300 \text{ COUNTS}$$

$$\text{Equivalent } C = 466 \pm 127 \text{ COUNTS}$$

$$\sigma/\mu = (21 \pm 7)\%$$



TOTAL (ADC-PEDestal)

figure 14a

HADRONS AT 20 GeV/c

$$E(\text{MEAN}) = 3500 \pm 400 \text{ COUNTS}$$

$$\text{FWHM} = 1700 \pm 400 \text{ COUNTS}$$

$$80 - \text{Equivalent } \sigma = 720 \pm 167 \text{ COUNTS}$$

$$\sigma/E = (21 \pm 5)\%$$

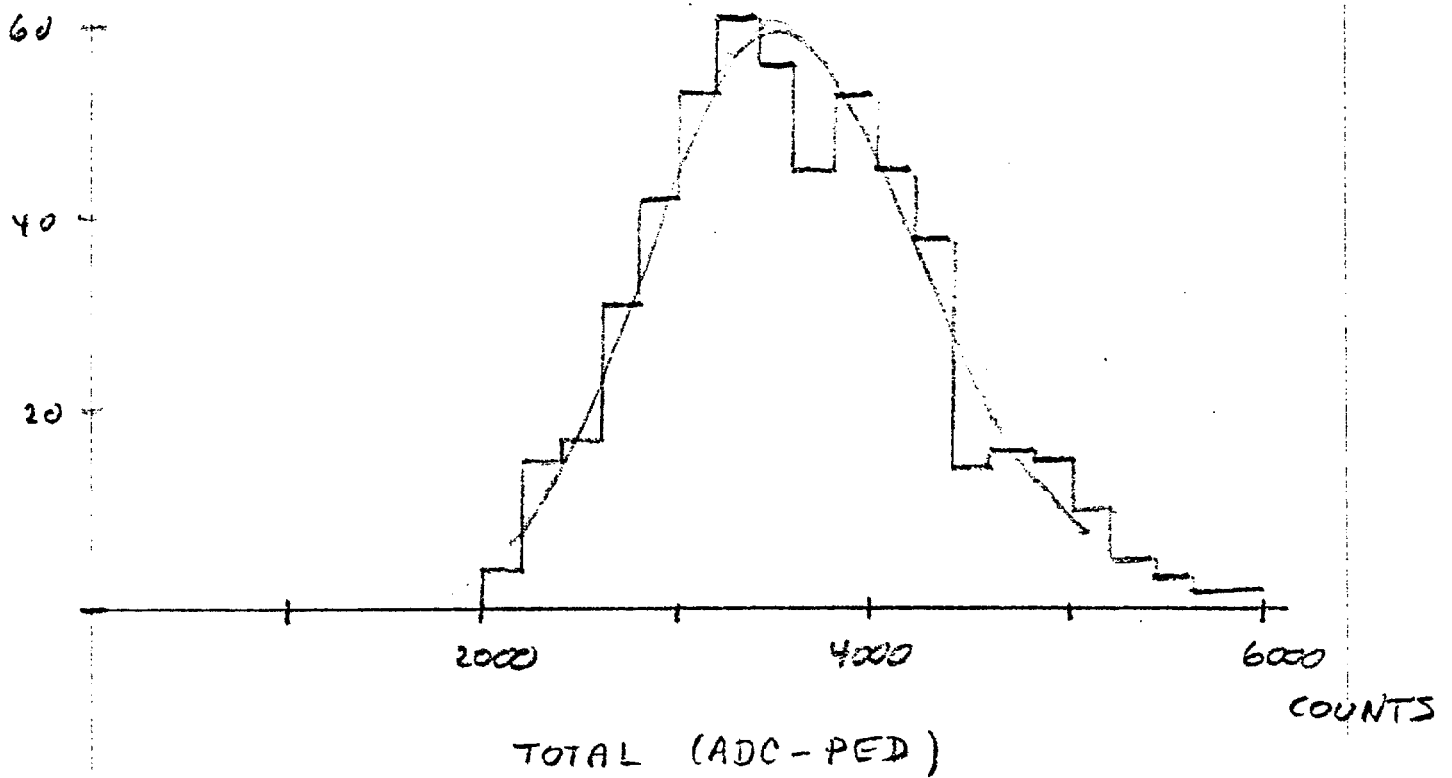


figure 14b

HADRONS AT 30 GEV/c

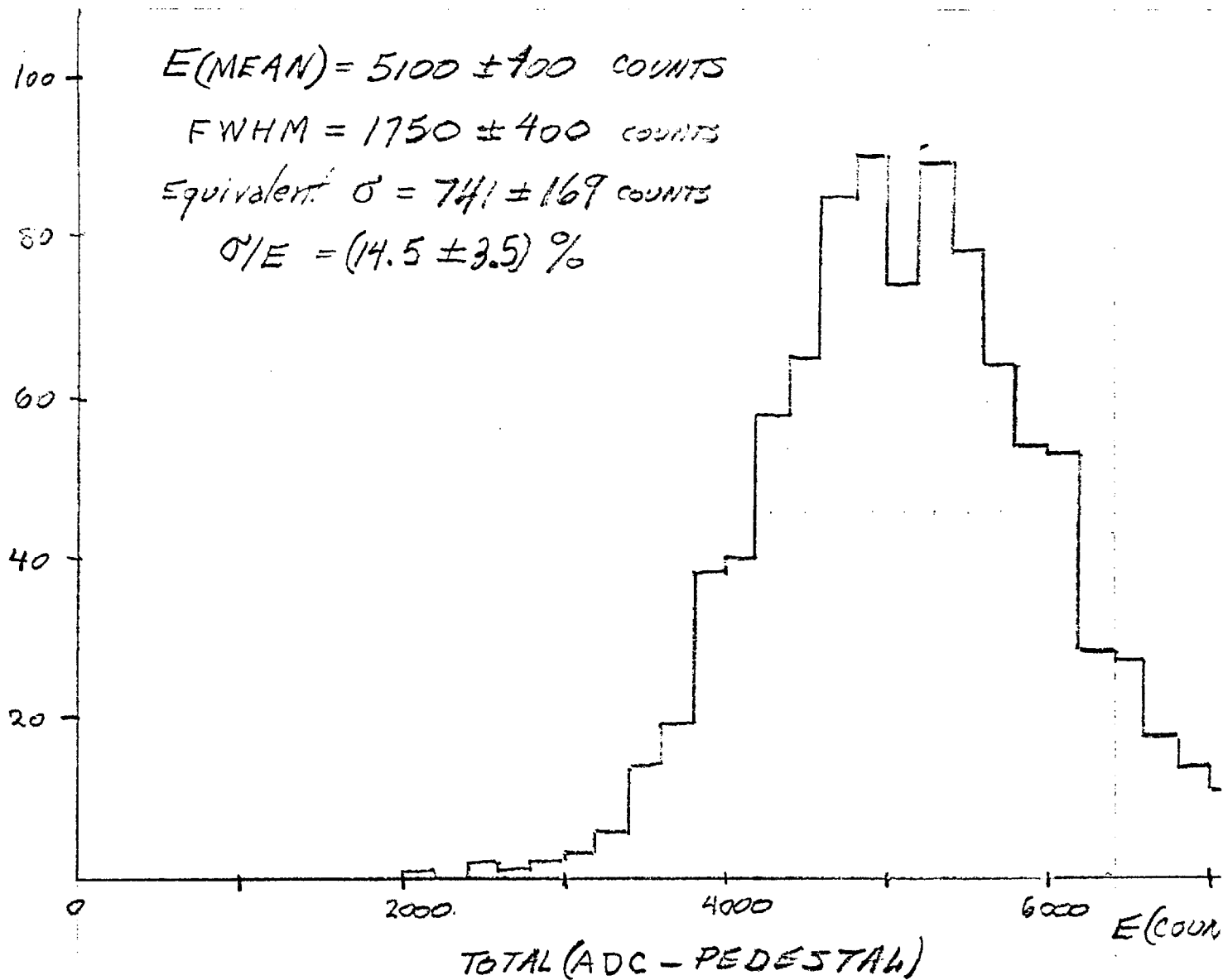


figure 14c

HADRONS AT 40 GeV

$$E(\text{MEAN}) = 6100 \pm 500 \text{ COUNTS}$$

$$\text{FWHM} = 2200 \pm 400 \text{ COUNTS}$$

$$80 - \text{Equivalent } \sigma = 932 \pm 170 \text{ COUNTS}$$

$$\sigma/E = (15 \pm 3)\%$$

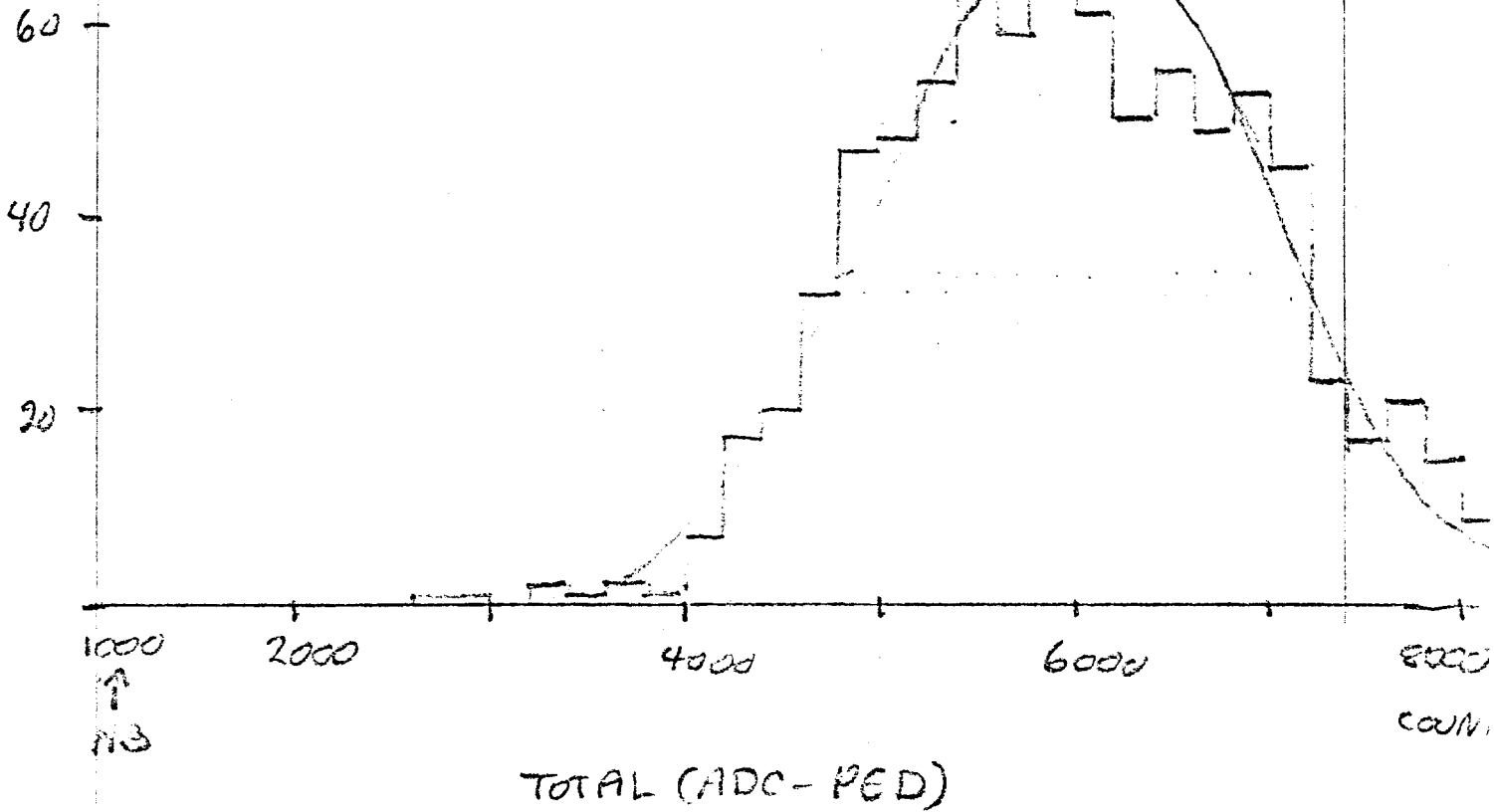


figure 14d

FROM CAL Ø27 - 8000 TRIG.

HADRONS AT 10 GEV/c

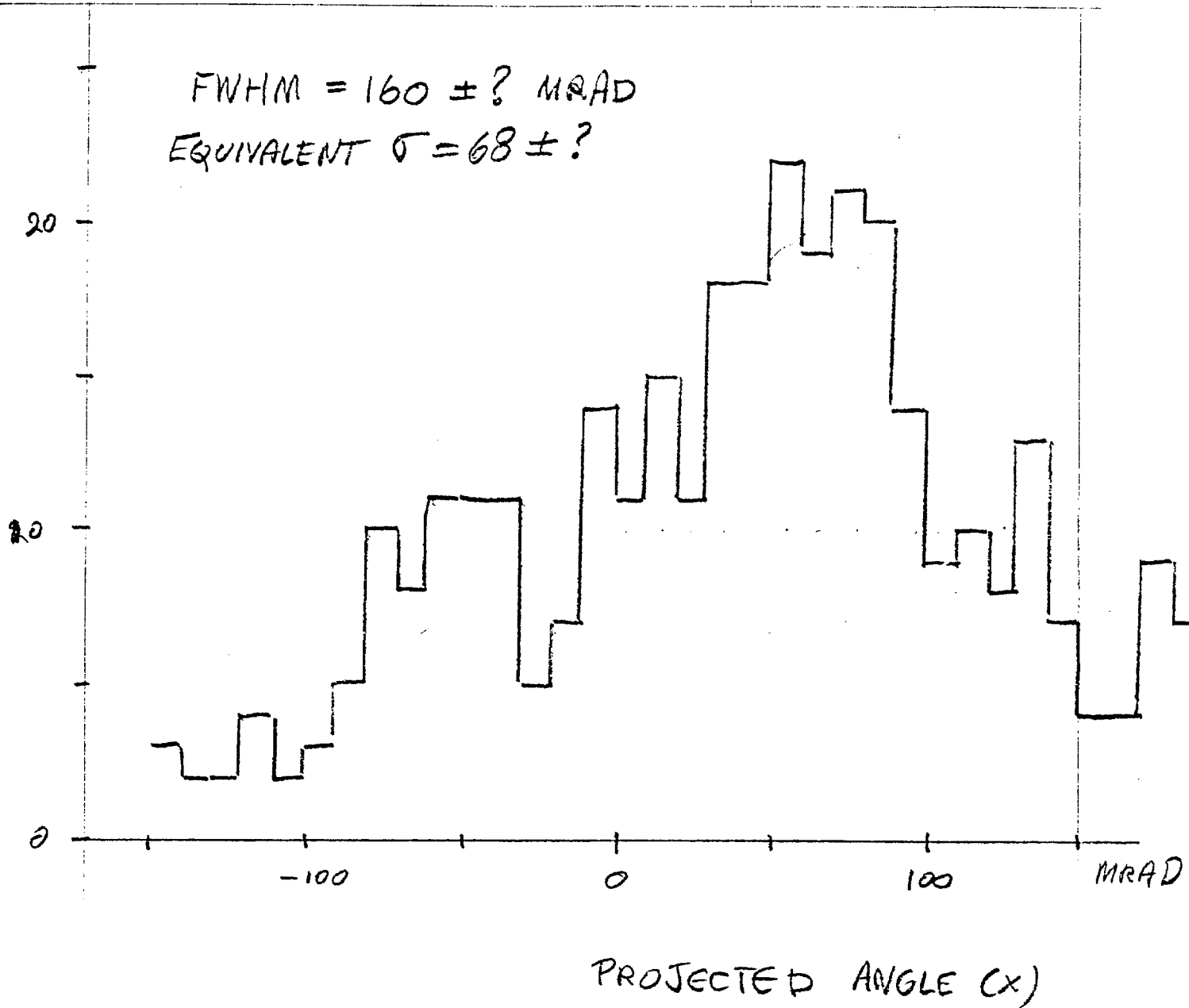


figure 15a

HADRONS AT 20 GEV/C

FWHM = 135 ± 40 MRAD

Equivalent $\sigma = 57 \pm 17$ MRAD

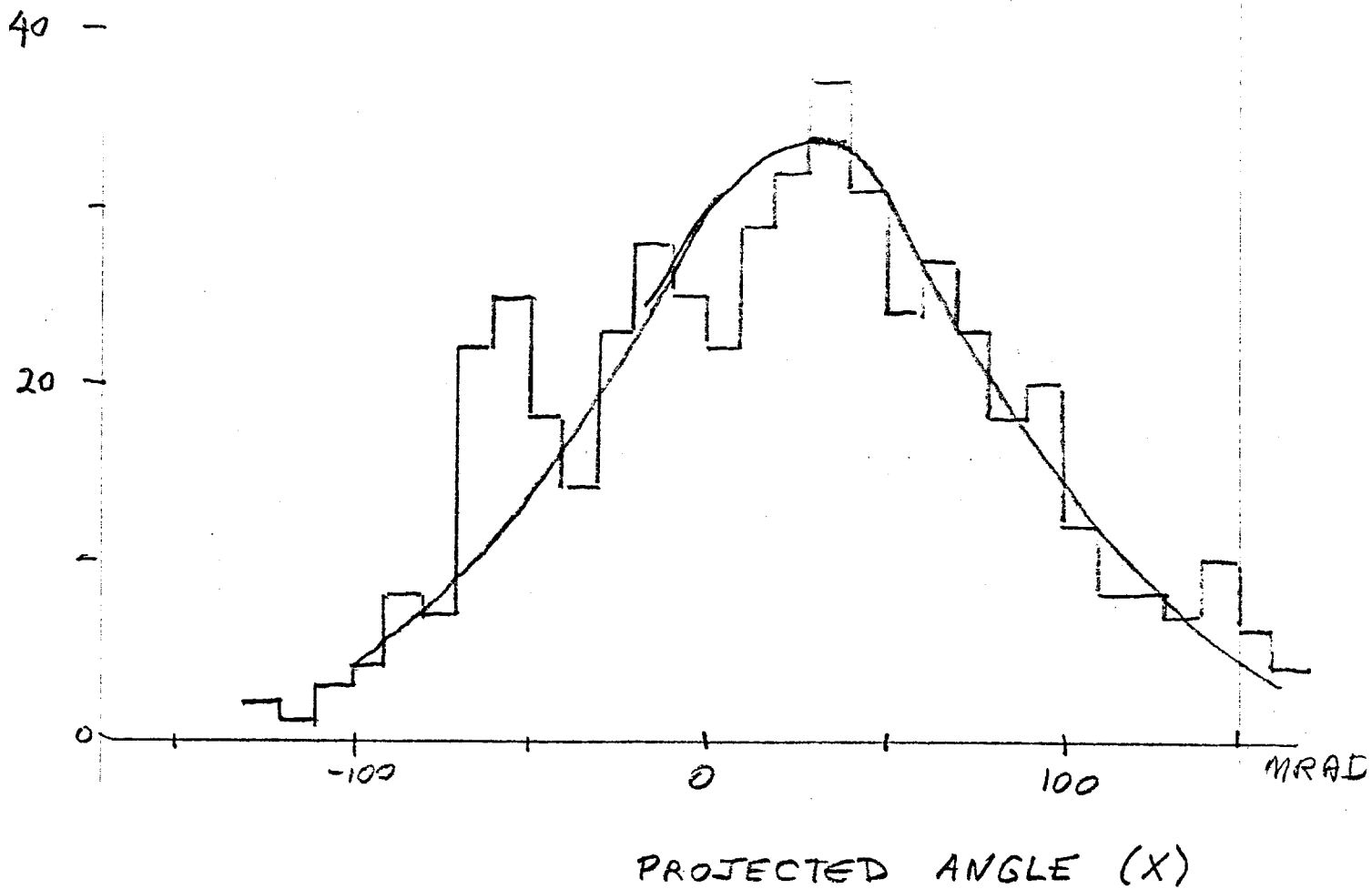


figure 15b

HADRONS AT 30 GEV

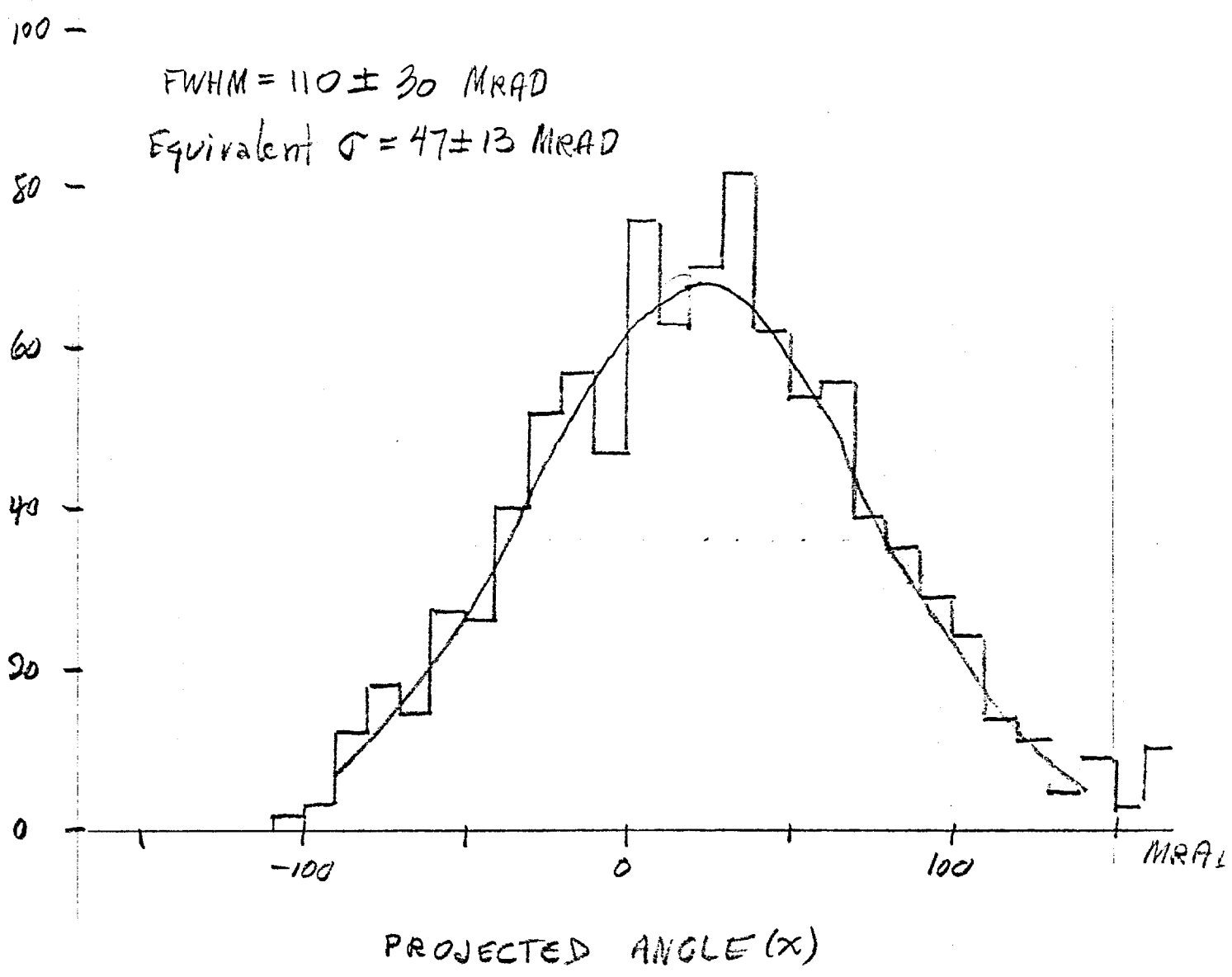


figure 15c

HADRONS AT 40 GeV/c

FWHM = 95 ± 20 MRAD
EQUIVALENT $\sigma = 40 \pm 8$ MRAD

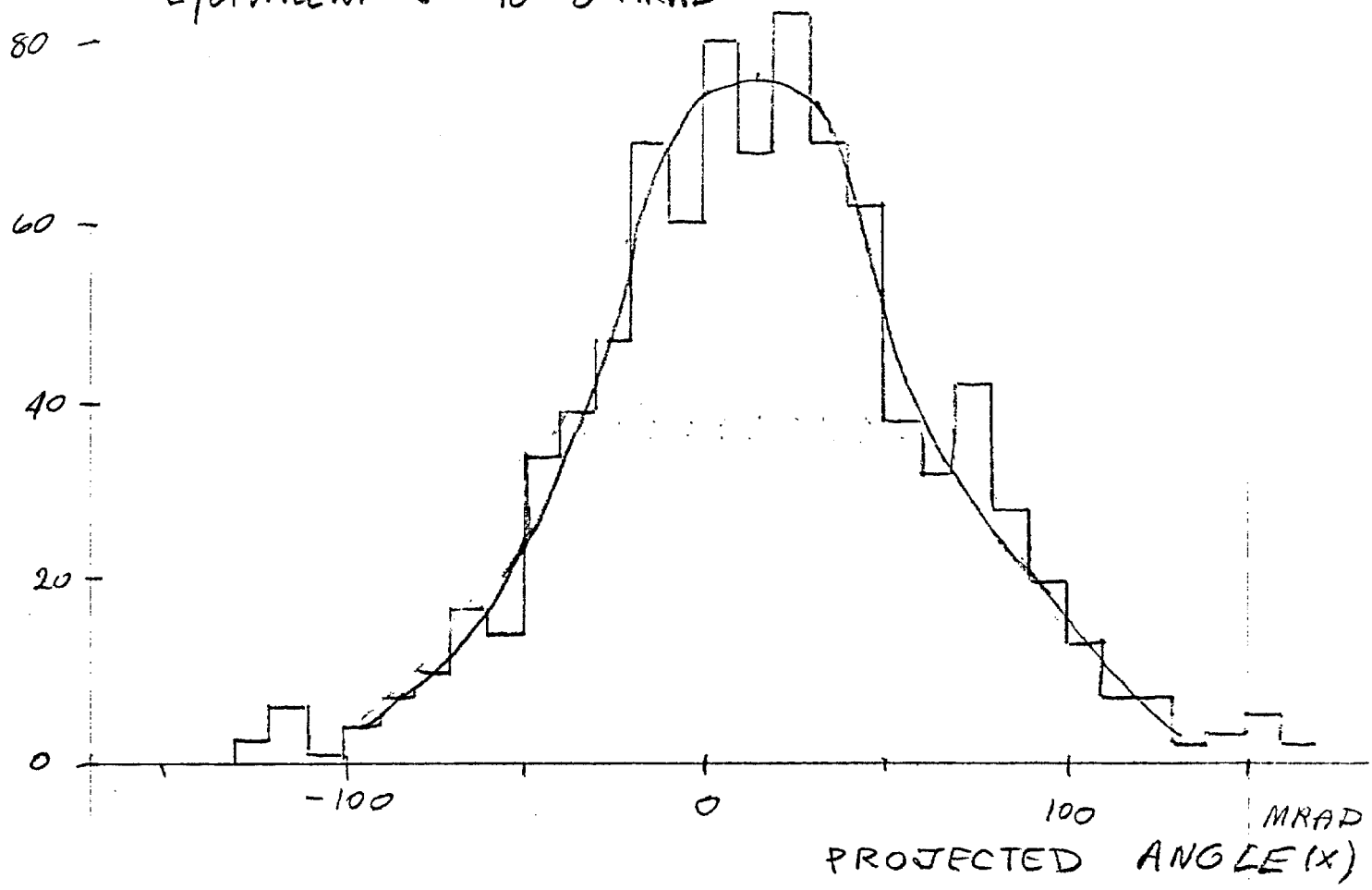


figure 15d

MUONS AT 30 GEV/c

FWHM = 25 ± 5 MRAD
Equivalent $\sigma = 11 \pm 2$ MRAD

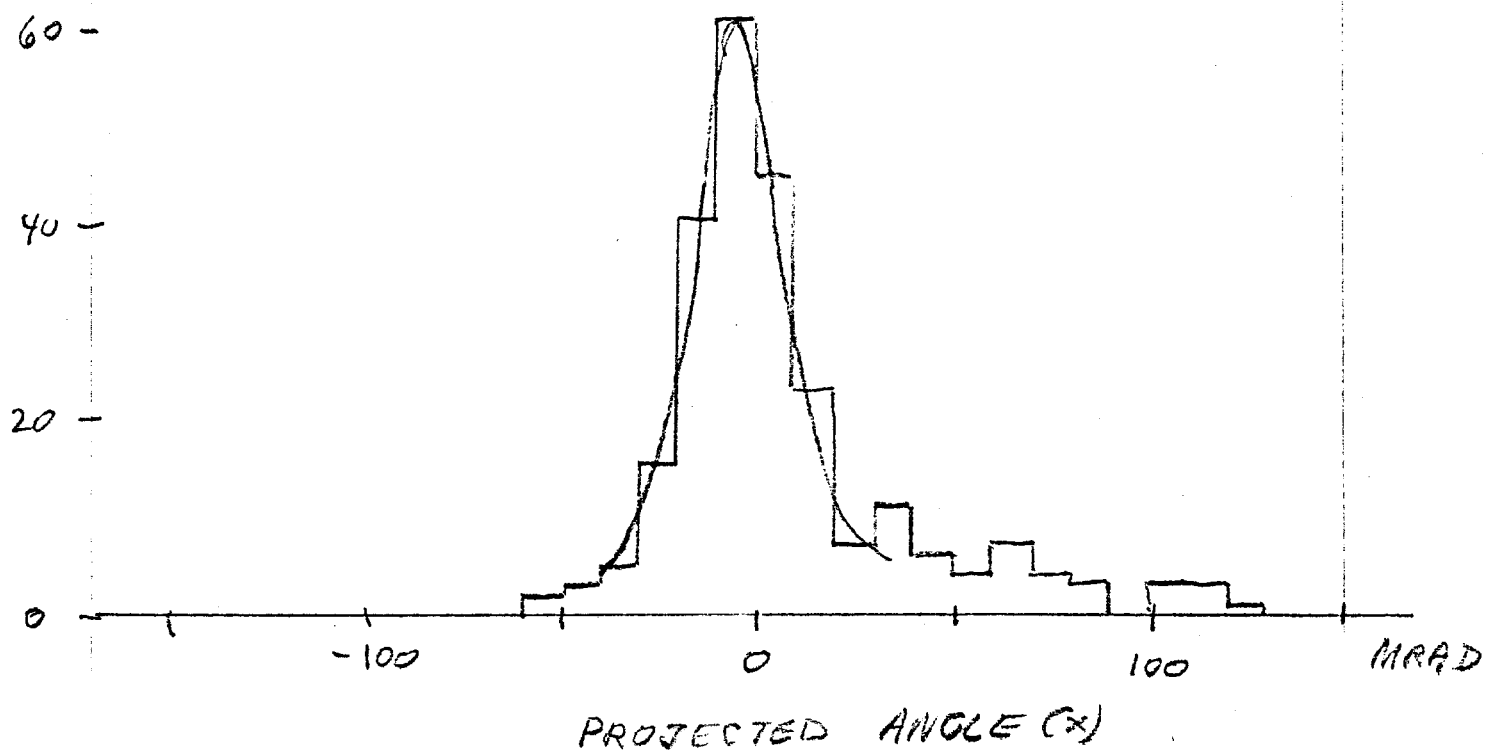


figure 15e

HADRONS

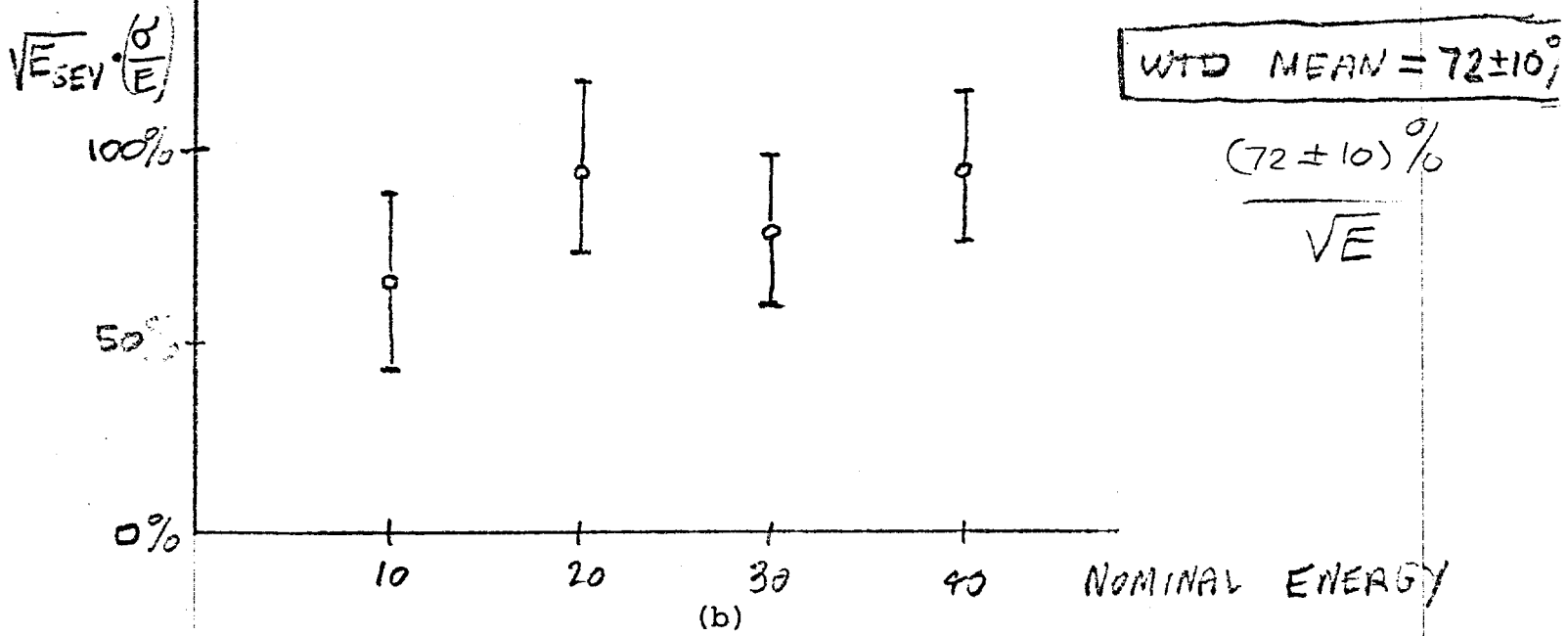
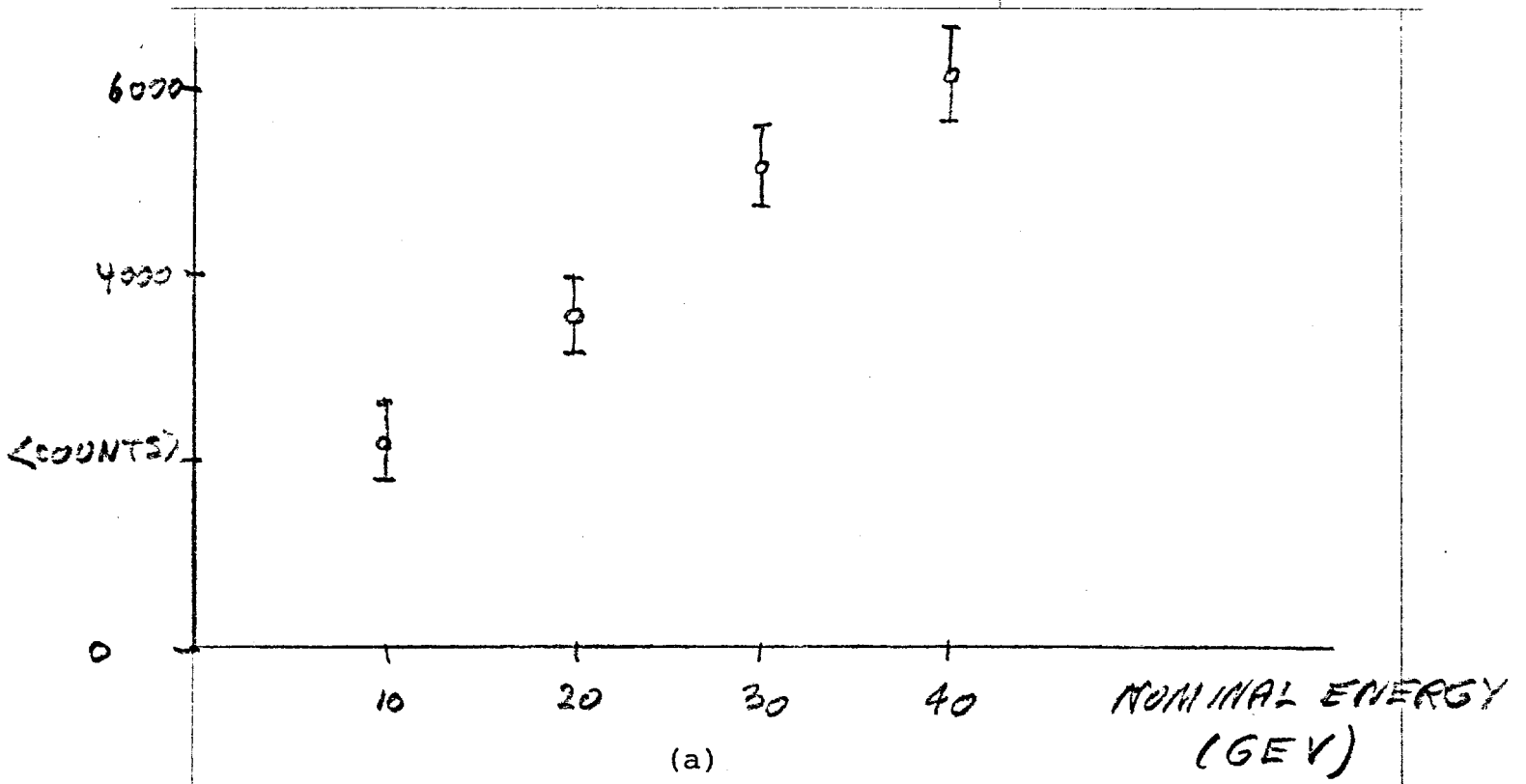


figure 16

References

- ¹A. L. Sessoms, *et al.*, to be published.
- ²W. J. Willis and V. Radeka, *NIM* 120, 221 (1974).
- ³C. W. Fabjan, *et al.*, "Iron Liquid Argon and Uranium Liquid Argon Calorimeters for Hadron Energy Measurement," CERN preprint, September 1976.

Appendix

Total cost of 960 channels of LARC electronics, including spare parts.

I. Parts

<u>Order no.</u>	<u>Company</u>	<u>Cost</u>
K17943	Gerber	73.20
K17940	Sterling	839.20
K17941	Sterling	682.65
K17942	Cramer	700.00
K17939	Cramer	501.00
K17945	H. Avnet	36.00
K17946	T.I. Supply	469.65
K18602	Impact Sales	771.80
K18606	Marshall	55.00
K18608	Appollo-Vera	78.62
K22201	T.I. Supply	62.75
K23408	Restart	530.00
K23409	Rogers	209.00
K50806	Sterling	444.30
K50803	Ferroxcube	70.00
K50810	T.I. Supply	145.60
K50812	Cramer	277.00
K50813	R.C. Component	96.00
K50820	Schweber	111.00
K50819	Impact Sales	135.00
K27306	Cramer	31.00
K27363	Cramer	178.00
K25193 (PC Boards)	Electrosonics	1400.25

II. Assembly

K27373	Whittman	<u>2370.00</u>
--------	----------	----------------

960 channels: cost/channel 10.69

III. Analog to Digital Converters

3-LeCroy 2259A at 1850/apiece	<u>5550.00</u>
-------------------------------	----------------

720 channels: cost/channel 7.71

TOTAL 18.40/channel

IV. Power Supplies

K71154	Lambda	583.00
	(other supplies on hand)	<u>800.00</u>

720 channels: cost/channel 1.92

Total Cost per Channel (includes labor, power supplies,
connectors, cables, and spare parts):

\$20.32

A LIQUID ARGON/IRON HADRON CALORIMETER

A. Strominger, A. L. Sessoms, E. S. Sadowski, M. Robbins and L. Holcomb

High Energy Physics Laboratory
Harvard University
42 Oxford Street
Cambridge, Massachusetts 02138

Abstract

We have built a liquid argon/iron calorimeter that will serve as a prototype for an instrument that will be used in an experiment at Fermilab. This calorimeter allows measurements of the direction of the hadronic shower, as well as its energy, to be made. The calorimeter is approximately 685 gms/cm^2 thick and so sufficient to contain hadron energies up to 150 GeV. Various design features of the system are discussed.

Presented at the
1977 Nuclear Science Symposium
October 19-21, 1977
San Francisco, California

To be published in
IEEE Transactions

We have built a liquid argon/iron hadron calorimeter that has the ability to measure the direction of a shower induced by hadronic matter, as well as its energy.

The resolution of calorimetric devices is limited by the fluctuations in the measured quantity, the distribution of charge deposited in traversing material, this generally taking the form of ionization loss by the shower particles. We list a few fluctuations specifically:¹

1) Sampling fluctuations. These are fluctuations associated with the fact that in most calorimeters not all of the ionization is measured, but only periodically sampled. Even in those detectors which use a homogeneously sensitive detector, dead regions in the absorber are unavoidable and therefore may contribute to a fluctuation of this type.

2) Noise. This includes effects of photon statistics in scintillation detectors, amplifier noise, and signal distortions due to slow neutrons from previous events or pile-up of events occurring within the time resolution of the detector.

3) Fluctuations due to non-uniform response. This effect would be absent in an ideal detector, but many calorimeters which have actually been built clearly suffered to some degree from this effect. We include here such effects as the non-uniform response across a given section of the detector, and different responses due to errors in calibration between different sections of the detector.

To try and minimize these fluctuations and to also have a large mass,

high density device we settled on the iron/liquid argon combination because of the:

- a) very small sampling step
- b) uniformity of response
- c) availability of low noise amplifiers
- d) high average density (4.17 gms/cm^3)
- e) low cost per unit mass.

At high energies most ($\sim 60\%$, at 100 GeV) of the energy in a hadronic shower ends up in the form of electromagnetic energy. In order to measure the direction of a shower, then, one must sample the profile of the shower in a step that is matched to an average radiation length in the material of the calorimeter. This measurement, made at several points along the shower length, allows its direction to be determined. This is done by fitting to the profile and finding its centroid, and then drawing a straight line through the (at least 5) centroids found, at least a couple of which are at the peak of the shower. Since the shower length depends on its energy, the profile must be sampled fairly often.

Our design consists of alternating solid (high voltage) iron plates, 3 mm thick, a 4 mm deep liquid argon gap, followed by steel strips, 3 mm thick and 2 cm wide, at ground potential. This is repeated throughout the device with strips of horizontal and vertical orientation alternating with each other. The configuration is shown schematically in Figure 1.

The calorimeter is made up of 40 modules, one of which is shown in Figure 2. The steel plates and strips are electroplated with approximately

10 microns of copper. This assures surface cleanliness and a good surface on which to make solder connections. This is crucial since all electrical connections to, and among, the strips and plates are solder connections. The strips and plates are separated by G-10 spacers 4 mm deep \times 1 cm \times 50 cm. These spacers are notched as shown so that the strips can be cemented in place with a 1 mm spacing between them. This space is necessary in order to minimize the cross coupling between strips.

The spacer is attached to the plates and strips with CREST 7410 cryogenic epoxy (manufactured by CREST Products Corporation, Santa Ana, California). This epoxy has excellent properties and can be relied upon to hold under the stresses of cool down to, and operation at, liquid argon temperatures.

The modules are placed in a support structure made of an aluminum egg crate type substructure and a G-10 superstructure. This is shown in Figure 3. The strips are ganged together in groups of 5 and coupled to the amplifiers through low inductance 30 conductor ribbon cable, each signal wire alternating with a ground wire. The "X" cables are shown on top of the module assembly shown in Figure 3. The two slots in the module assembly will hold two scintillation counters that serve as trigger counters. We have found that slow cool down to liquid argon temperatures does not affect the performance of the scintillator; the counters are wrapped in thin aluminum foil to maintain high collection efficiency.

The module assembly sits in a double walled vacuum insulated dewar to cut heat loss to a minimum. The cables are fed through a copper cooling shroud which is cooled by liquid nitrogen and thus serves as a heat sink.

The level of argon is monitored by a parallel plate capacitor and several resistors, and the temperature is monitored by a thermometer that is accurate to 0.1°C in this temperature range (manufactured by Omega Engineering, Inc. Stamford, Connecticut).

The cables, liquid nitrogen and argon, and gaseous argon and vacuum assembly are brought out through stainless steel flanges. The electronics are mounted on the outer dewar, and the flange.

The module assembly fits into the inner dewar as shown schematically in Figure 4. This whole assembly fits into the outer dewar in a similar fashion. The separation between the inner and outer dewar is evacuated and superinsulated.

A block diagram of the electronics is given in Figure 5. Briefly a trigger is generated by scintillation counters which starts the central circuitry. Signal G_1 is generated which opens a switch that allows integrate and hold circuits to collect charge from the calorimeter. At a later time signal G_2 is generated which decouples the amplifier from the integrate and hold and the data are ready to be read out. The computer takes over and, through a CAMAC address module, which we call a RIRODAC, begins switching the multiplexers through the 696 channels of data which are read into 36 channels of CAMAC ADC's (LeCroy 2259A). A circuit diagram of the electronics is given in Figure 6. Details of the calorimeter are given in Table 1.

The motivation to build such a device comes from the study of neutrino induced neutral current interactions at high energies. In order to get enough events to make meaningful statements about the physics of the process a target detector of large mass and high sensitivity is necessary. We have found that a liquid argon/iron calorimeter offers these features coupled with the high reliability.

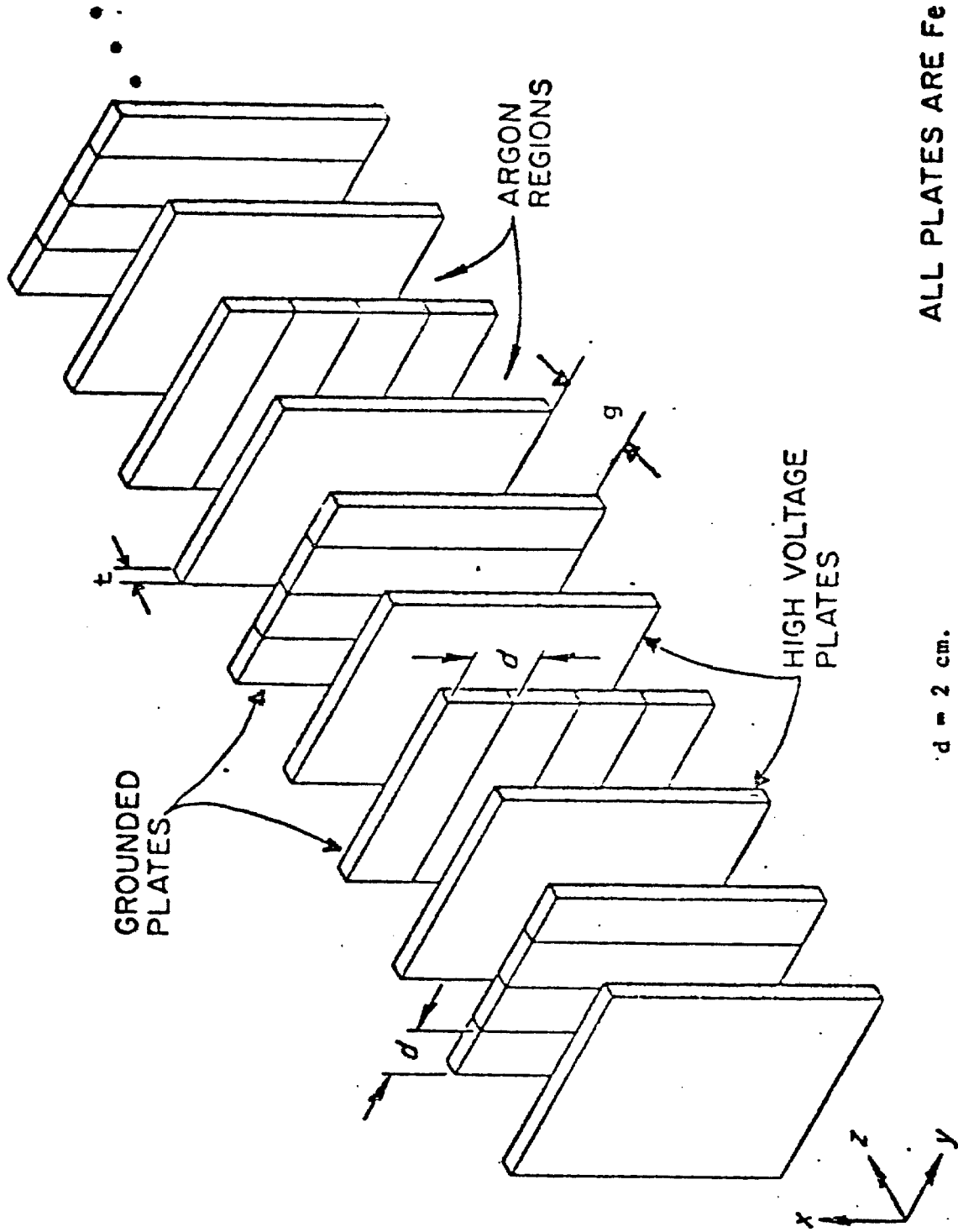
TABLE I

TEST CALORIMETER

Active dimensions	60 × 60 cm
Length	1.64 m
Sampling Step	3.0 mm iron (2.36 gm/cm ²)
Sampling Counter (Energy)	liquid argon, 4 mm thick
Sampling Counter (Angle)	liquid argon, 4 mm thick, iron plates 60 cm × 2 cm x and y, every 28 mm
Target thickness	684 gms/cm ²
Target Weight	2.7 tons
Channels of electronics	696
Average quantities	density: 4.17 gms/cm ³ radiation length: 3.52 cm interaction length: 19.0 cm

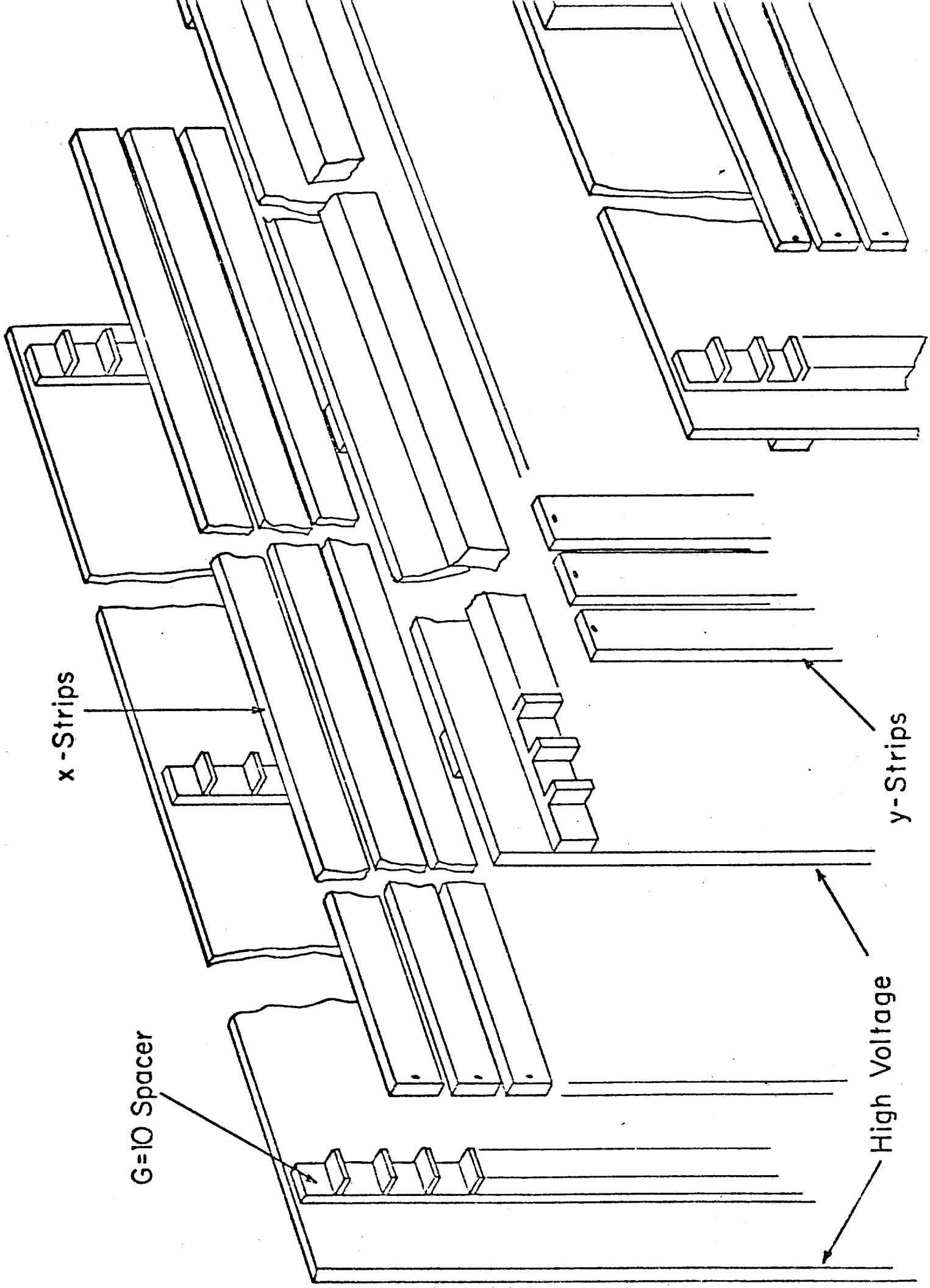
FIGURE CAPTIONS

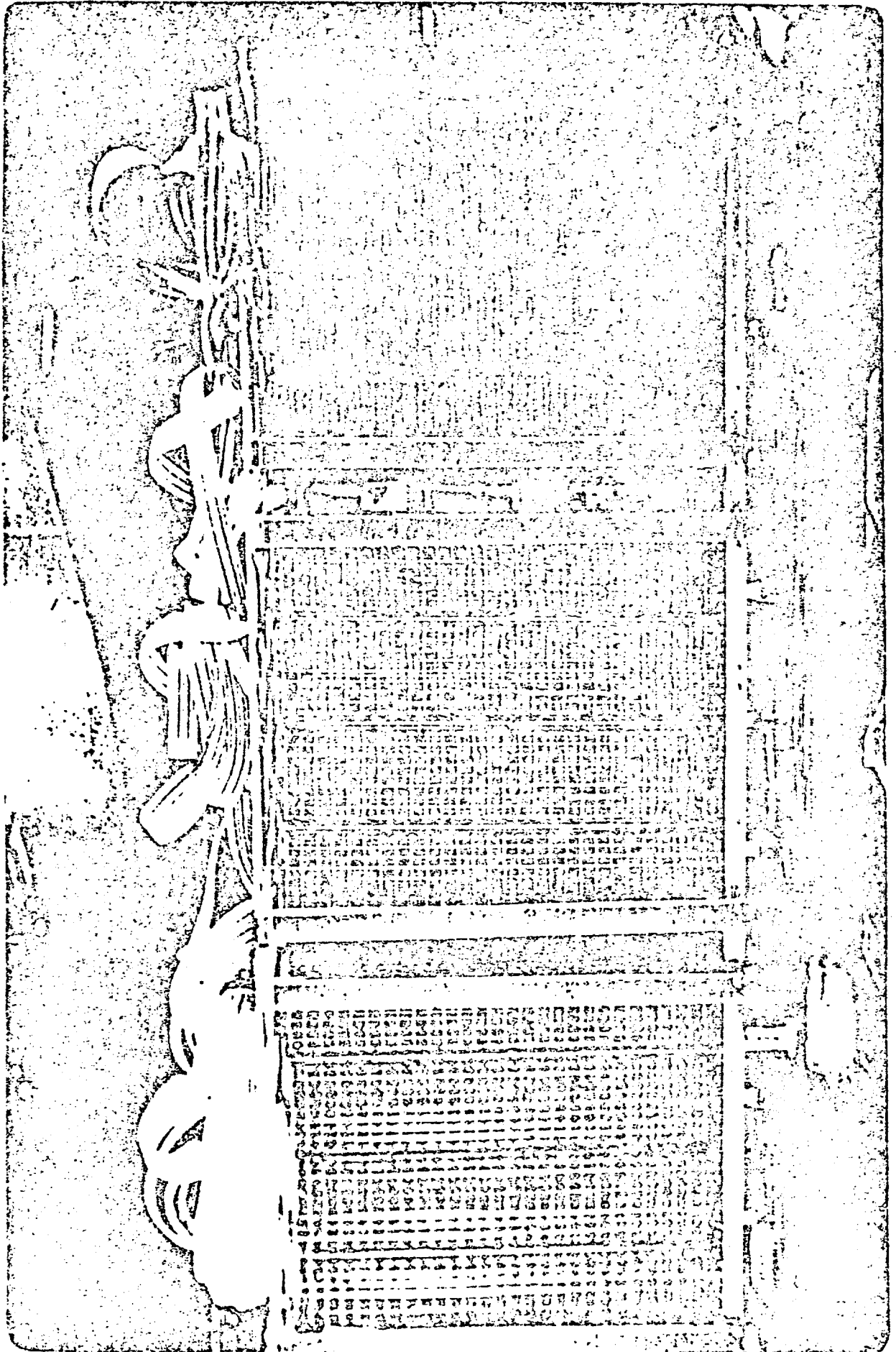
- Figure 1: Schematic diagram of the calorimeter configuration
- Figure 2: Schematic diagram of a calorimeter module
- Figure 3: Photograph of module support structure with modules and X wiring completed
- Figure 4: Schematic of module assembly-inner dewar mating
- Figure 5: Block diagram of the electronics
- Figure 6: Circuit diagram of electronics



- $d = 2 \text{ cm.}$
- $g = 4 \text{ mm.}$
- $t = 3 \text{ mm.}$

Figure 1





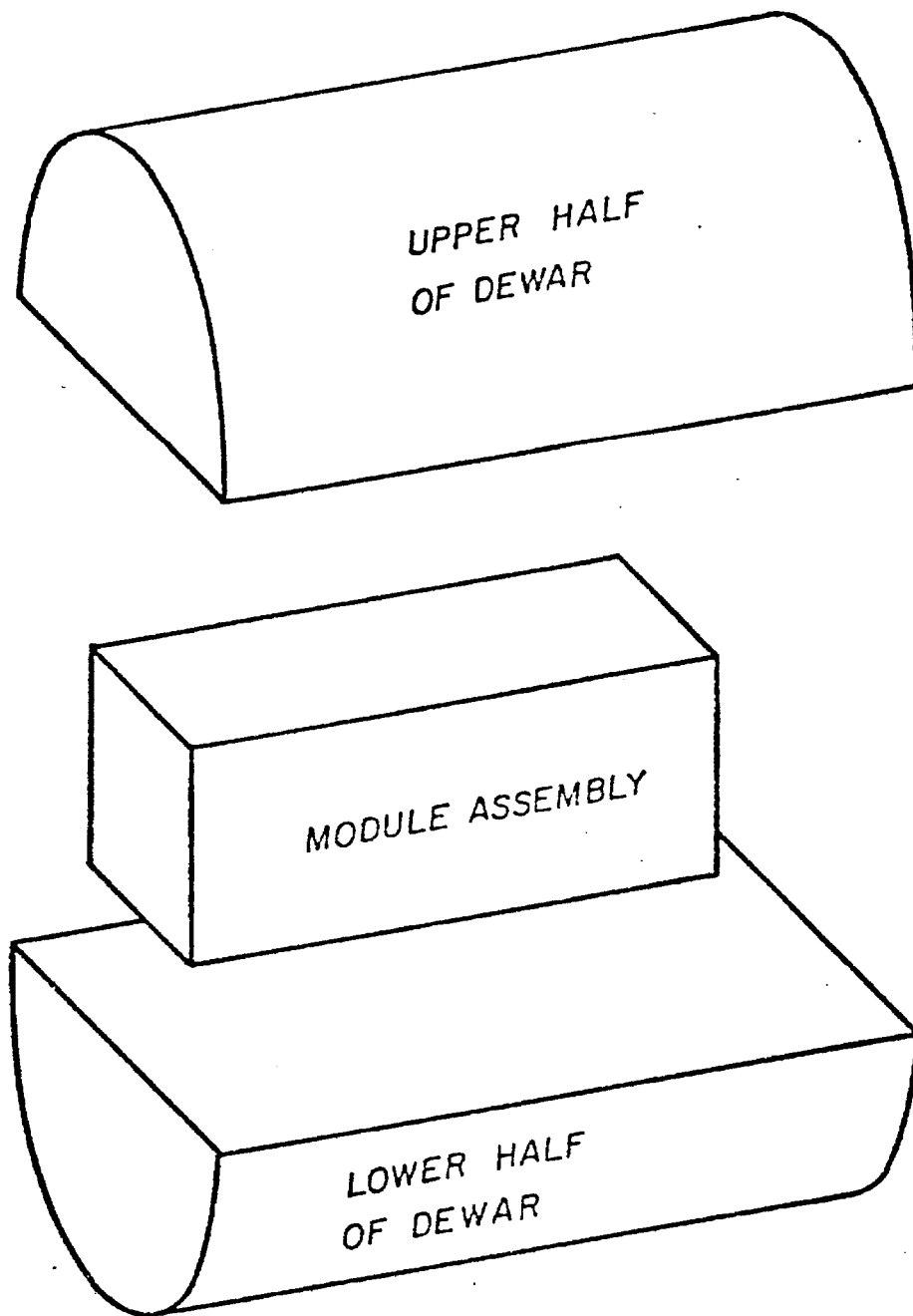


Figure 4

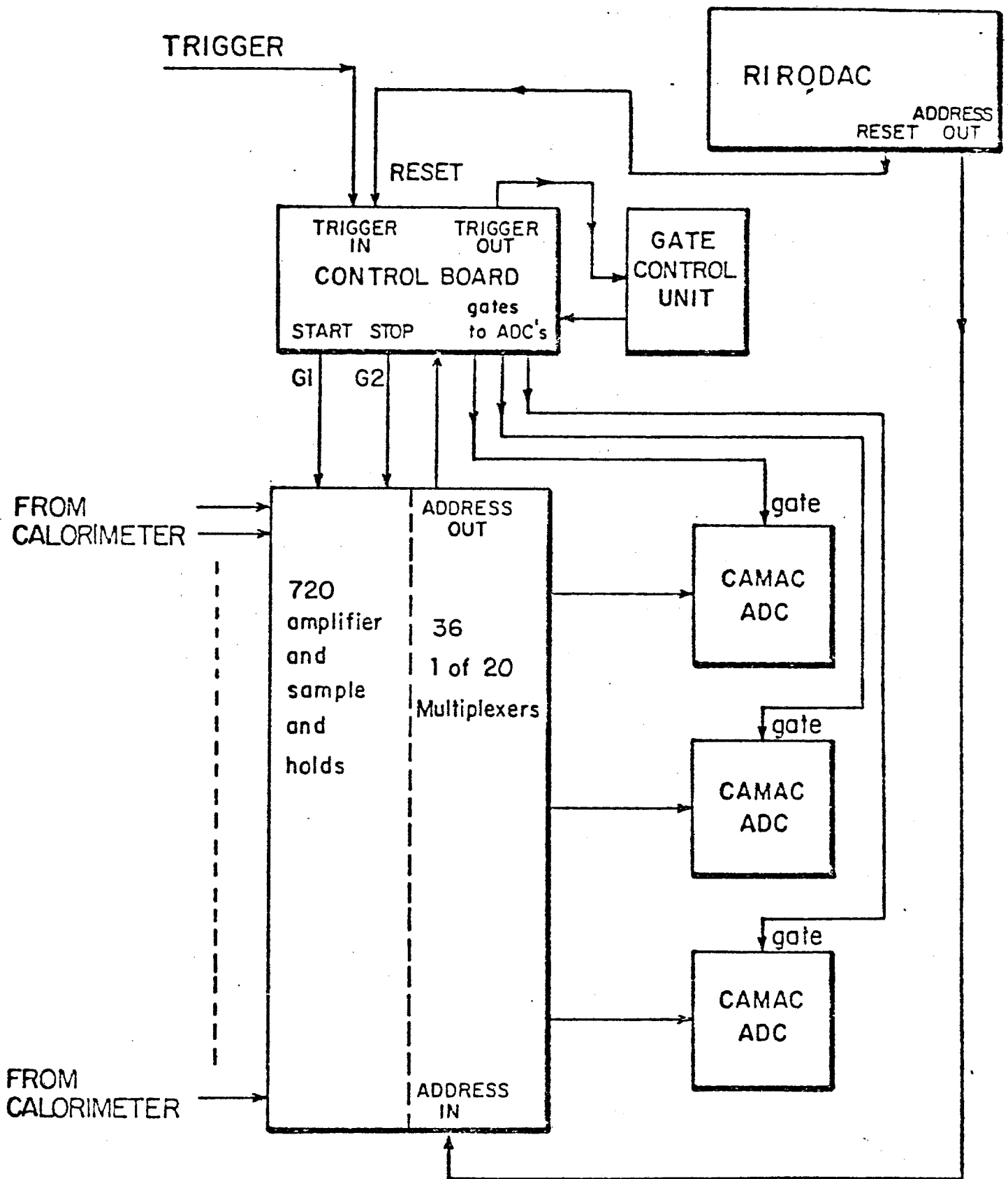
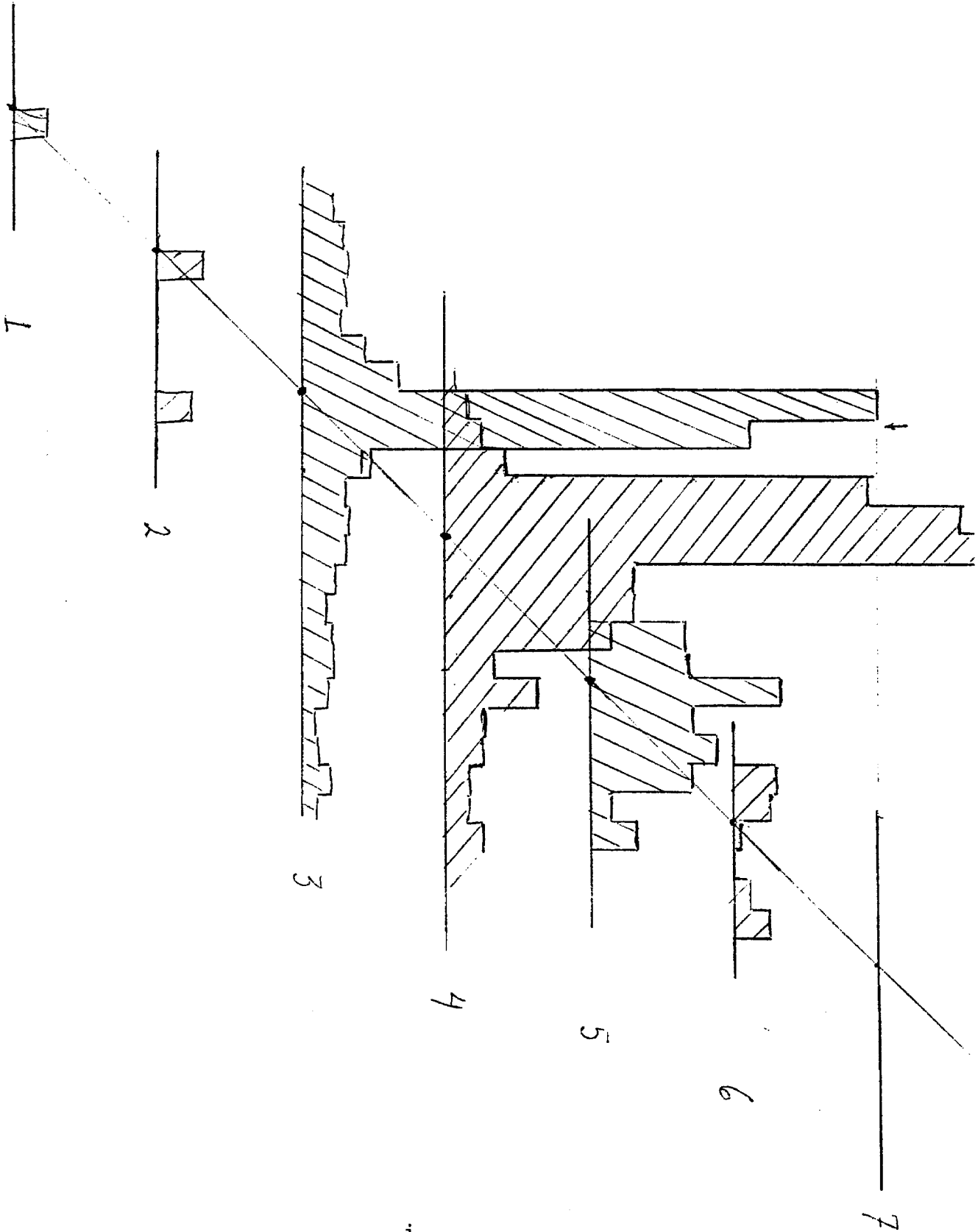


Figure 5

REFERENCES

1. W. J. Willis and V. Radeka. Nucl. Instr. and Methods 120, 221 (1974).
2. C. W. Fabjan, et al. "Iron Liquid Argon and Uranium Liquid Argon Calorimeters for Hadron Energy Measurement." CERN preprint 1976.
3. V. Radeka. IEEE Transactions in Nucl. Sci. October 1976. "High Resolution Liquid Argon Detectors, Electronic Noise and Electrode Configuration."
4. T. A. Gabriel and W. Schmidt. NIM 134, 271 (1976).
5. D. Hitlin, et al. SLAC Pub. 1761 (May 1976). "Test of a Lead Liquid Argon Shower Detecor."

8 JUNE 1978 ADDENDUM P-602



i.

"A PROPOSAL TO STUDY THE INTERACTIONS
OF NEUTRINOS AND ANTINEUTRINOS AT THE DOUBLER/SAVER"

M. Goodman
A. L. Sessoms
Harvard University

S. C. Wright
University of Chicago

B. Eisenstein
L. E. Holloway
W. T. Wroblecka
University of Illinois

T. Coffin
B. Roe
University of Michigan

(CHIM Collaboration)

Spokesman: A. L. Sessoms
Physics Department
Harvard University
Cambridge, MA 02138
(617) 495-3388

Summary

We have determined values for the angular resolution of the liquid argon/iron hadron calorimeter (LARC) using a very simple weighting scheme that does not try to enhance the centroid of the shower over the wings. More sophisticated analyses are in progress and initial indications are that the quoted resolutions will improve markedly. The 1st pass results are:

<u>E in GeV</u>	<u>σ_θ in Mrad</u>
10	59 ± 1
20	39 ± 1
30	30 ± 0.5
36	27 ± 0.5

We conclude that, for Doubler/Saver energies, no other existing or proposed detector offers resolutions or flexibility remotely comparable to the one proposed in P-602.

I. Statement of Purpose

We propose to build a detector that is explicitly designed to be used at the high neutrino and antineutrino energies that will be provided by the Energy/Doubler/Saver. At these energies the detector will provide energy and angular resolutions unmatched by any other existing or proposed device. The analog nature of this instrument and its very fine segmentation make it ideally suited for angle measurements of high energy showers. The "hot core" of hadronic showers, which gives most of the information on the direction and consists of upwards of 100 particles per 4cm^2 independent of calorimeter material, is easily dealt with in an analog manner without fear of saturation effects.

The aspect ratio of the device, long and narrow, provides an excellent match to the neutrino beam geometry provided by the Doubler/Saver. There is no "useless" tonnage as would exist in a broader, shorter detector and so the ratio of fiducial to total mass is maximized. For example in the energy range from 300-700 GeV it has about four (4) times the fiducial mass of the E-594 (Walker/Taylor) device.

It is important to note that if any new J/ψ or Upsilon type particles are produced giving rise to three muon final states the excellent acceptance and momentum resolution for muons, and the ability to track the muons back to the vertex with great accuracy, give this detector advantages over any that are coupled to iron toroid magnets. The short absorption length, 30cm, provides a much needed factor of two suppression of $\pi \rightarrow \mu$ decay over a device like E-594.

We have here a proven technology which is probably 2 to 3 years ahead in development over other proposed liquid argon devices.

Cont'd

In the short time we have had to analyze the data taken to date, we have already demonstrated many of the properties of the calorimeter, which points to the beautiful simplicity such a device offers and so the probability of small systematic biases.

The time scale for the construction of this detector is 2-1/2 to 3 years. It, therefore, fits very nicely into the time scale for construction of the Doubler/Saver. No other detector that is capable of dealing effectively with the energies and fluxes of neutrinos and antineutrinos that will be provided offers such compatibility.

This instrument is clearly a complement to existing and other proposed neutrino detectors. It will cover the high energy part of the neutrino spectrum at least as well as present detectors cover the lower energy part. It therefore fits nicely into a carefully reasoned approach to neutrino physics at Fermilab in the short and longer time scale.

II. We are proposing to pursue the following physics objectives:

1. Neutral current x and y distributions at high energies
2. Charged current x and y distributions at high energies
3. Multimuum physics

It should also be noted that we will be sensitive to asymptotic freedom effects, e.g. energy dependences of the cross sections. If these effects are well known from other sources, it is conceivable the vector boson propagator effects can be seen if the boson mass is around 70 GeV.

III. The collaboration presently consists of A.L.Sessoms and M.Goodman, Harvard University; S.C.Wright, University of Chicago; B.Eisenstein, L.E.Holloway and T.Wroblecka, University of Illinois at Urbana-Champaign; T.Coffin and B.Roe, University of Michigan.

Cont'd

IV. Design Update

We suggest adding an additional one (1) meter of drift chambers downstream of the magnet, which we now view as an air core superconducting solenoid turned on end and used as a toroid, followed by one (1) meter of iron to serve as an additional hadron filter, followed by one (1) meter of drift chambers. This increases the muon momentum measurement accuracy to about 2.3% at 100 GeV and reduces hadron punch through to less than the probability for hadron decay to muons in flight (See Fig. 1).

V. Data

The data were taken in far from ideal conditions in the M-5 beam line. A Cerenkov Counter in the beam served to tag particles as π/μ or e and a muon counter downstream of the calorimeter (LARC) behind 3 meters of concrete separated muons from pions. The Cerenkov counter was not very efficient and so the electron contamination in the hadron sample was substantial. The following step allowed subtraction of this electron contamination, and also served to illustrate the power of this device.

It is clear from the raw data that electronic and hadronic showers are significantly different in nature. In particular hadronic showers are more diffuse, e.g. they have much larger wings. If one suppresses all channels with less than 5 minimum ionizing particles, for example, one preferentially depresses the hadrons over electrons. This is illustrated in Figures 2. Figure 2a gives the total pulse height in the calorimeter for "hadrons" with vertices identified as occurring in the first 0.45 absorption lengths of LARC. The plot is number of events versus pulse height.

Cont'd

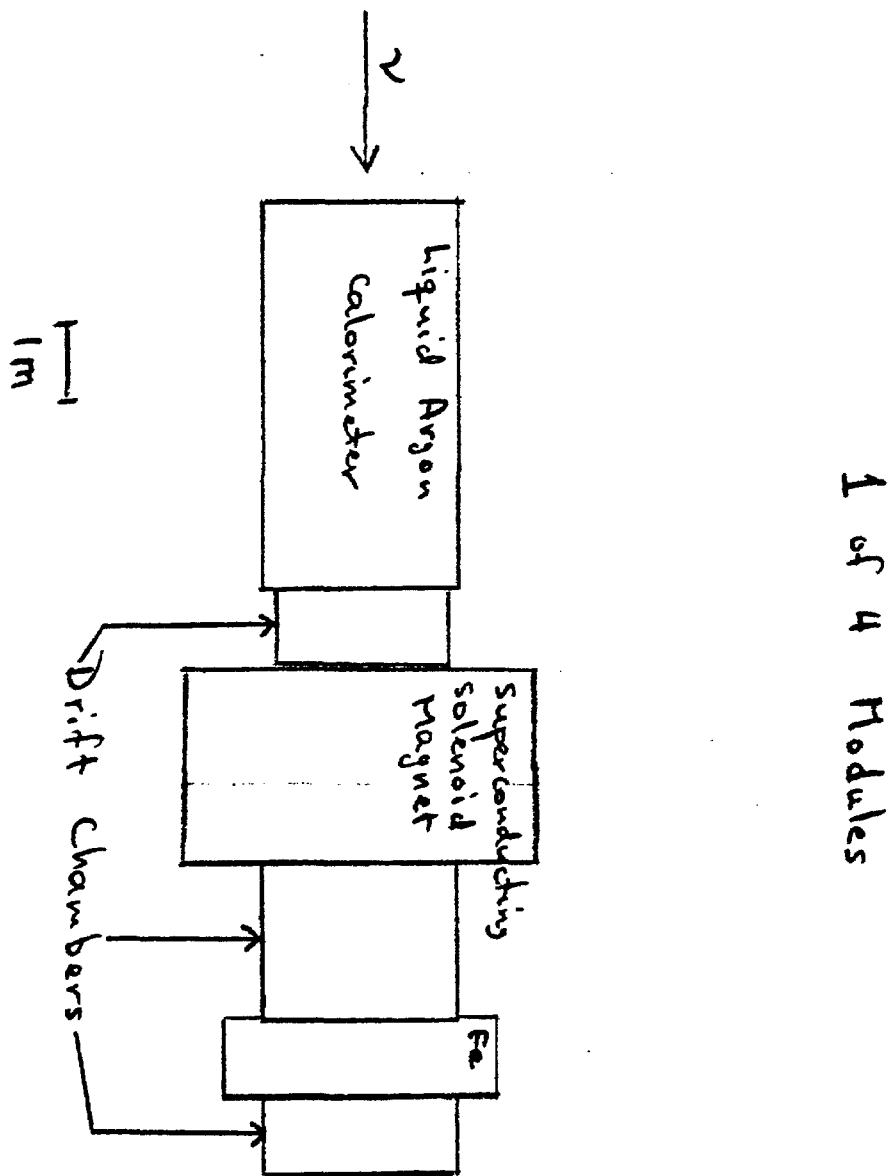


Figure 1. Schematic of One P602 Module

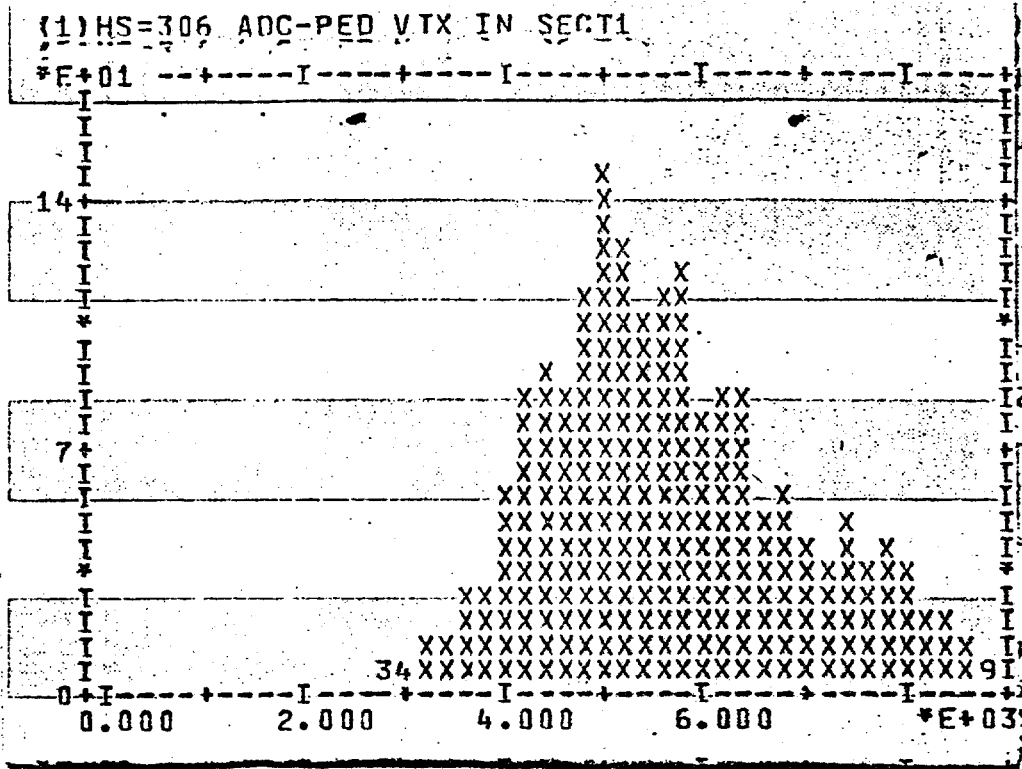


Figure 2a. Pulse Height Distribution for events with vertices in section 1. No minimum cut has been applied.

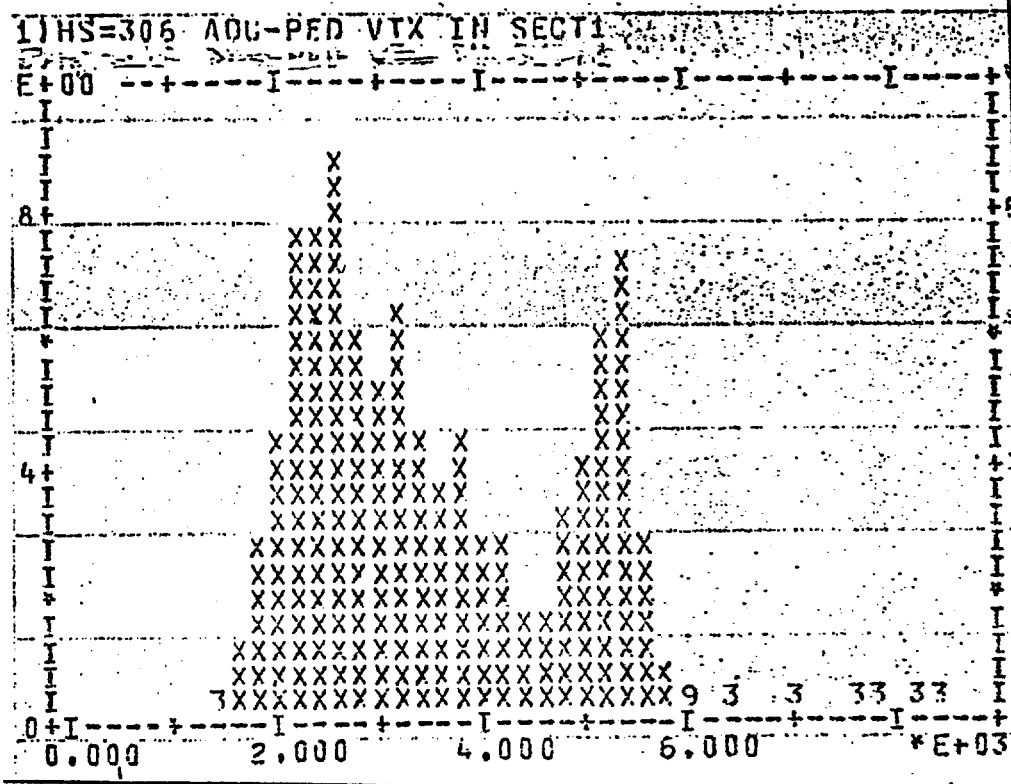


Figure 2b. Pulse Height Distribution for events with vertices in section 1. A minimum cut of 5 particles has been applied to each channel.

Figure 2b is the same data with the 5 minimum ionizing particle cut applied to all channels. The number of events in the plot decreases and the hadrons are shifted down much more than the electrons. The separation is striking and indicates how well the detector can do on electron-hadron separation with the most rudimentary of cuts. (No cut has been made on longitudinal shower development, for example.)

Before each pulse the pedestal for every channel was recorded, an average value was derived and each channel had the average value of its pedestal subtracted. The total pedestal subtracted, that is

$$\sum_{\substack{i = 1, 12 \\ j = 1, 29}} \text{Ped} (I, J)$$

for all 696 channels and its associated width is indicated in Figure 3. The width of this distribution must be subtracted from the width of the pulse height distribution in order to determine the energy resolution of LARC. The linearity of the system is illustrated in Figure 4. A typical pulse height distribution for 20 GeV hadrons, electrons subtracted, that have interaction vertices identified in Section 2 (approx. 0.68 absorption lengths into LARC) is shown in Figure 5. A plot of the upper limits on σ_E versus energy is given in Figure 6 along with data from Willis, et al. Most of the uncertainty in our values come from the electron subtraction. At this stage we have not pushed the resolution further because the upper limit is already reasonably good and sufficient for the physics we propose to do.

VI. Angles

The angle of the hadronic shower is calculated in two independent ways. Centroids are found for the charge distributions in each

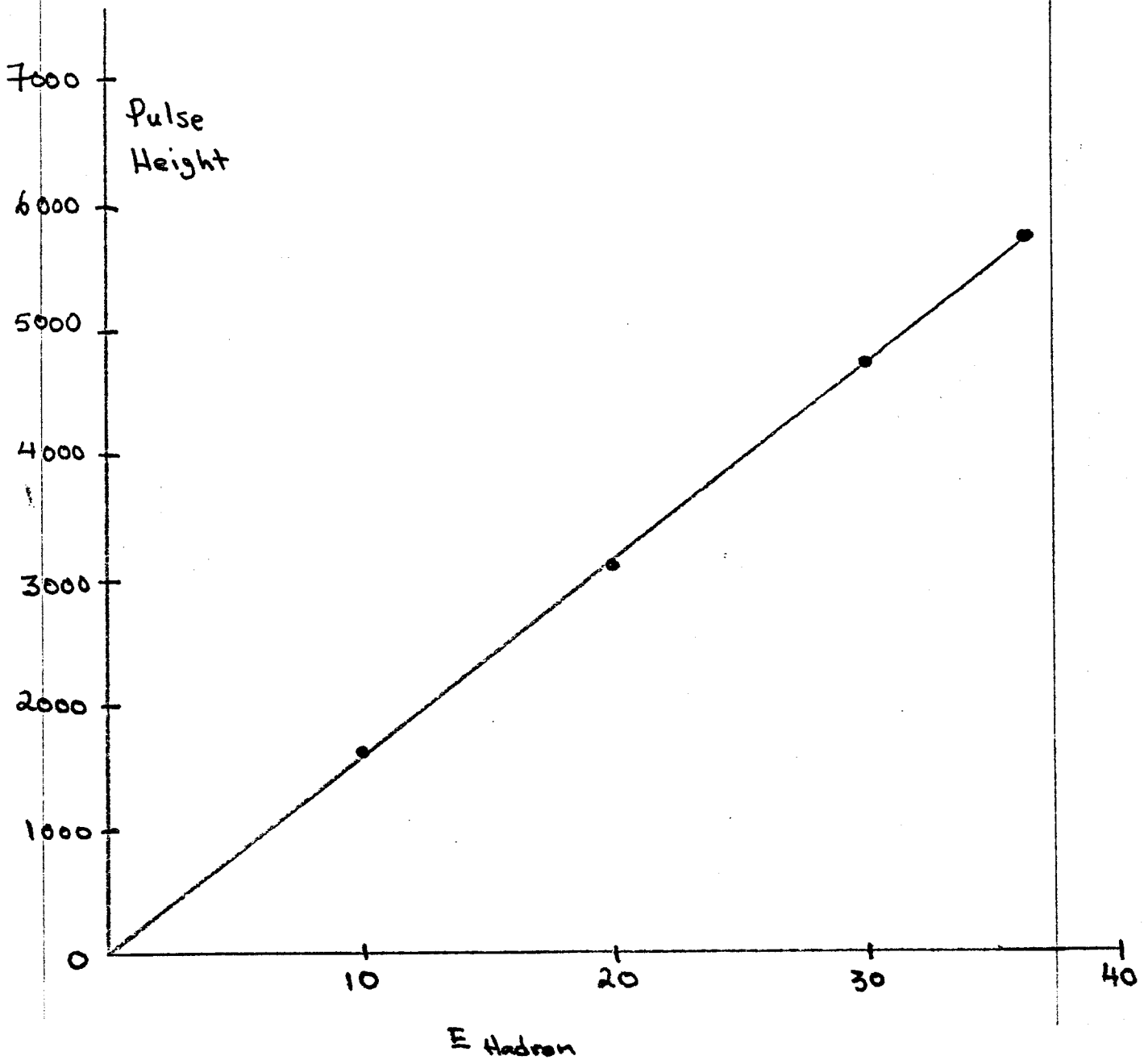
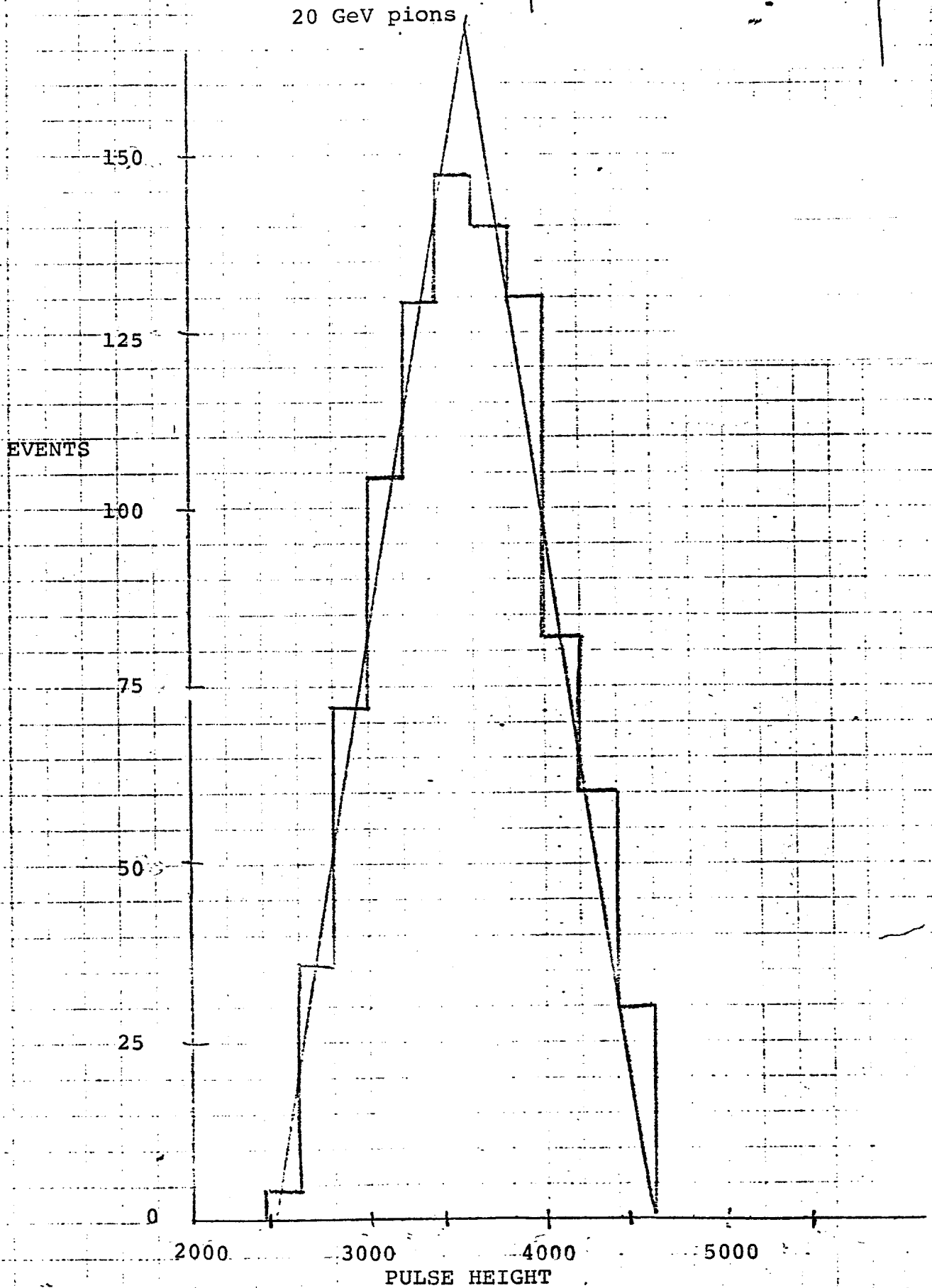


Figure 4. Pulse Height vs. Hadron Energy

Figure 5. Pulse Height Distribution for 20 GeV Pions



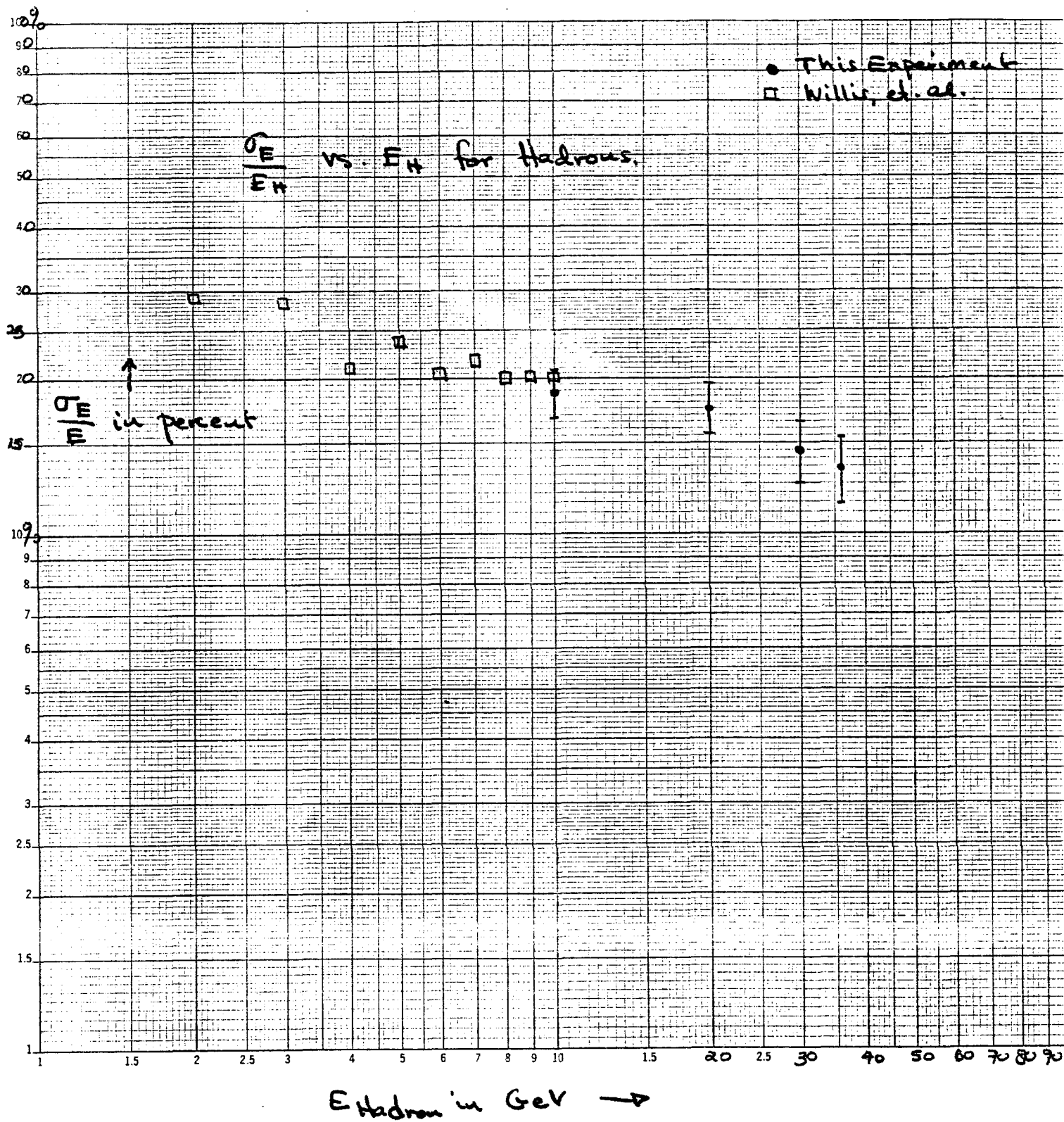


Figure 6.

plane downstream of the vertex. Each centroid has an error associated with it which is $\frac{\sigma}{\sqrt{N}}$, where N is the number of particles in the plane. Each point is weighted according to its error and a straight line is fit through the points. No other cuts are made.

In the other case we use an algorithm that does a momentum weighted average for each strip in the calorimeter downstream of the vertex. The weighting presented here is the most rudimentary; that is the ratio of the energy in the x(y) strip divided by the total energy in the shower in the x(y) view. The two algorithms give the same result.

Clearly we can now proceed to do center weighting that will enhance the "hot core" relative to the wings and make cuts on the longitudinal and transverse shower development. The difficulty in getting turn around on tape jobs at Fermilab has prevented us from getting completely tested results from these more sophisticated cuts; the initial results, however, are very encouraging.

The results of the initial analysis is shown in Figures 7-10 for 10, 20, 30 and 36 GeV respectively, and in Table I.

The results are plotted in Figure 11, along with the function:

$$\sigma_{\theta} = \left(6 + \frac{600}{E_H}\right) \text{ mrad for illustration.}$$

VII. Conclusions

The analysis is at the part where the characteristics of the liquid argon/iron calorimeter (LARC) are becoming clear. Even though the running conditions during the test were not the best (e.g. there was a lot of material upstream of us going in and out of the beam at random times, the beam was poorly configured and tuned, etc.), the results are encouraging and we are even more convinced (if this is possible) that we have the best device for

Cont'd

10 GeV

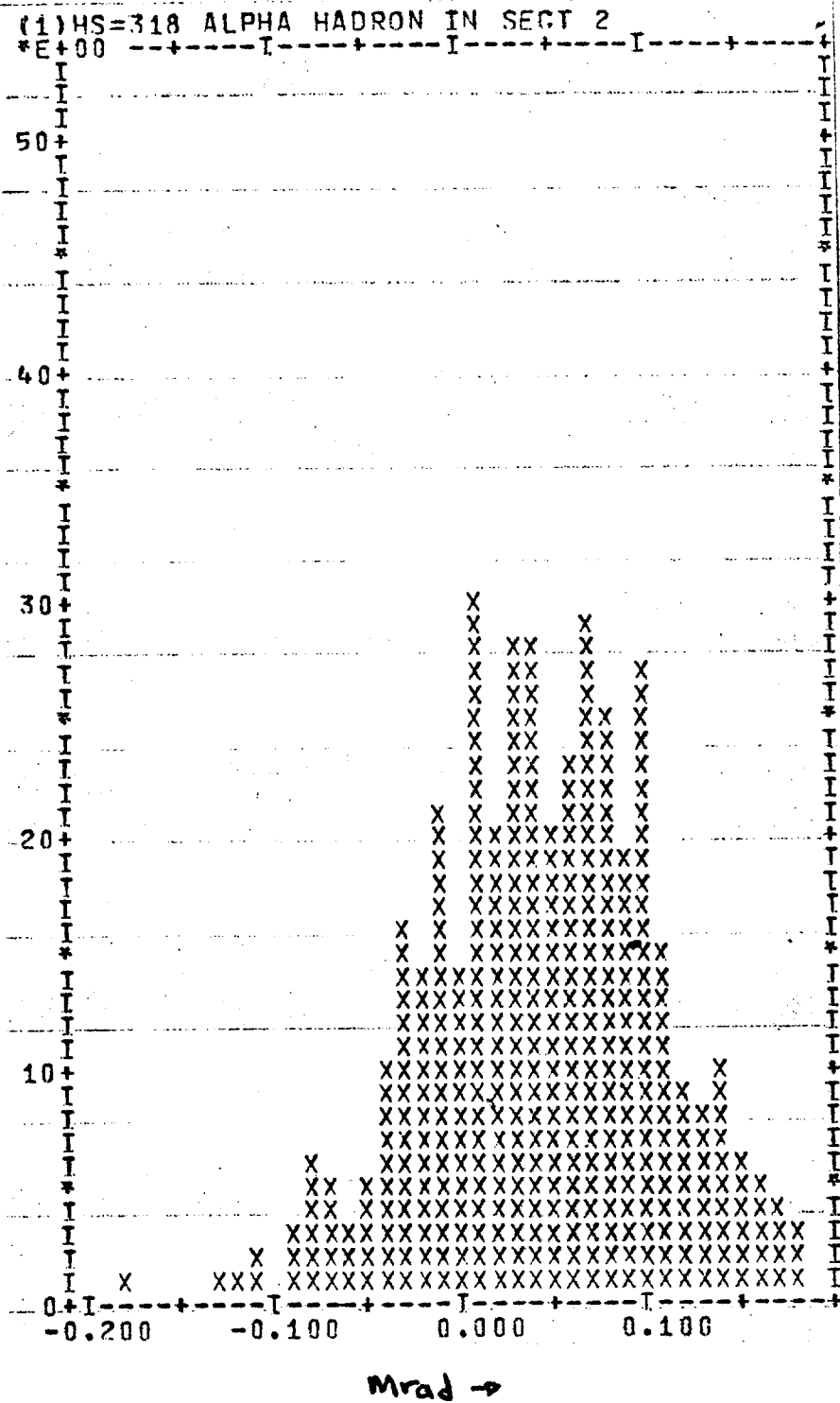


Figure 7.

36 GeV

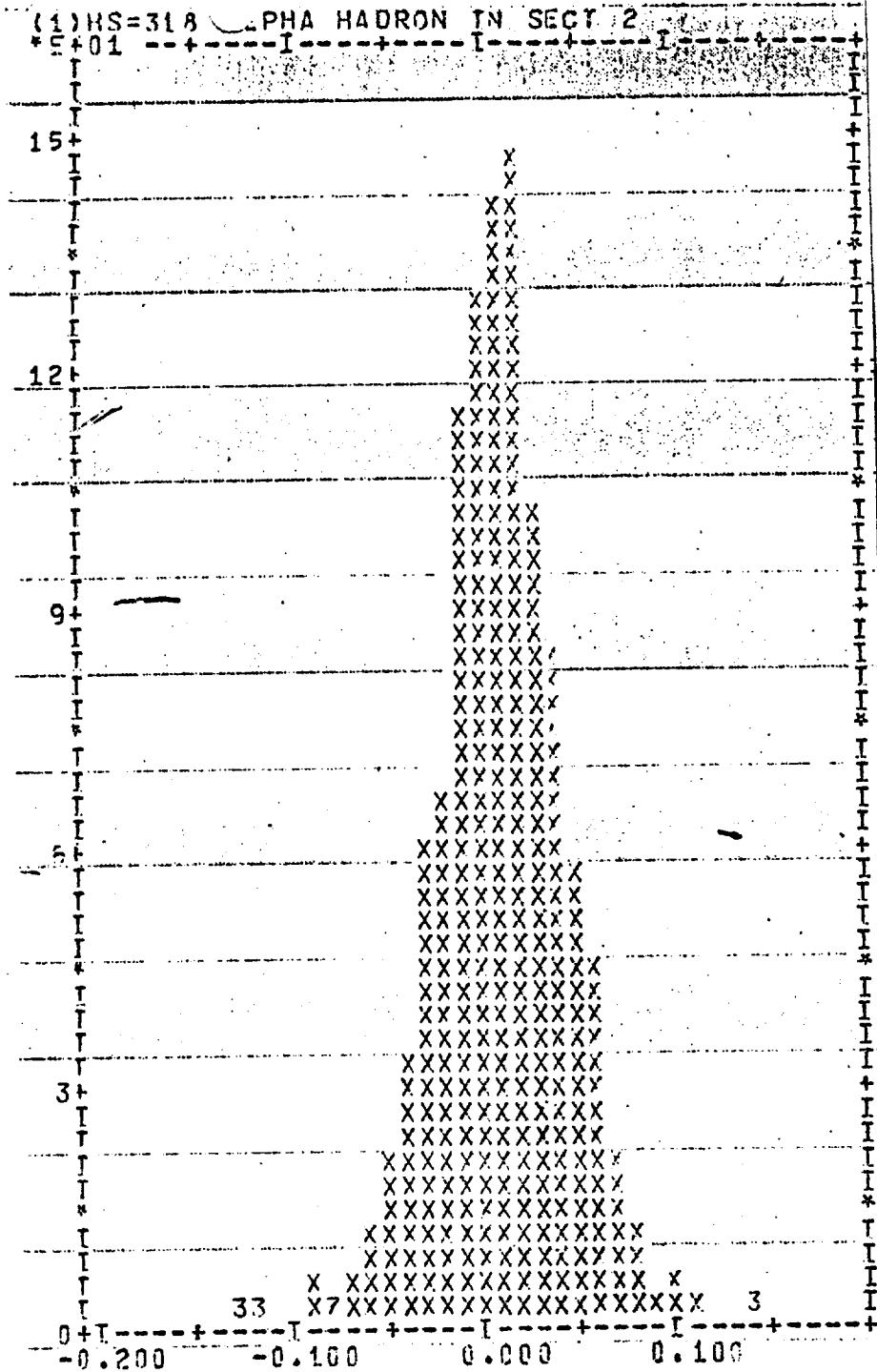


Figure 10.

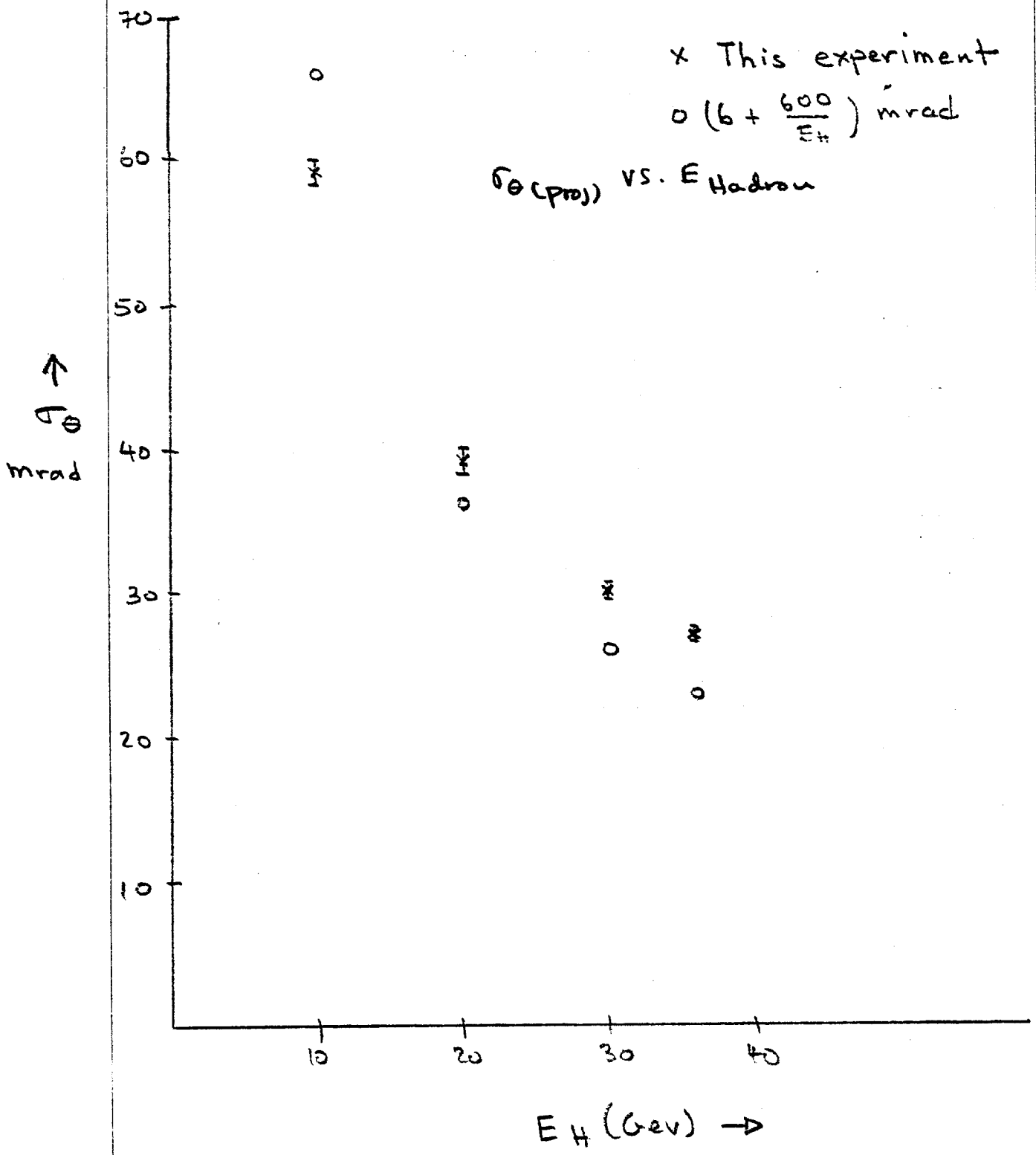


Figure 11.

TABLE I

<u>E (GeV)</u>	<u>σ_{θ}</u> (proj)
10	59 \pm 1
20	39 \pm 1
30	30 \pm 0.5
36	27 \pm 0.5

neutrino physics at Doubler/Saver energies. The angular resolutions have improved markedly since the first report even though we have not used all of the information available to us. More sophisticated algorithms are presently being developed.

We are heartened that our colleagues from the University of Michigan have elected to join in this endeavor. With approval from the PAC we expect that others, especially from Fermilab, will elect to join and further strengthen the collaboration.

ALS:dla
6/8/78

A Proposal To Study The Interactions
of Neutrinos and Antineutrinos at
The Energy Doubler/Saver

M. Goodman
A. L. Sessoms
Harvard University

S. C. Wright
University of Chicago

B. Eisenstein
L. E. Holloway
W. T. Wroblecka
University of Illinois

Spokesman: A. L. Sessoms
Physics Department
Harvard University
Cambridge, MA 02138
(617) 495-3388

MAY 8 1978

Abstract

We propose to build a modular neutrino detector based around liquid argon-iron calorimeters to study the weak interactions of neutrinos and antineutrinos. The device consists of four modules, each made up of a calorimeter, drift chambers and scintillation counters, and a 10 kilogauss superconducting magnet. This has the unique feature of having both good hadronic and muonic energy resolutions and will allow detailed studies of charged and neutral current reactions to be made.

Introduction

High energy neutrino physics has been tremendously productive over the past few years. We have seen the dramatic success of the simple scaling picture and quark model in describing the general features of high energy neutrino scattering. We have seen the accumulation of evidence establishing the existence of weak neutral currents, one of the most important developments in particle physics in recent times. We have also seen the discovery of dimuon events, which undoubtedly were the first direct observations of charm.

The opening of a new energy regime to experimentation, with the advent of the energy doubler/saver holds great excitement, especially when one considers the history of neutrino physics. It has always been true that with the advent of higher energy machines, new phenomena have been discovered that have vastly increased our knowledge of nature. Therefore we anticipate that energy doubler/saver neutrinos will be rich in new phenomena. This, hopefully, will lead to new understanding. Several questions immediately come to mind:

- 1) What happens to the total cross sections at high energies?
- 2) Are charged and neutral currents the same at high energies?
- 3) How do neutrino and antineutrino cross sections compare?
- 4) What is the structure of the weak interaction?
- 5) Where are the new thresholds?
 - a) New quantum numbers
 - b) New leptons
 - c) ?

The complexity of deep inelastic neutrino events with and without final state muons or energetic electrons demands increased detector capabilities to unravel their full

content. This is especially true of neutrino events at the highest energies, the highest four-momentum transfers Q^2 , and the highest final state "hadron" energies $E_H = E_{\nu_{in}} - \sum_{out} (E_{\mu} + E_{\nu})$ (this will contain direct electron components). The instrument we propose in this document is a major advance in detector sophistication. It will obtain significant improvements with respect to both quality and quantity of information from neutrino interactions. Moreover it is well designed for the physics of the energy doubler/saver.

Physics Discussion

I. Energy Dependence in the Charged Current Reaction

At Fermilab-SPS energies there is, at present, no resolution of the question of some energy dependent effects in the charged current reaction. For example, data presented at the recent Hamburg conference from the Caltech-Fermilab collaboration¹ and from BEBC² indicated some energy dependence, especially when compared with low energy data. CDHS data³ on the other hand gave no such indications in the range 30-200 GeV. Some dependence would be expected from scaling violations of the kind seen in deep inelastic electron and muon scattering, beyond that due to the excitation of new thresholds. This is one of the first questions that one would address in neutrino interactions at energy doubler/saver energies.

II. Neutral Current Reactions

It is of major importance to continue the study of weak neutral currents to higher energies and to perform a high-statistic comparison between charged and neutral currents under the same conditions. There is more to neutral currents than the study of the Weinberg angle; e.g. are there charm or bottom or anything else changing neutral currents? Do the neutral currents behave like the charged currents or are

there profound although so far hidden differences? These questions could be immediately addressed with the dichromatic energy doubler/saver.

III. Multimuon Events

It is now clear that "normal" neutrino induced dimuon events are of charmed origin. Questions still remain regarding the existence and characteristics of the same sign dimuons. These events would presumably have an origin other than charm and deserve to be investigated at higher energies.

The discovery of spectacular trimuons at Fermilab,⁴ confirmed at CERN,³ with thresholds at or near the highest energies we can now obtain cannot be explained by any known process. These multimuon events portend more spectacular types at higher energies.

IV. The Challenge

The physics of these remarkable phenomena at the energy doubler/saver is the motivation for this proposal.

The surprisingly large number of $\nu_{\mu}e$ scattering events recently seen in BEBC at CERN⁵ (approximately seven times the number expected from Weinberg-Salam theory) raises many questions about our understanding of the weak interaction. This serves to underscore the importance of extending current measurements to the highest possible energies with the best detector that can be produced.

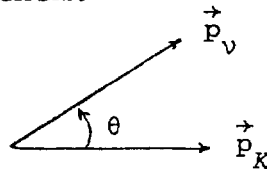
Beam and Detector

A possible dichromatic beam for the energy doubler/saver was discussed during the 1976 Summer Study. Detailed calculations for the present N-30 dichromatic beam have been done by Edwards, Mori, and Press⁶ and by Edwards and Sciulli.⁷ We can extend these calculations to energy doubler/saver

energies in the following way.⁸

Consider a K -meson beam. The decay $K \rightarrow \mu \nu$ is isotropic in the center of mass and the beam acceptance is small enough (11 microsteradians) so that, at all interesting energies, the beam line covers a flat part of the rapidity distribution.

Define p_ν to be the momentum of the neutrino from this decay, and p_K to be the momentum of the K -meson with θ being the angle between them:



Then

$$p_\nu^{\max} = p_K [1 - (m_\mu^2/m_K^2)] = 0.95 p_K$$

$$p_\nu = p_\nu^{\max} \frac{1}{1 + (\theta/\theta_0)^2},$$

where θ_0 is the characteristic angle, $\theta_0 = m_\mu/p_K$. For the Edwards, et al. calculation $p_K = 300$ GeV. For the energy doubler/saver $p_K = 700$ GeV. Thus

$$\theta_0^{300} = 1.65 \text{ mrad}$$

$$\theta_0^{700} = 0.71 \text{ mrad.}$$

Now, for neutrinos within an angle θ

$$p_\nu^{\min} = \frac{p_\nu^{\max}}{1 + (\theta/\theta_0)^2}.$$

Define

$$f \equiv \frac{p_\nu^{\max} - p_\nu^{\min}}{p_\nu^{\max}}$$

as the fraction of the neutrino spectrum accepted by the beam line. Then

$$f = 1 - \frac{1}{1+(\theta/\theta_0)^2} = \frac{\theta^2}{\theta^2+\theta_0^2} .$$

Assume a detector with an acceptance $\theta = 1$ mrad. Then we can construct the following table

p_K	p_ν^{\max}	θ_0	f
700	668	0.71mr	0.66
300	286	1.65mr	0.27

One sees approximately 2.5 times the flux of neutrinos at the higher energy. One loses, however, because of the longer lifetime in the lab by $\frac{300}{700} = 0.43$, so that the relative flux is of the order of 1. So we expect roughly the same flux from the energy doubler/saver N-30 beam line as from the present beam. The expected flux for neutrinos and antineutrinos is given in figures 1a and 1b. If one separates the detector into 25 cm bands one gets the spectrum shown in figure 2 for neutrinos;⁹ a similar spectrum obtains for antineutrinos.

We are interested in neutrinos and antineutrinos with energies of 250 GeV and up. This gives reasonable overlap with measurements that will be made at CERN and Fermilab and also permits the detector to be reasonably small. The fiducial

radius is taken to be 1 meter. We allow 30 cm on all sides to assure full containment of large angle hadronic showers. This gives a total active detector of 2.6 meters.

With this beam the total mass in the neutrino detector must be approximately 300 tons in order to be sensitive to a cross section of $\sim 10^{-44}$ cm². With our proposed technique, namely a liquid argon/iron calorimeter of modular design,¹⁰ we would achieve approximately 290 tons of fiducial mass for 620 tons total.

We want the best possible muon momentum measurement for the study of events with one or more muons in the final state. This demands the use of air core magnets and drift chambers and helps to define the segmentation of the instrument. We would like 95% muon acceptance for normal charged current events.

Consider a calorimeter that has a volume of 2m×2m×5m, and demand that all accepted events be initiated in the first 3 meters. This assures total containment and clearly underestimates the muon acceptance. Imagine that this calorimeter is followed by 1 meter of drift chambers, a 10 kilogauss magnet with a 2m×2m×2m gap, followed by 1 meter of drift chambers. This is shown schematically in figure 3. We can easily calculate the muon acceptance using the front face of the magnet as the defining aperture. Doing this we have found that out of 5000 events the apparatus accepts 4697 muons for an acceptance of 94%.

We can calculate the momentum resolution such a system would have in the following way. Consider the arrangement in figure 4 for 100 GeV muons. Assume normal drift chambers with resolutions of 100 microns. Then

$$p_{\perp} = 0.03 \int B dl = 0.6 \text{ GeV},$$

$$\alpha = \frac{0.6}{100} = 6 \text{ mrad},$$

$$\delta\alpha = \frac{2 \times 100 \text{ microns}}{1 \text{ m}} = \frac{2 \times 10^{-4}}{1} = 0.2 \text{ mrad},$$

$$\frac{\delta\alpha}{\alpha} = \frac{\delta p}{p} = \frac{0.2}{6} = 3.3\%.$$

The total mass of a single calorimeter unit with gap width and plate thickness identical to the prototype calorimeter described in the accompanying document is

$$(2.6\text{m} \times 2.6\text{m} \times 5\text{m}) \times 4.17 \text{ gm/cm}^3 = 140946 \text{ kg or } 155 \text{ tons}.$$

The average fiducial length of a calorimeter module is 4 meters. The fiducial width was defined to be 2 meters. This gives a fiducial mass of 66727 kg or 73.4 tons.

The detector configuration is shown in figure 3. We propose 4 modules, each consisting of a liquid argon/iron calorimeter, drift chambers, and scintillation trigger counters and 10 kilogauss air core magnet. The total liquid argon detector mass is 620 tons. The total fiducial mass is 294 tons. Details of the module construction are given in table 1 and figure 5.

The electronics we propose is essentially identical to that used on the prototype liquid argon/iron calorimeter and so need not be discussed in detail here. A block diagram of the system is given in figure 6. Briefly, a trigger is generated and sent to the liquid argon calorimeter (LARC) control unit, a NIM module placed near the detector. This device generates gates G1 and G2, with a separation appropriate to the time constant of the device (720 ns in this case) and gates the sample and hold circuit on (G1) to collect the charge and off (G2) after all the charge is collected. The computer then addresses the multiplexers via a CAMAC unit called a Read In/Read Out Digital to Analog Converter (RIRODAC). The RIRODAC is capable of sending digital signals to the multiplexers as well as analog signals, through the LARC control unit, directly to the amplifier inputs for test and calibration purposes. There are 580

channels of Lecroy 2259A or equivalent analog to digital converters (ADC's), these to service 11600 channels of electronics per calorimeter module. There are $48\frac{1}{3}$ 2259A or equivalent 12-channel units. We note that this number of channels is not large when compared to some of the detector arrays being built for colliding beam detectors (20,000 channels just for the inner chamber in the CESR detector at Cornell, to give only one example).

A detailed cost estimate of the electronics for 720 channels (plus 240 spares), including labor, for the prototype device is given in the appendix.

Drift Chambers

The drift chamber design will be very similar to that presently being used at Fermilab for experiment 490. The chambers are 2.3m×2.3m in active area. The drift space is 10 cm. The 100 micron resolution can be achieved by using either the system designed and implemented by T. Droege at Fermilab or the commercial system marketed by W. LeCroy, Inc. We would have 3 sets of chambers in front and 3 in back of the magnet. A set consists of xx' yy' vv' planes to define a space point. A schematic of the construction technique is given in figure 7.

Magnets

A sketch of one of the proposed magnets with drift chambers is given in figure 8a. Briefly, we propose superconducting split solenoids, 2 meters in diameter with a 2 meter gap. The field uniformity need only be good to a few percent. The proposed field is 10 kilogauss. This gives $\int Bdl = 200 \text{ kG-m}$ as required and the high muon acceptance for charged current events. Figure 8b gives some of the considerations used by Joe Heim¹¹ of Fermilab to make his cost estimate of \$384K per magnet, based on an extrapolation from

the conversion of the Chicago cyclotron magnet (CCM). It has been pointed out by Paul Mantsch¹¹ that there may be ways to cut the cost down to our projected \$300K. For example, by putting some material in the aperture, 7 inches of aluminum, say, the coil assembly could be made self supporting, thereby avoiding costly support columns. Once the iron no longer supports the magnetic load it could be removed, as in the 15 foot bubble chamber, or used only as a magnetic shield. One could also take advantage of new techniques such as high current density, intrinsically stable coils. We assume a cost of \$300K per magnet henceforth.

Beam

Monte Carlo studies indicate that resolution for E_ν , and therefore $y = E_H/E_\nu$, for neutral currents will be dominated by the hadron beam divergence for divergences as small as 0.22 mrad (see figures 9-11). We suggest that care be taken so that the meson beam divergence be kept less than 0.11 mrad if at all possible.

It is obvious that the berm must be hardened. We suggest the use of muon spoilers if feasible. The muon background is likely to be limiting if care is not taken early on to insure a clean environment.¹²

Event Rate

Using the N-30 dichromatic beam calculations discussed above we have calculated the event rate for a coulomb of protons (6.25×10^{18}) on target for the proposed detector. These rates, as a function of energy, are given for neutrinos and anti-neutrinos in tables 2 and 3 respectively. A plot of event rate versus neutrino energy is given in figure 12. The event rate peaks at 600 GeV for the 700 GeV meson beam tune. This is a significant increase over the present (almost) peak

of ~ 200 GeV. The size of the data sample allows one to probe cross sections of the order of 10^{-44} cm², assuming that $\sigma_{\nu N} \propto E_{\nu}$. If the cross section does not remain proportional to neutrino energy the statement above is of great import since it signals the first direct evidence for an intermediate vector boson of finite mass.

Time Schedule

<u>Time</u>	<u>Goal</u>
t_0 : June 1978	Approval of proposal. Begin engineering of full-sized calorimeter, superconducting magnet, drift chambers, and building.
t_0+4 mos: October 1978	Begin construction and testing of first complete module (includes calorimeter, magnet, and drift chambers).
t_0+12 mos: June 1979	Complete building. Begin beam tests of full module in building.
t_0+16 mos.: October 1979	Begin construction of remaining three modules.
$t_0+2\frac{1}{2}$ yrs : January 1981	Begin calibrations and tests with muons and hadrons. Begin data taking.
t_0+3 yrs : June 1981	Complete operating experiment.

Cost Estimate

	<u>\$M</u>
a) 11600 channels/module 4 modules @ 15.00/channel (large quantities reduce cost from 20.00/channel)	0.70 ¹
b) 4 dewars @ 100K/dewar	0.40 ²
c) 328 tons of steel strips and plates, copper plated @ 500.00/ton	0.16
d) 4 superconducting 10 kG magnets, 2m×2m×2m (solenoids) @ 300K/magnet	1.20 ³
e) 8 sets of drift chambers, 2.3m×2.3m @ 34K/set	0.27 ⁴
f) LA storage (tank cars) LN ₂ supply dewars (from surplus list)	0.25 ⁵ 0.25 ⁵
g) Assembly of calorimeters in place 10 man-years @ 30K/man-year	0.30 ⁵
TOTAL	\$3.53M

Note: A new building on the other side of Wilson Road, in back of the bubble chamber, will be needed. We estimate the total cost for 50m×10m×20m, with crane, to be \$0.5M.

¹see appendix on electronics cost

²extrapolated from the prototype cost of \$11300.00

³see section on magnet designs and costs

⁴M. Atac, private communication

⁵reasonable estimates

Table 1

Target Calorimeter Module

Active Dimensions	2.6 x 2.6 m ²
Length	5.0 m
Fiducial Volume	2.0 x 2.0 x 4 m ³
Total Mass	155 tons
Fiducial Mass	73.4 tons
Sampling Step	3.0 mm iron (2.36 gm/cm ²)
Energy Sampling	liquid argon 4 mm thick
Angle Sampling	2 cm wide x and y every 2.8 cm
Density (average)	4.17 gms/cm ³
Radiation Length	3.52 cm
Interaction Length	19.0 cm
Number of Channels of Electronics	11600

Table 2

Number of Events for Neutrinos
1 Module

E_ν (GeV)	# Evts/ 10^{13} protons
250	1.6×10^{-1}
300	1.0×10^{-1}
350	4.8×10^{-3}
400	3.2×10^{-3}
450	1.1×10^{-2}
500	5.8×10^{-2}
550	1.4×10^{-1}
600	1.5×10^{-1}
650	6.6×10^{-2}
700	3.0×10^{-2}
750	8.0×10^{-3}
800	1.6×10^{-3}

Total $0.738/10^{13}$ protons

885 evts/day/module

(day $\equiv 10^{13}$ protons/pulse $\times 1$ pulse/min $\times 20$ hrs)

Total number of events 3540/day

Table 3
 Event Rate Per Module for $\bar{\nu}$

$E_{\bar{\nu}}$ (GeV)	# Evt $s/10^{13}$ protons
250	2.8×10^{-3}
300	1.1×10^{-3}
350	3.9×10^{-5}
400	3.9×10^{-5}
450	1.1×10^{-4}
500	4.4×10^{-4}
550	7.0×10^{-4}
600	5.9×10^{-4}
650	1.7×10^{-4}
700	8.9×10^{-5}
750	2.6×10^{-5}
800	5.1×10^{-6}
	<hr/>
	$6.1 \times 10^{-3} / 10^{13}$ protons
	8 evt $s/day/module$
	Total number of events 32/day

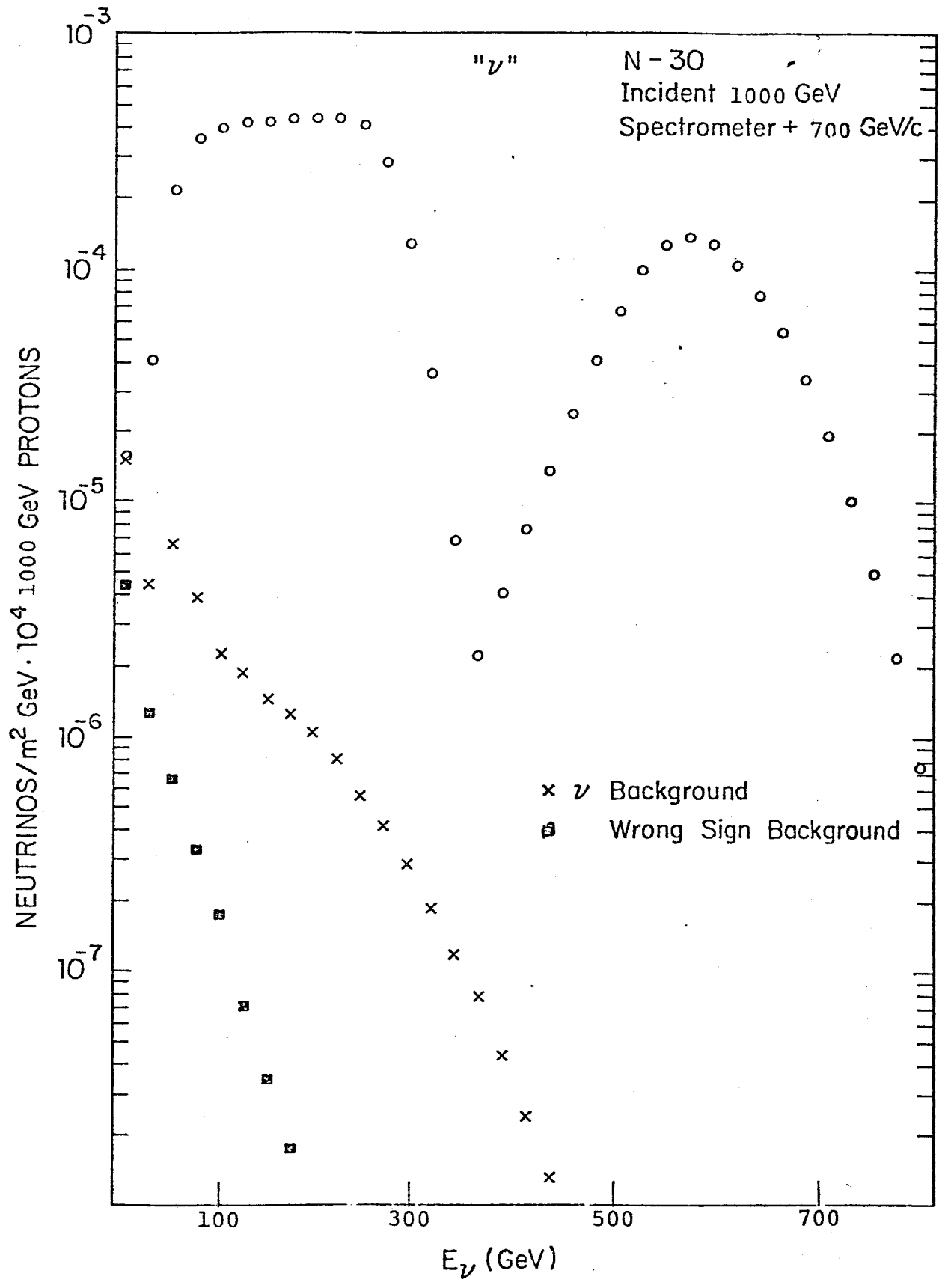


FIGURE 1a

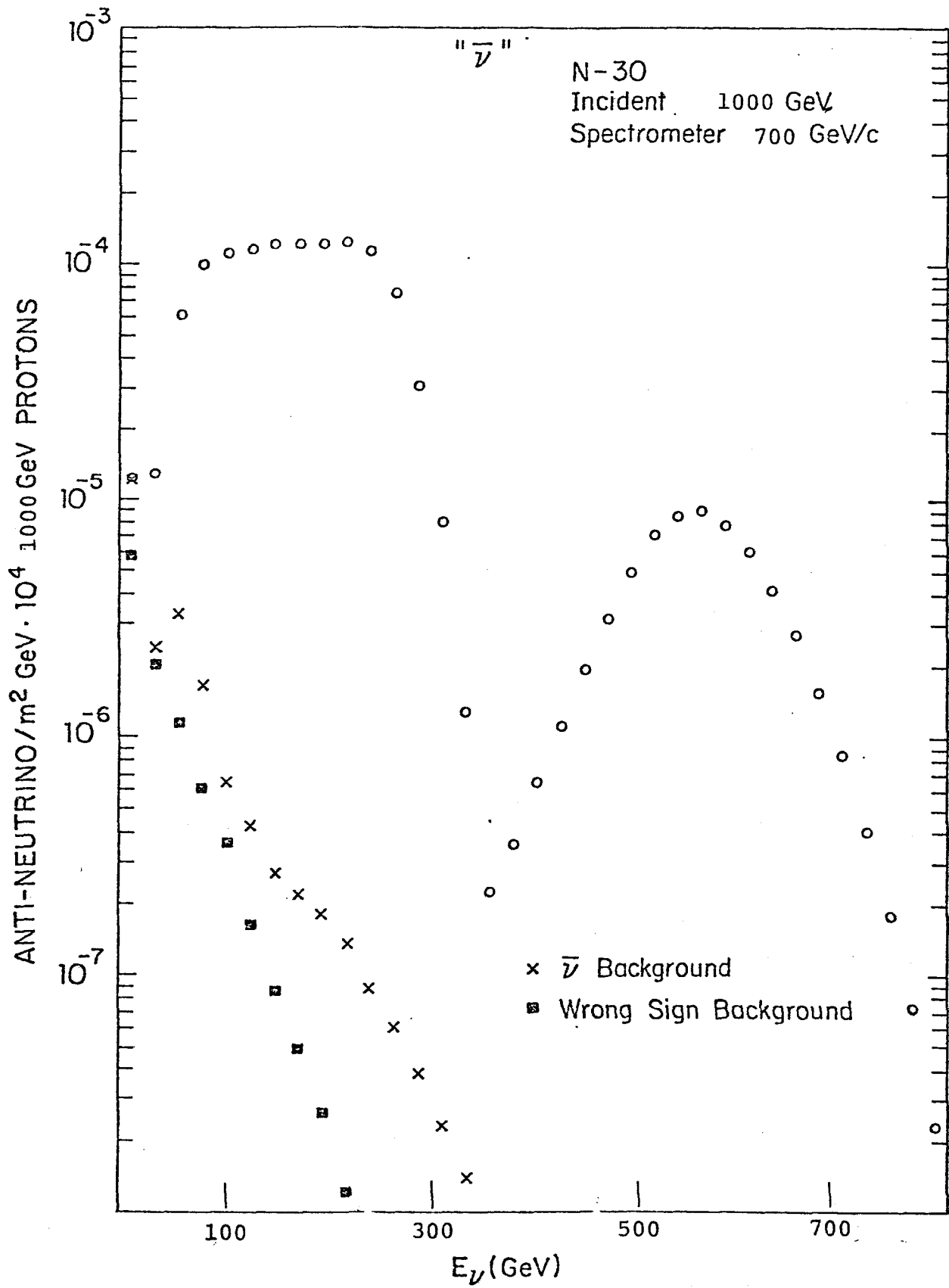
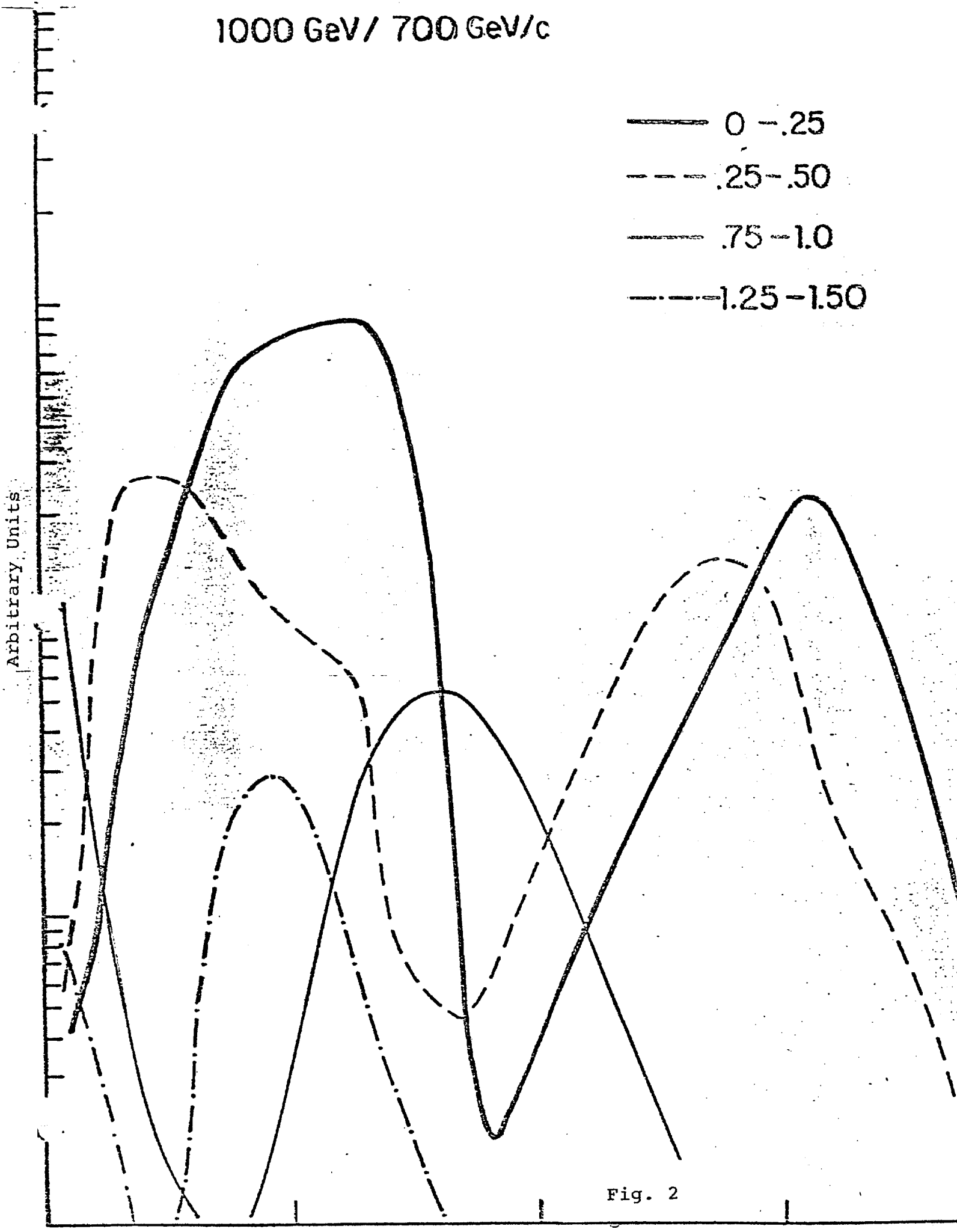
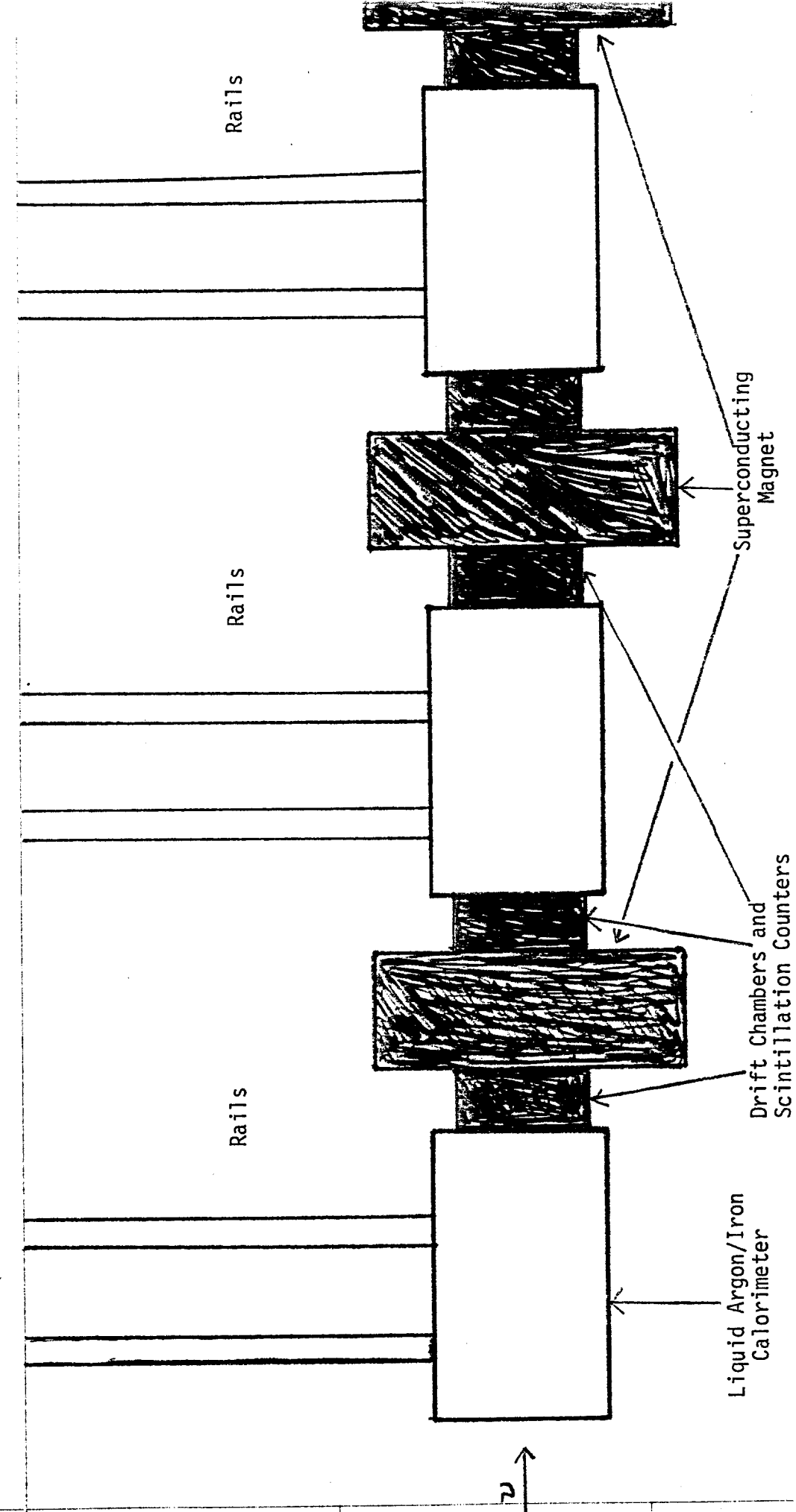


FIGURE 1b

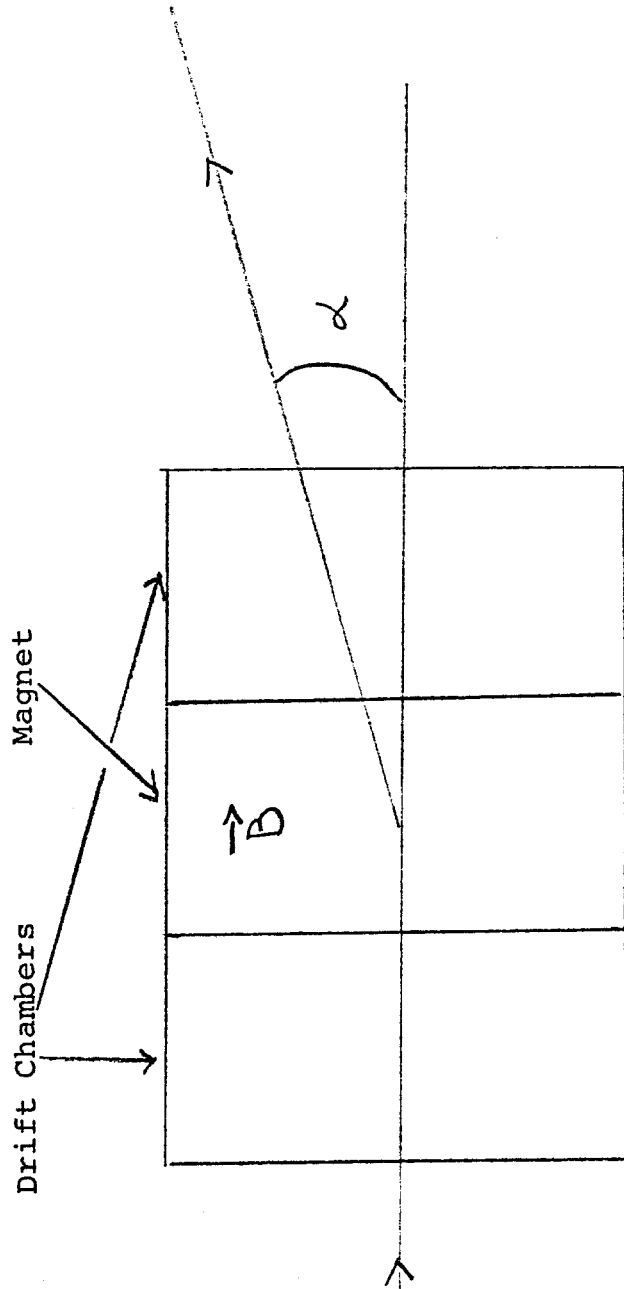
1000 GeV / 700 GeV/c





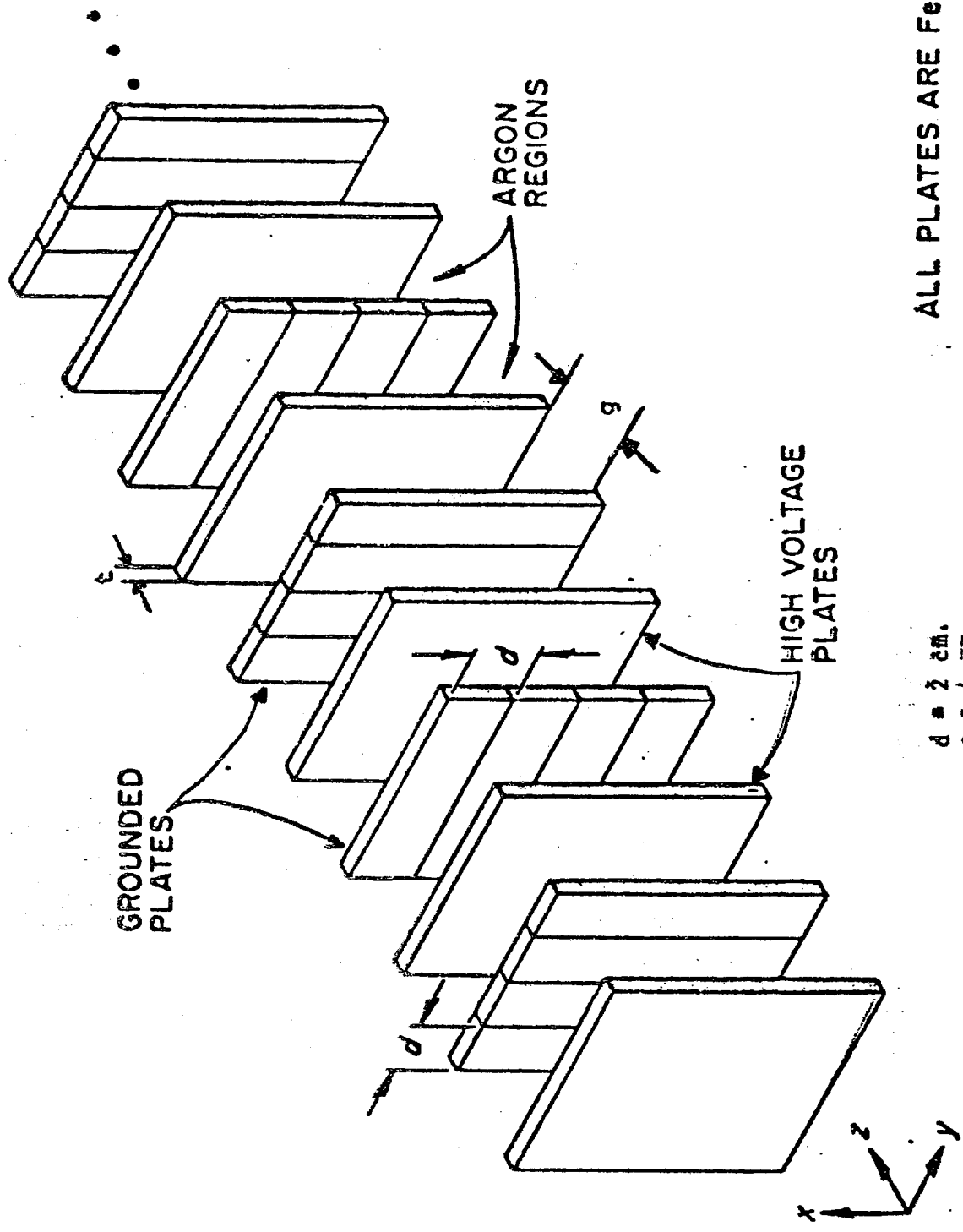
1 cm = 1 m.

Figure 3.



Drift Chamber Resolution 100 microns
 $\int_{BDL} = 20$ Kilogauss-meters

Figure 4



ALL PLATES ARE Fe

- $d = 2 \text{ mm.}$
- $g = 4 \text{ mm.}$
- $t = 3 \text{ mm.}$

figure 5

figure 6

SCHEMATIC OF ELECTRONICS FOR ONE CALORIMETER MODULE

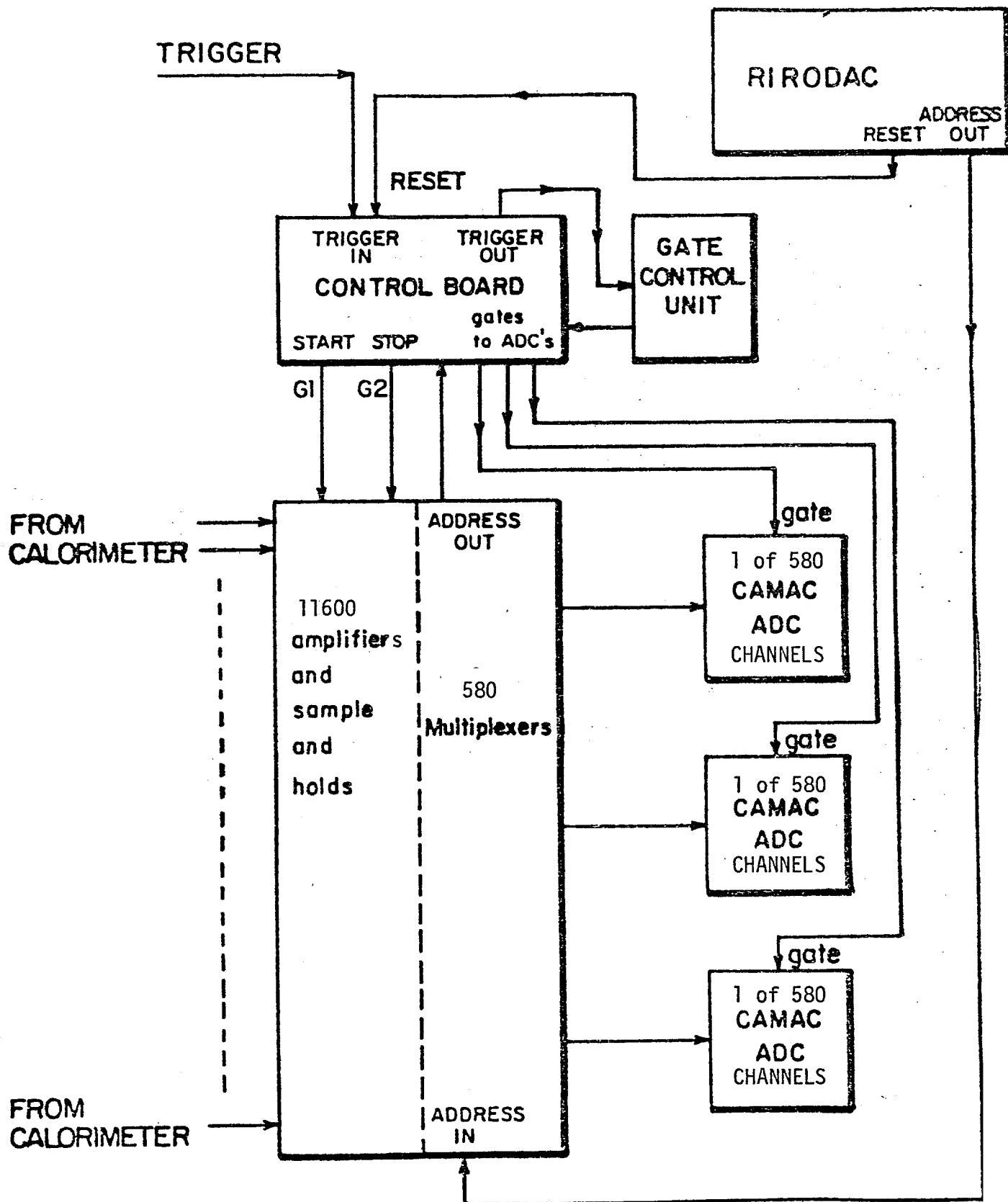
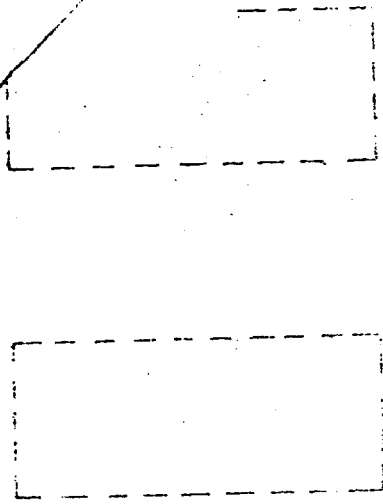


figure 7



4

BUSS

$\frac{1}{4}$ HEX CELL PAPER EPOXY TO G-10 PLATES
 USE SCOTCH WELD #2216 TYP.

12

1

4

6

.146

.394 TYP. 163-WIRED = 71.708

SECTION A-A

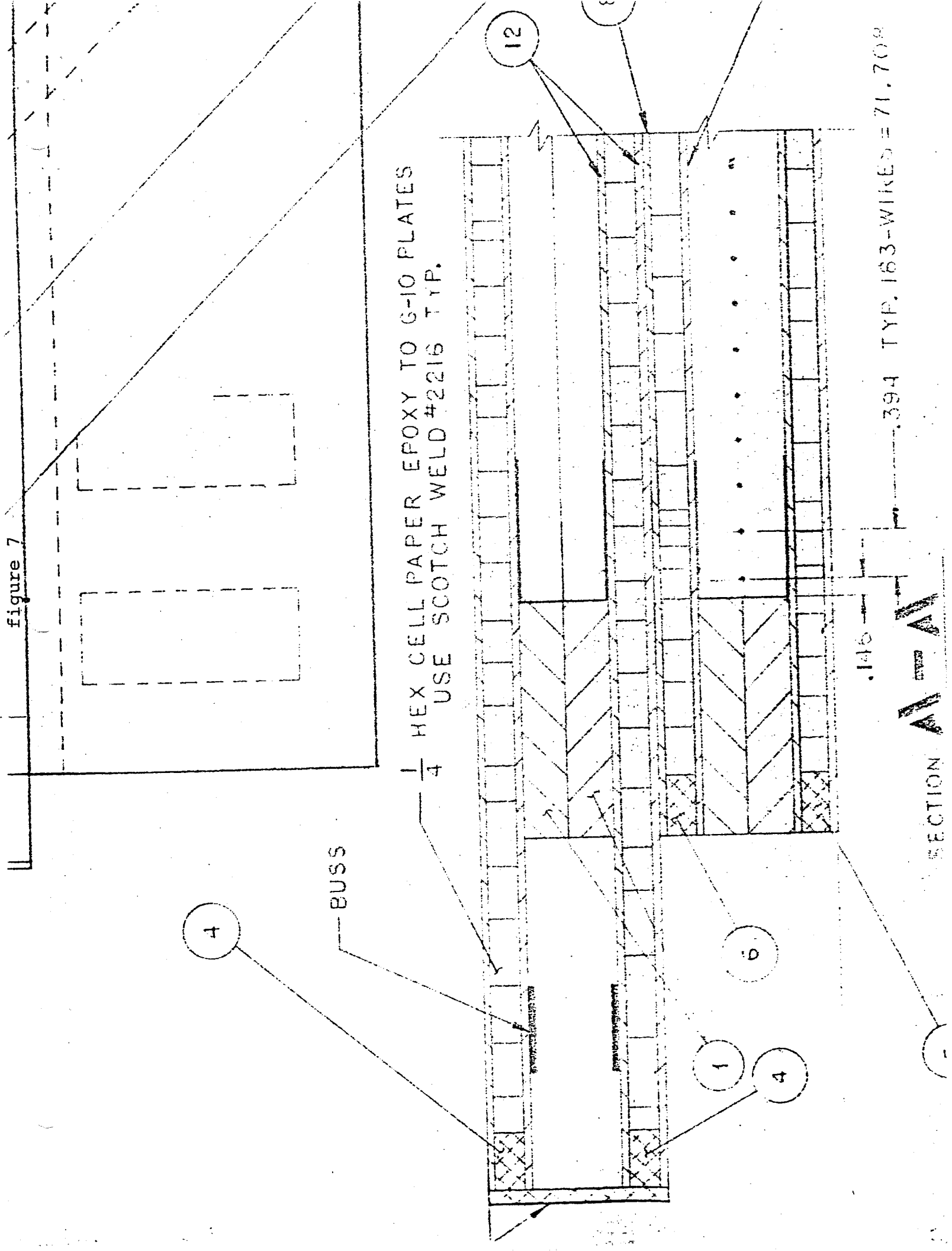
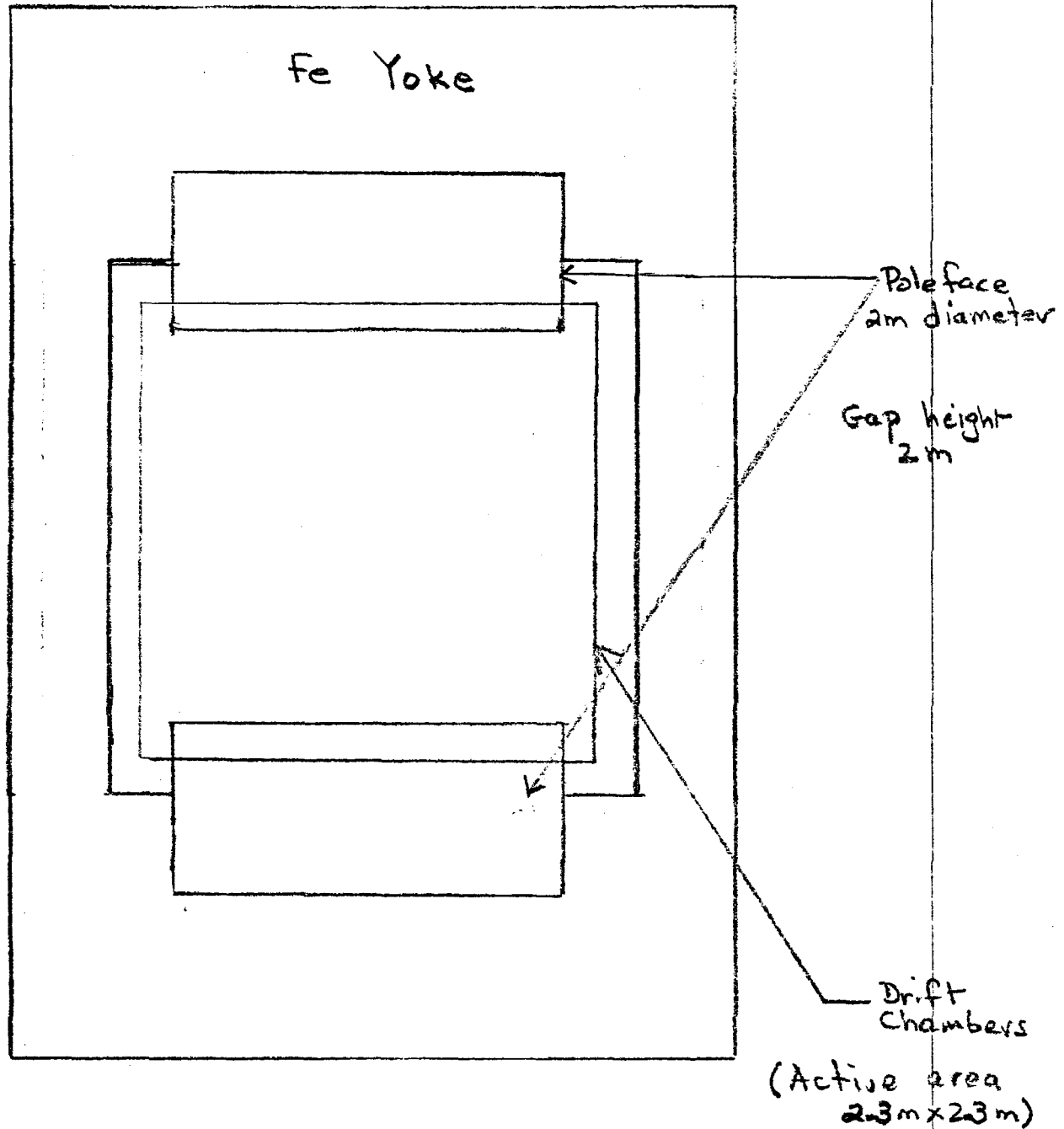


figure 8a

Split Solenoid Magnet $B = 10$ Kilogauss

$$\frac{\Delta B}{B} \approx 2\%$$



$$3\text{cm} = 1\text{m}$$

figure 8b

Magnet for energy doubler/saver experiment

10 amp turns per coil

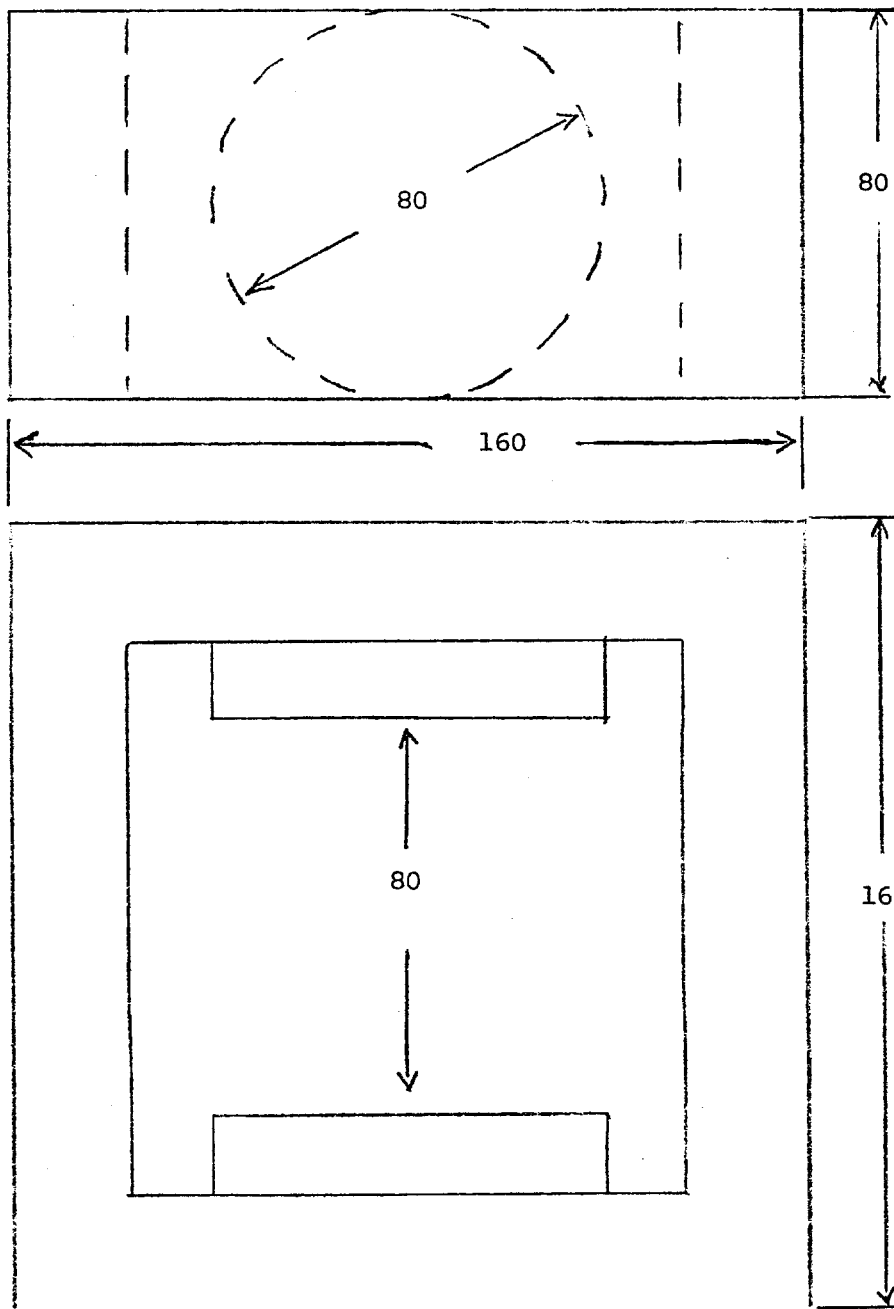
1 Tesla

Cryostat of same type design as CCM

6 support columns and 60° segment polygon

\$275,000

Iron size - return leg driven at 19 kG approx.



180.8 ton
@\$600/ton
\$108,480

Total Cost
\$384,000

figure 9

E_{γ}

beam divergence = 0. radian

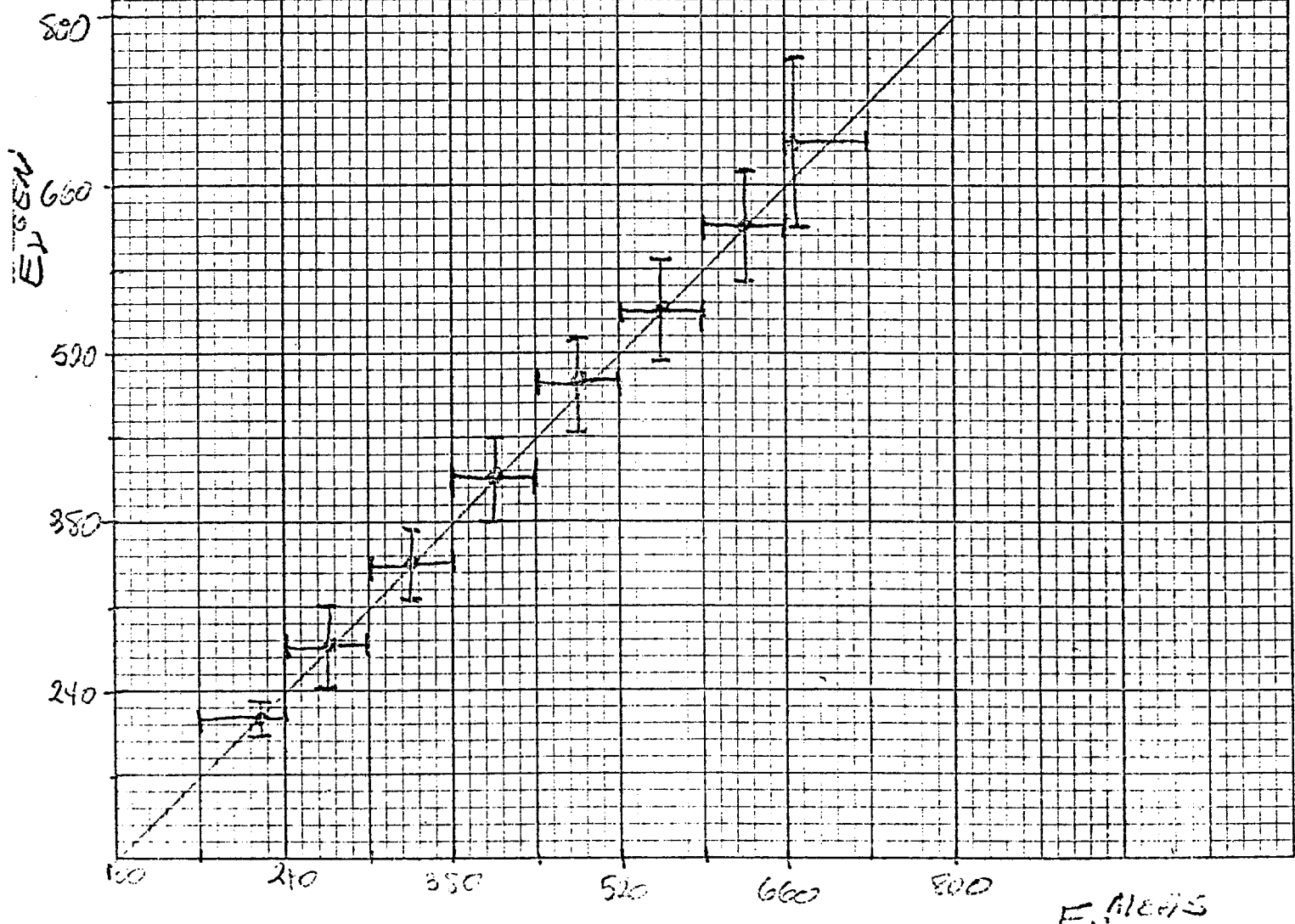


figure 10

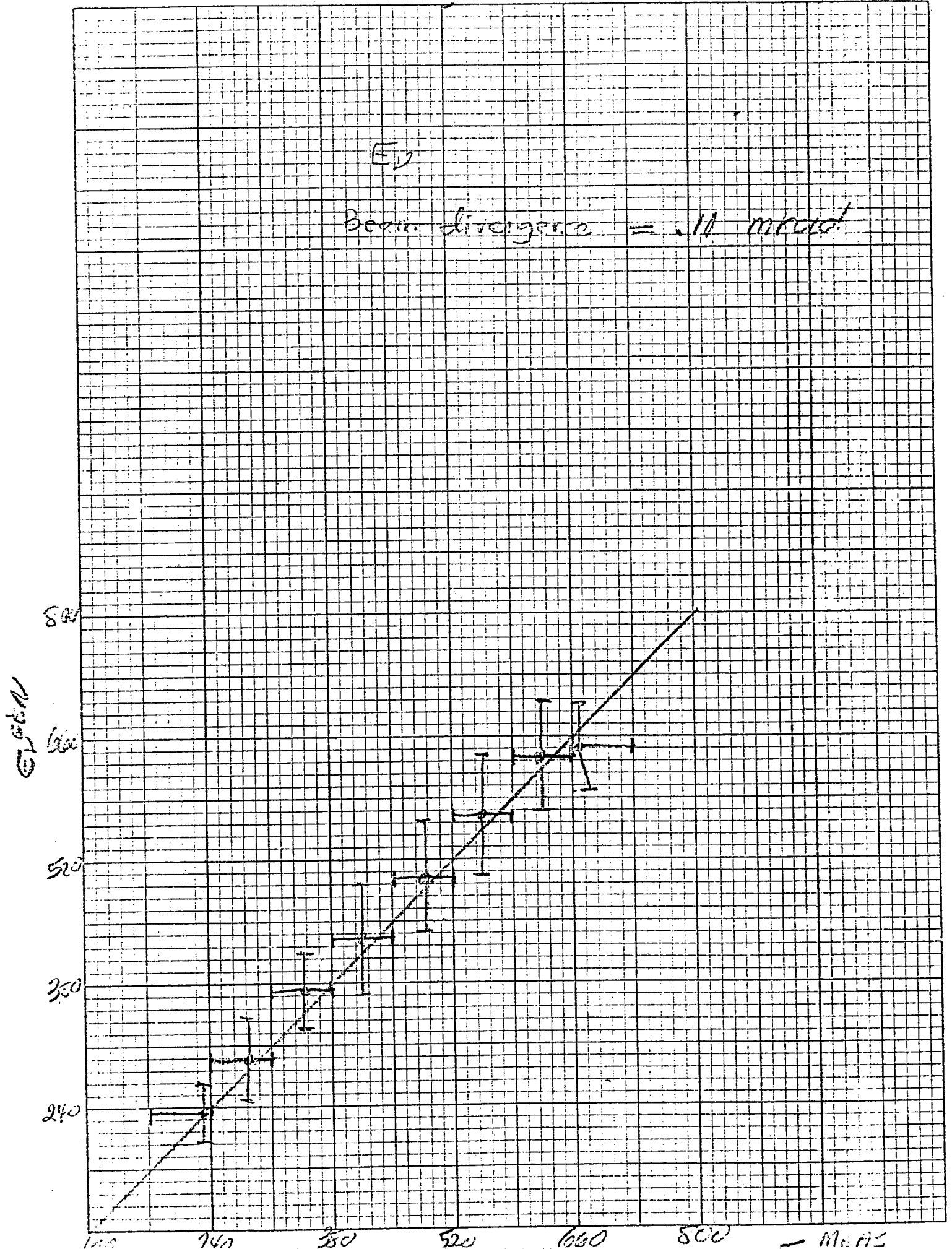


figure 11

E_V
Normal

Beam divergence = 22 mrad
 $\epsilon_{p(\text{meson})} = 9\%$
 $\sigma_{\text{meson}} = 5 \text{ cm}$

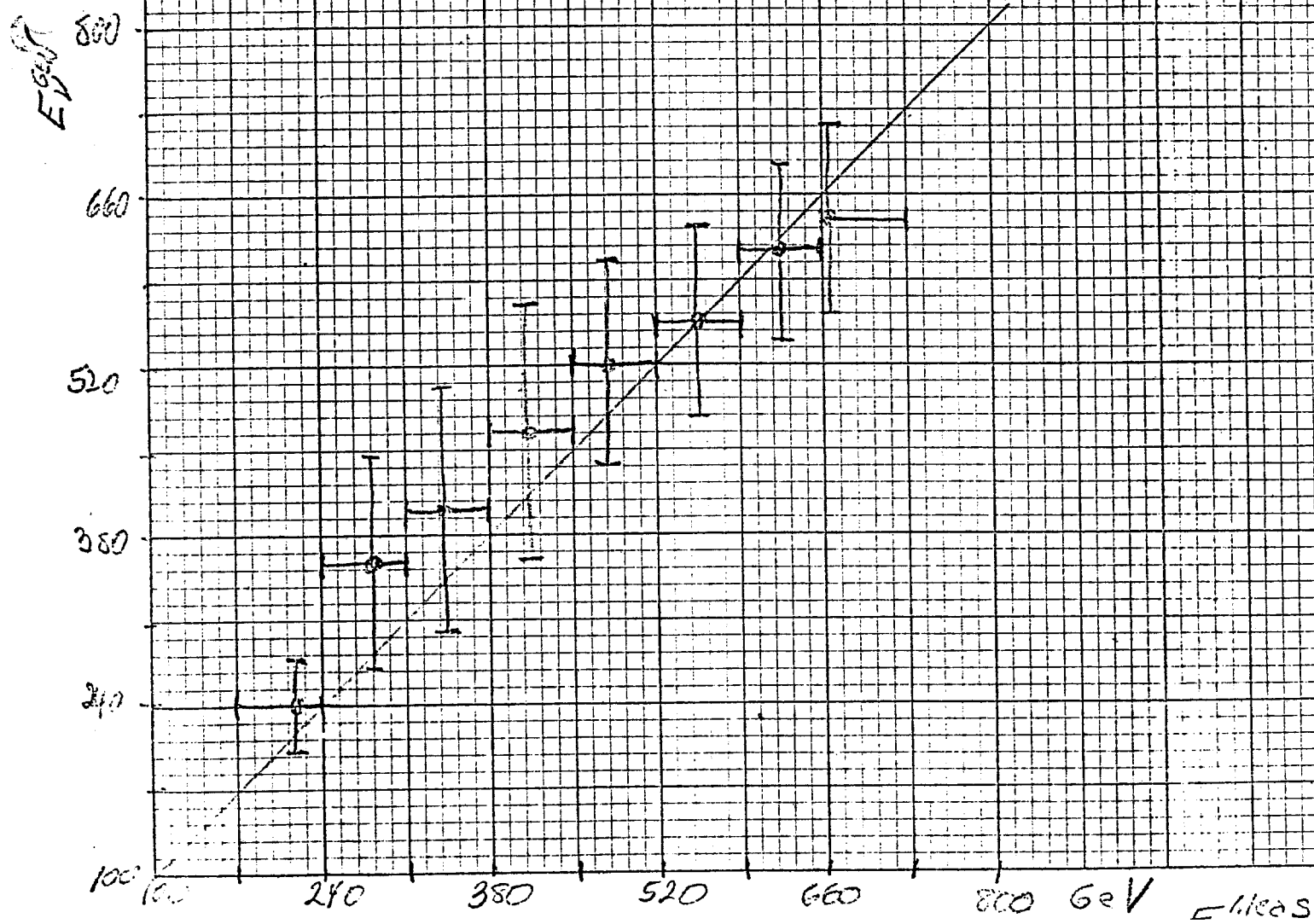
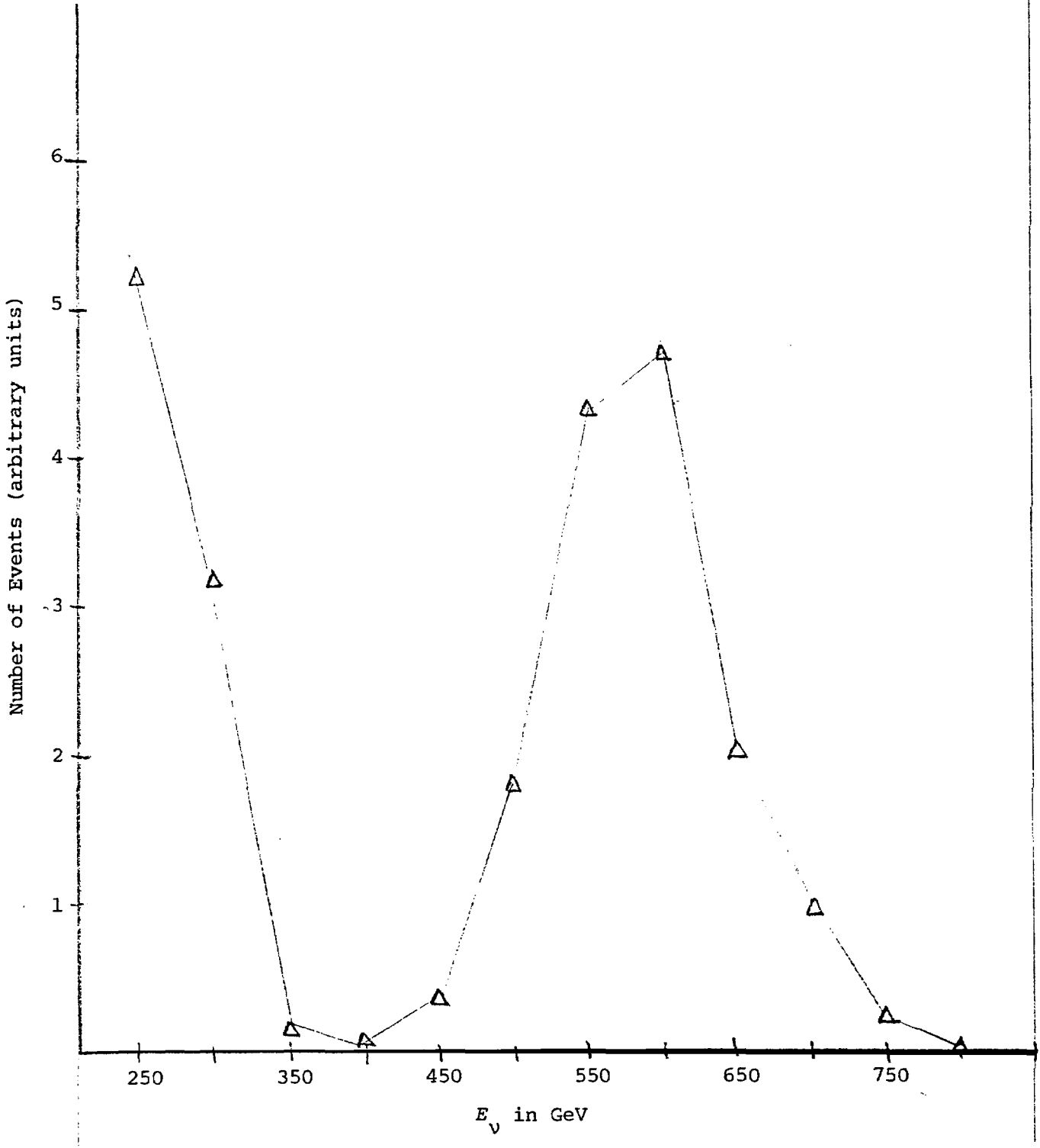


figure 12

ν Event Rate



References

¹B. Barish, "A Critical Summary of Neutrino Results" in *Proceedings 1977 International Symposium on Lepton and Photon Interactions at High Energy (Hamburg)*, pp 748-753; F. Sciulli, "Total Cross Sections and Mean y from Charged Current ν_{μ} and $\bar{\nu}_{\mu}$ Collisions," *ibid.*, pp 239-258.

²K. Schultze, "Study of Neutrino and Antineutrino Interaction in Neon-Hydrogen Mixture Using the CERN Narrow Band Beam," *ibid.*, pp 359-386.

³K. Keinknecht, "First Charged Current Data from the CERN-Dortmund-Heidelberg-Saclay Neutrino Experiment," *ibid.*, pp 271-292; P. Bloch, "Multilepton Production," *ibid.*, pp 293-308; K. Tittel, "Study of Semileptonic Neutral Currents of ν - and $\bar{\nu}$ Interactions in the CERN SPS Narrow Band Beam by the CERN-Dortmund-Heidelberg-Saclay Collaboration," *ibid.*, pp 309-322.

⁴D. Cline, "Charged Current Weak Interactions at High Energy," *ibid.*, pp 749-784; D. D. Reeder, "Multimuon Production by High Energy Neutrinos," *ibid.*, pp 259-270.

⁵P. Musset, Private Communication.

⁶D. Edwards, S. Mori, and S. Press, "350 GeV/c Dichromatic Neutrino Target Train," Fermilab TM-661, 2972.000, May 6, 1976.

⁷D. A. Edwards and F. J. Sciulli, "A Second Generation Narrow Band Neutrino Beam," Fermilab TM-660, 2972.000, May 1976.

⁸We are indebted to Frank Sciulli for this discussion.

⁹S. Mori, Private Communication.

¹⁰See the attached report to the PAC on the P-541 liquid argon/iron calorimeter studies for a detailed description of the construction techniques.

¹¹P. Mantsch, Private Communication.

¹²See, for example, J. Allaby, *et al.*, in the proceedings of the 1976 Fermilab Summer Study.

Appendix

Total cost of 960 channels of LARC electronics, including spare parts.

I. Parts

<u>Order no.</u>	<u>Company</u>	<u>Cost</u>
K17943	Gerber	73.20
K17940	Sterling	839.20
K17941	Sterling	682.65
K17942	Cramer	700.00
K17939	Cramer	501.00
K17945	H. Avnet	36.00
K17946	T.I. Supply	469.65
K18602	Impact Sales	771.80
K18606	Marshall	55.00
K18608	Appollo-Vera	78.62
K22201	T.I. Supply	62.75
K23408	Restart	530.00
K23409	Rogers	209.00
K50806	Sterling	444.30
K50803	Ferroxcube	70.00
K50810	T.I. Supply	145.60
K50812	Cramer	277.00
K50813	R.C. Component	96.00
K50820	Schweber	111.00
K50819	Impact Sales	135.00
K27306	Cramer	31.00
K27363	Cramer	178.00
K25193 (PC Boards)	Electrosonics	1400.25

II. Assembly

K27373	Whittman	<u>2370.00</u>
--------	----------	----------------

960 channels: cost/channel 10.69

III. Analog to Digital Converters

3-LeCroy 2259A at 1850/apiece	<u>5550.00</u>
-------------------------------	----------------

720 channels: cost/channel 7.71

TOTAL 18.40/channel

IV. Power Supplies

K71154	Lambda	583.00
	(other supplies on hand)	<u>800.00</u>

720 channels: cost/channel 1.92

Total Cost per Channel (includes labor, power supplies,
connectors, cables, and spare parts):

\$20.32